UNIVERSITÀ DEGLI STUDI DI MILANO
Facoltà di Scienze Matematiche, Fisiche e Naturali
Scuola di Dottorato in Scienze biologiche e molecolari
DOTTORATO DI RICERCA IN BIOLOGIA VEGETALE
XXIV CICLO
Settore scientifico Disciplinare: BIO/01

Maternal control of seed development: the role of the MADS-box genes *SEEDSTICK* and *ARABIDOPSIS B sister*

Tutor:
Dott.ssa Elisabetta Caporali

Coordinatore:
Prof. Carlo Soave

Tesi di Dottorato di:
Chiara Mizzotti

Anno Accademico 2011-2012

To see things in the seed, that is genius
Lao Tzu

To Roby, Sonia e Sarah

Table of Contents

Abstract 3

Introduction 5
The importance of seed 5
Ovule formation and development 7
Integuments development 10
Double fertilization 12
Embryo and endosperm development 15
Seed coat development 18
Genetic control of proanthocyanidins accumulation 21
Genetic control of mucilage accumulation and release 25
References 28

Chapter 1 33
Summary 34
Introduction 35
Results 39
STK and ABS play a maternal role in ovule and seed development 39
Loss of the endothelium layer in the *abs stk* double mutant causes fertilization defects 44
Discussion 54
Experimental Procedures 61
Acknowledgements 66
References 68
Supporting Information 72

Chapter 2 75
Summary 76
Introduction 77
Result 82
STK is involved in seed coat development and proanthocyanidins accumulation 82
STK is involved in mucilage release 88
STK is a key regulator controlling metabolic network during seed coat development 93
Discussion 98
The MADS-box gene *STK* plays a crucial role during seed development in *Arabidopsis* 98

STK regulates the expression of genes involved in seed coat differentiation and PAs production 99
STK has a key role in outer seed coat differentiation and mucilage release 102
Experimental Procedures..... 106
References..... 114
Supporting Information..... 118

Discussion 123
The role of the integuments during ovule development..... 124
The role of the integuments during the fertilization process ... 125
The role of the integuments during seed development..... 127
References..... 131

Abstract

The haploid generation of flowering plants develops within the sporophytic tissues of the ovule that protect the female gametophyte developing inside. After fertilization the maternal seed coat develops in a coordinated manner with the embryo and endosperm and undergoes several changes including accumulation of secondary metabolites such as proanthocyanidins and mucilage. The research performed in these three years had the goal to investigate the interaction between the two generations. In particular we have identified key factors, expressed in the seed integuments (maternal tissue) controlling several aspects of seed development.

In the *arabidopsis bsister* (*abs*) mutant, the endothelium does not accumulate proanthocyanidins and cells have an abnormal morphology (Nesi et al., 2002). ABS encode for a transcription factor belonging to MADS box family. *SEEDSTICK* is another MADS-box gene that regulates, redundantly with *SHATTERPROOF 1 (SHP1)* and *SHP2*, ovule identity (Pinyopich et al., 2003). Here we describe the characterization of the *abs stk* double mutant. This double mutant develops very few seeds due to both a reduced number of fertilized ovules and seed abortions later during development. Morphological analysis revealed the total absence of the endothelium in this double mutant. Additionally, massive starch accumulation was observed in the embryo sac. The *abs stk* analysis strongly suggests a maternal role in the regulation

of the fertilization process and highlights the importance of the endothelium for the development of the next generation. Here we also report new functions of the MADS-box transcription factor *STK* during seed development. *stk* mutant seeds present defect in seed coat morphology and abnormal proanthocyanidins accumulation. In addition, *stk* mutant seeds present problems in mucilage release. Our data reveal new functions of *STK* after fertilization highlighting the importance of this transcription factor indicated as a key regulator of seed development.

Nesi, N., Debeaujon, I., Jond, C., Stewart, A., Jenkins, G.I., Caboche, M., Lepiniec, L. (2002). The TRANSPARENT TESTA16 locus encodes the *ARABIDOPSIS BSISTER MADS* domain protein and is required for proper development and pigmentation of the seed coat. *Plant Cell **14**, 2463-2479.*

Pinyopich, A., Ditta, G.S., Savidge, B., Liljegren, S.J., Baumann, E., Wisman, E., and Yanofsky, M.F. (2003). Assessing the redundancy of MADS-box genes during carpel and ovule development. *Nature* **424**, 85-88.

Introduction

The importance of seed

Morphological innovations in reproductive strategies have played a fundamental role in the diversification of plants, since they have been associated with adaptive radiations in new territories. The most successful strategy is the ability of developing seeds, which allowed plants to extensively colonize the Earth.

The seed can be considered as a functional unit required for the protection and propagation of the offspring. Seeds have several features that make them an excellent survival, dispersal and nutrition unit: they have a reduced metabolism and they germinate only under favourable condition; they are responsible for the dispersion in space and time of the plant offspring; and they are

also involved in providing food at the developing embryo (Nowack et al., 2010).

A key characteristic for evolutionary fitness of the plants is the seed size. This feature is also important as an agronomic trait during crop domestication (Orsi and Tanksley, 2009). The number of seeds produced by a plant is negatively associated with seed size due to the limited resources of the mother plant (Harper et al., 1970). Several studies suggest that seed size is linked to colonization and stress tolerance abilities: seedlings of large-seeded plants can better tolerate stresses encountered during seedling establishment, whereas small-seeded plants have higher colonization abilities because they produce large numbers of seeds (Westoby et al., 2002; Moles et al., 2005). Larger seeds often have higher probability of germination (Jacobson 1998; Westoby et al., 2002) and seedlings of larger seeds tend to have greater survival and improved performance under a wide range of environmental conditions (Krannitz et al., 1991; Westoby et al., 1996; Manning et al., 2009). Thus, the existence of such variation is puzzling because seed size is expected to have a strong effect on fitness and be under strong selection (Silvertown 1989; Manzaneda et al., 2009; House et al., 2010).

Scientific interest in seed size is related not only to plant fitness, but also to crop domestication. Crops domesticated for consumption of their seeds (e.g. rice and wheat) often produce seeds significantly larger than their wild ancestors (Fan et al., 2006; Song et al. , 2007; Gegas et al., 2010).

Ovule formation and development

The first step in seed development is the formation of ovules: the ovule provides the structural support at the female gametophyte that develops into seeds after fertilization. Ovule primordia arise from the placental tissue and appear as a finger like protrusions. Along the proximal distal axis of the developing ovule three elements can be distinguished: the funiculus, the chalaza, and the nucellus (Schneitz et al., 1995).

The funiculus connects the ovule to the placenta and includes the vascular strand, which channels nutrients through the chalaza to the nucellus and the rest of the developing ovule. The chalaza forms the integuments that protect the developing gametophyte; while in the nucellus, the megaspore mother cell differentiates to form the embryo sac (Figure 1).

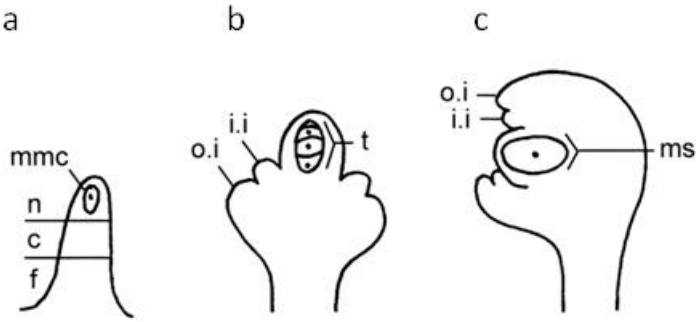


Figure 1 Ovule formation in Arabidopsis (from Gross-Hardt et al., 2002). The ovule primordium (a) is a finger-like structure that arises from the placenta. Along the proximal–distal axis of ovule primordia three domains can be distinguished: the distal nucellus that protects the megaspore mother cell (mmc), the central chalaza, and the proximal funiculus. The megaspore mother cell divides meiotically to give rise to a tetrad of haploid cells (b) and simultaneously integuments grow to enclose the nucellus. The three distal cells of the tetrad die (c) and the functional megaspore undergoes three rounds of mitotic division.

(c) chalaza; (f) funiculus; (i.i) inner integument; (mmc) megaspore mother cell; (ms) megaspore; (n) nucellus; (o.i) outer integument; (t) tetrad.

The gametophytes develop within sporophytic tissues. The male gametophyte, namely pollen grain, develops within the anther and is composed of two sperm cells and a vegetative cell (McCormick 1993, 2004). The female gametophyte develops within the ovule, which develops inside the carpels. The female gametophyte encloses egg cell and is critical to many steps of the reproductive process such as pollen tube guidance, fertilization and seed development upon fertilization (Yadegari and Drews, 2004). The megasporangium produces meiotic cells, one of which undergoes megagametogenesis. In Arabidopsis, the megaspore enlarges and undergoes two rounds of mitosis without cytokinesis. The result of this process is a four-nucleate coenocyte with two nuclei at each pole separated by a large central vacuole (Figure 2b, stage FG4). During the third mitosis, the cellularization process begins and the female gametophyte cells become completely surrounded by cell walls (Figure 2b, stage FG5). One nucleus from each pole (the polar nuclei (pn)) migrates toward the center of the developing female gametophyte and fuse together forming the diploid central cell (ccn) (Schneitz et al., 1995; Christensen et al., 1998). These events result in a seven-celled structure consisting of three antipodal cells, one diploid central cell, two synergid cells, and one egg cell (Figures 2a, b, stage FG6). The egg cell and central cell are polarized and their nuclei lie very close to each other (Figure 2a, b). This is important for double fertilization process when the two sperm cells reach the egg and the central cells. Furthermore,

the region between the egg, synergid, and central cells, is devoid of the cell walls or the cell wall is discontinuous such that the plasma membranes of these cells are in direct contact with each other (Mansfield et al., 1991; Kasahara et al., 2005). This absence provides direct access of the sperm cells to the fertilization targets because the pollen tube releases its two sperm cells into one of the synergid.

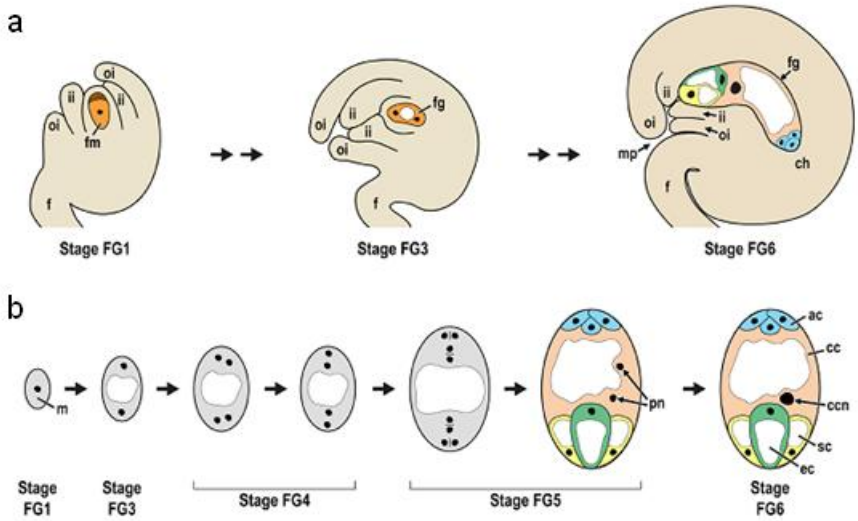


Figure 2 Megagametogenesis in Arabidopsis (from Drews and Koltunow, 2011). Megagametogenesis emphasizing development within the ovule (a) and a detail scheme of the megagametogenesis process (b)

(ac) antipodal cells; (cc) central cell; (ccn) central cell nucleus; (ch) chalaza; (ec) egg cell; (f) funiculus; (fg) female gametophyte; (fm) functional megaspore; (ii) inner integument; (m) megaspore; (mp) micropyle; (oi) outer integument; (pn) polar nuclei; (sc) synergid cells.

Integuments development

The seed coat (testa) consists of several layers of specialized maternal cells that provide an essential interface between the embryo and the external environment during seed development, dormancy and germination (Haughn and Chaudhury, 2005). Differentiation of the seed coat from the ovule integuments includes some dramatic cellular changes and culminates in the death of the seed coat cells.

The inner integument is initiated through a series of cell divisions in the dermal layer at a short distance behind the apex when the ovule primordia arise form the placenta tissue (Figure 3a, b). The cell proliferation determines the formation of a ring-like belt that delimits the nucellus as the apical portion of the primordium. Immediately after, the outer integument is initiated, followed by the inner integument, through a series of similar cell divisions (Figure 3c). Afterwards extensive growth and development occur (Figures 3d to 3f) (Robinson-Beers et al., 1992). As the body of the ovule enlarges and the funiculus elongates, the ovule begins to exhibit the effects of asymmetric growth. The larger number of cells on the convex side, relative to the concave side, indicates that this morphology results from a greater number of cell divisions on the convex side. During this process, both the nucellus and integuments curve forward and the outer integument overtakes the inner integument (Figure 3e), such that it begins to cover nucellus and the micropyle appears as a small cleft surrounded by markedly elongated cells of the outer integument (Figure 3f). At mature stage, the micropyle is closed to the funiculus, and the curvature of the funiculus strictly follows the outer integument (Figure 3g).

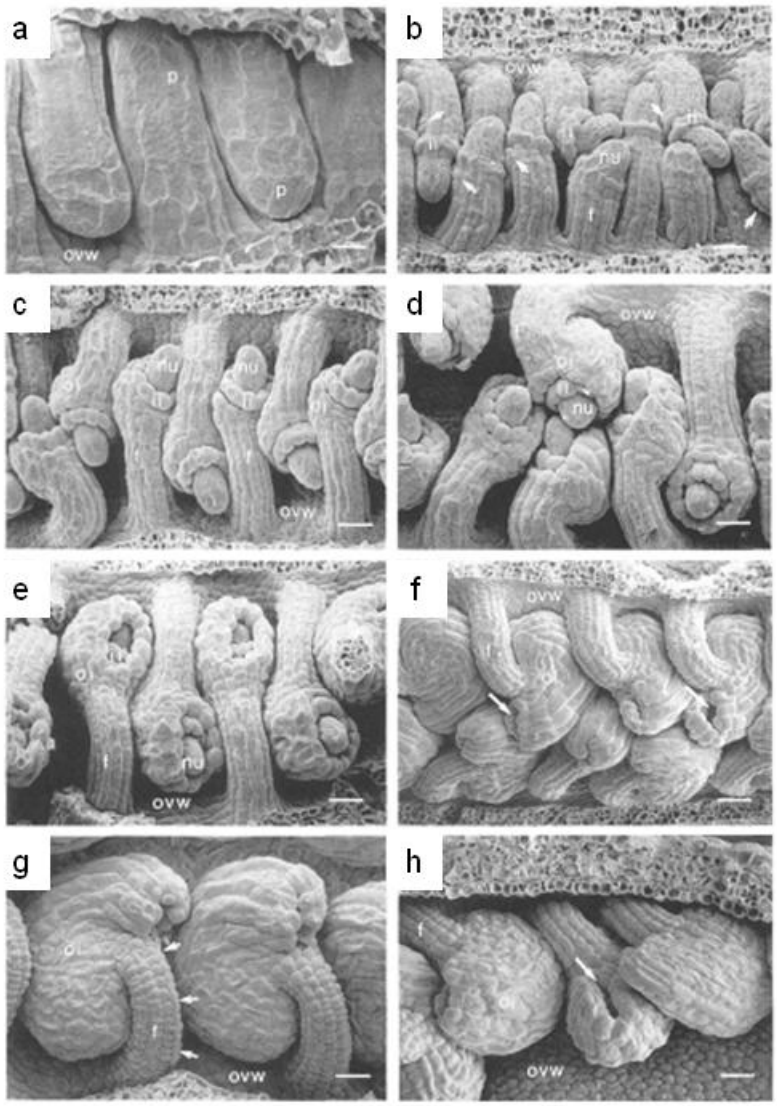


Figure 3 Integument and ovule development (from Robinson-Beers et al., 1992). Elongate ovule primordial (a) with newly initiated inner and outer integuments (b). The funiculus curves (c) and the integuments grow upward (d). The outer integument has covered both the inner integument and the nucellus (e) and both integuments completely envelop the nucellus (b). (g) and (h) views of mature ovules. f, funiculus; ii, inner integument; nu, nucellus; oi, outer integument; owv, ovary wall; p, ovule primordium.

Double fertilization

Carpels are the female reproductive unit of flowers. They enclose the ovules that wrap the female gametophyte, and they provide a screen that is penetrated only by appropriate male gametophyte. The carpels consist of a stigma, a style and an ovary joined to the floral receptacle by a short stem. The upper region of the carpels narrows into a short style that is capped by a dry stigma. Inside the style develops a core of transmitting tract cells that secrete an extra-cellular matrix that supports pollen tube growth (Smyth et al., 1990; Alvarez and Smyth, 1999). One of the primary functions of the stigma is to provide the desiccated pollen grains with sufficient water and nutrients for germination. In plants with a dry stigma surface, like Arabidopsis, hydration of foreign pollen is often inhibited (Preuss, 1995).

Soon after pollen is transferred from anther to stigma, the male gametophyte forms a pollen tube that grows through the carpel's sporophytic tissue to reach the female gametophyte. Multiple steps of guidance by the female sporophytic tissues and the female gametophyte allow directional growth of the pollen tube to the ovule (Johnson and Lord, 2006). Several mechanisms appear to be involved in pollen tube guidance, including chemo-attraction, mechanical guidance, growth stimulation, adhesion, re-orientation and competence control that enables the pollen tube to respond to the attraction signal (Higashiyama and Hamamura, 2008). However the major player responsible for pollen tube guidance in the pistil is a chemo-attractant that is still unidentified (Dresselhaus, 2006; Higashiyama and Hamamura, 2008). Studies in this decade have shown that attractants definitely exist in the

final phase of pollen tube guidance by the female gametophyte: for instance in *Torenia fournieri*, pollen tubes are attracted by a diffusible signal derived from synergids (Higashiyama et al., 1998, 2001; Higashiyama and Hamamura, 2008). After entering the embryo sac, the pollen tube ceases growth and discharges its contents into one of the two synergid cells penetrating through a structurally elaborated portion of the micropylar cell wall known as the filiform apparatus (Figure 4b). The penetrated synergid cell undergoes cell death soon before or upon pollen tube arrival. Immediately after arrival, pollen tube growth ceases, the pollen tube tip broke down, and the contents of the pollen tube, including the two sperm cells, are released rapidly into the degenerating synergid cytoplasm. Once the two sperm cells reach the female gamete, specific recognition signals are likely to take place, leading to plasmogamy (gamete membrane fusion) (Figure 4 c). Double fertilization occurs when the two sperm cells migrate to the egg and central cells and their plasma membranes fuse with the respective target cell to transport the sperm nuclei for karyogamy (van Went and Willemse, 1984; Russell, 1992, 1996; Berger et al., 2008).

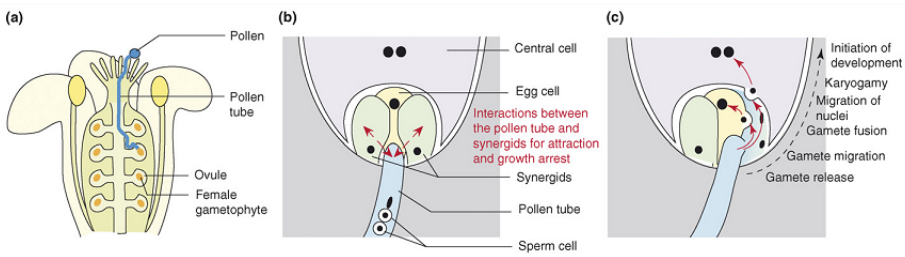


Figure 4. Double fertilization in Arabidopsis (from Berger et al., 2008). Pollen grains germinate on the stigma (a) to produce pollen tubes that grow within the pistil. Each

pollen tube, containing two sperm cells and a vegetative nucleus, is attracted by the synergids towards the ovule and is precisely guided to the micropile (b). After pollen tube arrival, direct interaction between the pollen tube and the synergids causes growth arrest of the pollen tube. The pollen tube discharges the two sperm cells into one of the two synergid cells of the embryo sac. Double fertilization follows: one sperm cell fuses with the egg cell to form the embryo and the second with the central cell to produce endosperm. Many steps, including gamete migration and fusion, nuclei migration, karyogamy, and initiation of active transcription, are required to achieve double fertilization

Embryo and endosperm development

During seed development, the fertilized egg cell develops into the embryo, the fertilized central cell develops into the endosperm, and the ovule integuments form the seed coat. These developmental events that culminate with the production of a mature seed are precisely coordinated and relatively conserved in the majority of angiosperms (Goldberg et al., 1994; Drews et al., 1998). Development of the embryo occurs in two distinct phases. A first phase of morphogenesis followed by the maturation phase. During the second phase all the processes related to the embyro's entry into metabolic quiescence and subsequent germination take place.

Following fertilization, the zygote elongates approximately three fold and divides into a large basal cell and a small apical cell (Figure 5). The apical cell and its daughters adopt an isotropic growth pattern and divide to give rise to the proper embryo. The basal cell and its daughters continue to expand longitudinally and divide transversely to produce a file of cells divided in uppermost daughter, that form hypohysis, and the remaining daughters that form the suspensor responsible of the contact with maternal tissues.

The apical cell that gives rise to the embryo undergoes two longitudinal divisions followed by a transverse division to form an eight-celled embryo. Each cell of the embryo undergoes a periclinal division generating a 16-celled embryo that continuously divides, giving rise to a globular embryo. Localized cell divisions lead to the emergence of cotyledon lobes. By the torpedo stage, the basic embryonic elements of the plant body are in place. Along

the apical–basal axis are the shoot apical meristem, cotyledons, hypocotyl, radicle and the root apical meristem.

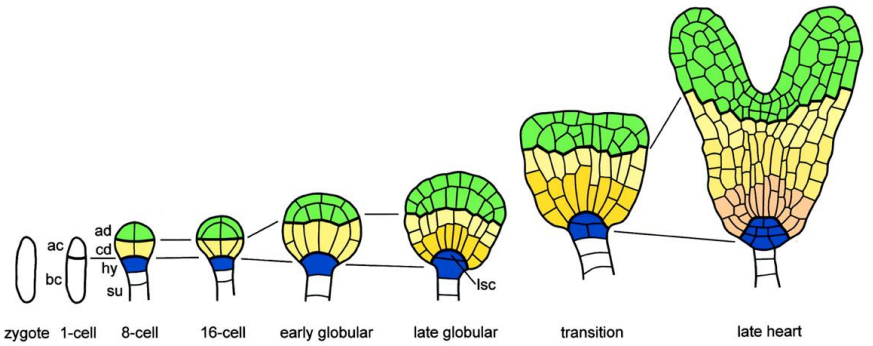


Figure 5. Schematic representation embryogenesis in Arabidopsis (from Laux et al., 2004). The zygote divides to from an embryo composed of a suspensor, that maintains contact with maternal tissues, and a proper embryo.
(ac) apical daughter cell; (ad) apical embryo domain; (bc) basal daughter cell; (cd) central embryo domain.

While one sperm cell fertilized the egg cell to form the embryo, the second sperm cell fertilized the central cell to form the endosperm. In Arabidopsis, the endosperm plays a crucial role in the control of nutrient delivery to the embryo (Hirner et al., 1998). Endosperm development is characterised by four phases: syncytial, cellularisation, differentiation and death. Endosperm development is initiated by successive divisions of the triploid cell formed upon fertilization, without cytokinesis. Therefore, during initial stages of development, the endosperm is a syncytium. Later, each nucleus becomes isolated by the development of cell walls. This process, called cellularisation, is gradual and is followed by a differentiation

of functional tissues and, eventually, cells death during seed maturation (Berger 1999; 2003).

Seed coat development

In response to fertilization, the Arabidopsis seed coat differentiates over a period of 2–3 weeks (Beeckman et al., 2000; Western et al., 2000; Windsor et al., 2000; Debeaujon et al., 2003). Cells in both layers of the outer integuments (Figure 6a, layers 1,2) and all three layers of the inner integuments (Figure 6a, layers 3–5) go through a dramatic period of growth in the first few days after fertilization through both cell division and expansion. Integument development initiates with a phase of cell proliferation followed by a phase of cell elongation. Cell proliferation is observed in the integument of mature ovules also before fertilization: the beginning of seed coat development is characterized by an increase in mitotic activity followed by a sharp decline that lead to a complete absence of cell division 4 days after pollination. The five cell layers have different fates (Figure 6c–e). Cells of the innermost layer, called the endothelium (Figure 6a, layer 5) synthesize proanthocyanidin (also known as PAs or condensed tannins), which accumulate in the central vacuole during the first week after fertilization and later oxidize, imparting a brown color to the seed coat (Debeaujon et al., 2003). On the contrary, the cells of the other two inner integument layers (Figure 6a, layers 3,4) do not appear to differentiate further and are crushed together as the seed develops (Figure 6d,e). Cells of both outer integument layers (Figure 6a, layers 1,2) accumulate amyloplasts during the growth phase (Figure 6b). Moreover the cells of the epidermal layer (Figure 6a, layer 1) synthesize and secrete a large quantity of mucilage into the apoplast. The mucilage is secret at the junction of the outer tangential and radial cell walls (Figure 6c). As mucilage deposition proceeds, the

vacuole contracts, leaving a cytoplasmic column in the center of the cell surrounded by a donut-shaped space filled with mucilage. Subsequently, a secondary cell wall is deposited and it completely fills the space occupied by the cytoplasmic column, forming the columella (Figure 6d,e). During the later stages of seed development, the cells of all seed coat layers die. The structure of the epidermal cells is preserved by the mucilage and columella, and the remaining layers are crushed together by the end of seed maturation (Figure 6e).

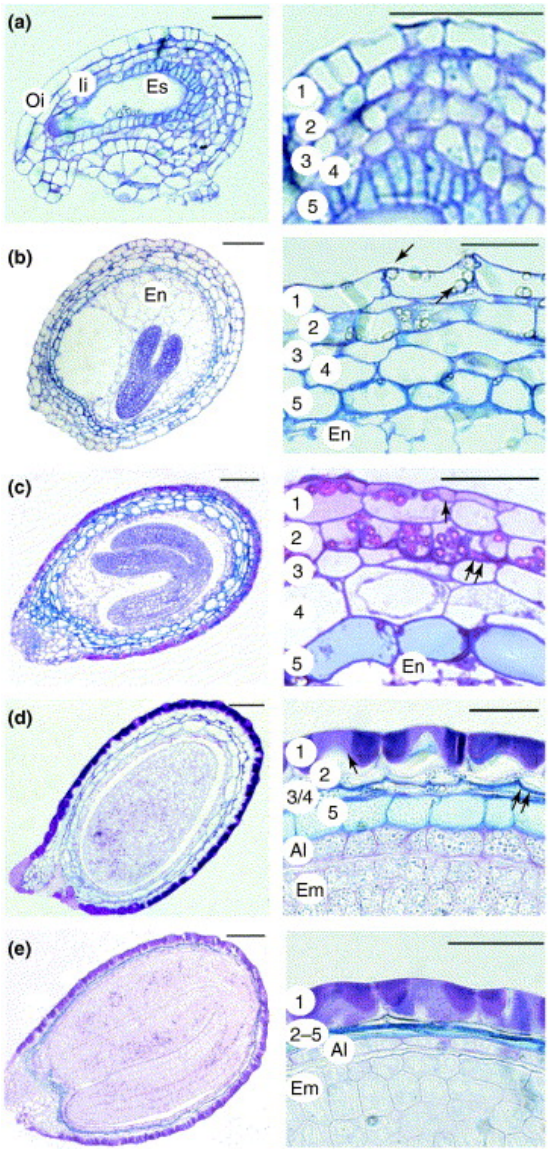


Figure 6. Ovule development (on the left) and a detail analysis of integuments development (on the right) (from Haughn and Chaudhury, 2005). The two cell layers of the ovule outer integument (a, layers 1,2) and three cell layers of the inner integument (a, layers 3–5) undergo an intensive period of growth (b) within 4 days after fertilization. Cells of individual layers differentiate (c, d) into

specialized cell types. By seed maturity (e), cells of all layers are dead and have been crushed together, except for the epidermis, the shape of which is maintained by the thick secondary cell wall of the columella.
(Al) endosperm aleurone; (Em) embryo; (En) endosperm; (Es) embryo sac; (Ii) inner integument; (Oi) outer integument.

Genetic control of proanthocyanidins accumulation

Fertilization of the female gametophyte induces the cells of the innermost layer of the integuments to produce and accumulate proanthocyanidins (PAs or condensed tannins). PAs biosynthesis starts around 1 to 2 days after fertilization (DAF) at the micropyle, and the deposition progresses in the endothelium toward the chalaza until 5 to 6 DAF (Debeaujon et al., 2003; Lepiniec et al., 2006). PAs have several functions in seeds: they act as defense against predators and pathogens (Dixon et al., 2002), increase seed coat dormancy (Debeaujon et al., 2000), and protect against UV radiation (Winkel-Shirley, 2002a). In Arabidopsis testa, PAs consist of oligomers of the flavan-3-ol 2,3-cis-epicatechin (Abrahams et al., 2003). PAs are synthesized as colourless polymers in vesicles that merge into the central vacuole.

The PAs pathway has been depicted through mutants' characterization: *transparent testa* (*tt*) and tannin-deficient mutant seeds, that present altered seed coat colour, allow pathway elucidation (Winkel-Shirley, 2002b; Abrahams et al., 2003). *BANYULS* (*BAN*) is the core gene of the PAs biosynthesis: it encode for an anthocyanidin reductase (ANR) that catalyze the formation of cis flavan-3-ols (epicatechin; Devic et al., 1999; Abrahams et al., 2002; Routaboul et al., 2006). The expression of flavonoid biosynthetic genes is regulated by several transcription factors (for review see Lepiniec et al., 2006).

The proteins required for the regulation of PAs biosynthesis are classified according to modalities of action. The first group of regulators involves TT2, TT8, and TTG1. PAs biosynthesis is

under the control of an endothelium-specific transcription complex, composed by the proteins TRANSPARENT TESTA GLABRA1 (TTG1), TRASPARENT TESTA8 (TT8) and TT2, which are necessary for *BAN* expression (Walker et al., 1999; Johnson et al., 2002; Baudry et al., 2004). These factors positively regulate *BAN* expression in the seed coat (Nesi et al., 2000; Debeaujon et al., 2001). Also the genes *TRANSPARENT TESTA1* (*TT1*) and *TRANSPARENT TESTA16* / *ARABIDOPSIS* B_{SISTER} (*TT16*/*ABS*) are necessary for PAs accumulation and normal cell morphology however they are necessary for PA accumulation in the endothelium but not in the micropyle and chalazal region defining a separate pathway for PAs accumulation in the endothelium and in the micropyle and chalazal region. Another gene involved in PAs biosynthesis is *TTG2* a zinc finger–like transcription factor of the plant-specific WRKY gene family (Johnson et al., 2002). *TTG2* is required for PA biosynthesis in the seed coat, like *TT2*, *TT8*, and *TTG1*, but it acts downstream of TTG1 in the PA pathway (Johnson et al., 2002), so TTG2 constitutes a different group of regulators. Four genes are thought to be involved in vacuolar transport of flavan- 3-ols. The *TT12* gene encodes a transporter exhibiting strong homology with putative Multidrug and Toxic Compound Extrusion (MATE) secondary transporters (Debeaujon et al., 2001). *AHA10* encodes a H+-ATPase (Baxter et al., 2005), while *TT19* encodes a GST whose mutation affects both PA and anthocyanin biosynthesis (Kitamura et al., 2004). The *tt12*, *tt19* and *aha10* mutants exhibit an aberrant vacuolar structure in endothelial cells.

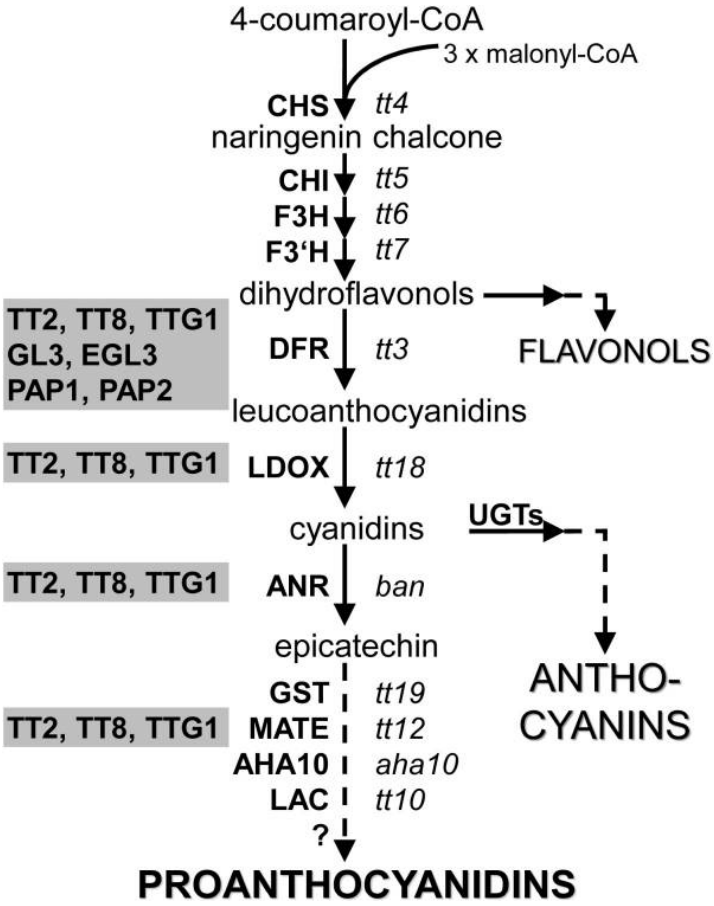


Figure 7 Simplified, schematic representation of proposed regulatory pathway for flavonoids and PAs biosynthesis (from Kleindt et al., 2010). Essential steps of the flavonoid biosynthesis leading to proanthocyanidins (PAs) in the seed are presented. Enzymes and transcriptional regulators (grey shaded) are indicated by bold, capital letters; corresponding mutant plant lines are in *italics*. Dashed arrows tag multiple steps that are not fully understood. The question mark indicates a limited knowledge of this biosynthetic step and a restricted understanding of the involvement of the associated factors.

(*ANR/BAN*) anthocyanidin reductase; (*AHA10*) P-type H^+-ATPase; (*CHS*) chalcone synthase; (*CHI*) chalcone isomerase; (*DFR*) dihydroflavonol 4-reductase; (*EGL3*) enhancer of glabra3; (*F3 H*) flavanone 3β-hydroxylase; (*F3'H*) flavonoid 3'-hydroxylase; (*GL3*) glabra3; (*GST*) glutathione S transferase; (*LAC*) laccase-like; (*LDOX*) leucoanthocyanidin dioxygenase; (*MATE*) multidrug and toxic compound extrusion-type transporter; (*PAP*) production of anthocyanin pigments; (*TT*) transparent testa; (*TTG*) transparent testa glabra; (*UGTs*) UDP dependent glycosyltransferases.

Genetic control of mucilage accumulation and release

Fertilization of the female gametophyte induces the epidermal cells of the outer ovule integument to differentiate into a specialized seed coat cell type with a unique morphology and containing large quantities of polysaccharide mucilage composed of pectin. The production of mucilage seems to be dispensable during seed development (Western et al., 2000). Seed mucilage is necessary for neither viability nor germination under normal laboratory conditions; however mucilage is essential in conditions of reduced water potential and maintaining seed viability under harsh desert conditions (Western et al., 2000; Penfield et al., 2001; Huang et al., 2007).

During seed coat formation, the cells of the external layer, the epidermal layer, synthesize and secrete large quantities of pectinaceous carbohydrate mucilage into the apoplast under the outer cell wall. Deposition of the mucilage begins specifically at the junction of the outer tangential and radial cell walls. As mucilage deposition proceedes, the vacuole contracts, leaving a cytoplasmic column in the centre of the epidermis cell, which is surrounded by a donut-shaped apoplastic space filled with mucilage. Following mucilage synthesis, a secondary cell wall is synthesized and deposited that completely fills the space occupied by the cytoplasmic column, forming the columella (Western et al., 2000). Upon contact with water, the mucilage is hydrated and released from the seed coat epidermis through rupture of the outer cell wall junctions to the radial walls. The swelling mucilage absorbs water

to form a gelatinous coating around the seed (Penfield et al., 2001).

Seed mucilage formation has been well studied and several mutants have been isolated and mapped (Western et al., 2001). Several transcription factors were shown to be involved in mucilage synthesis and seed coat development: for instance *APETALA2* (*AP2*) is required for differentiation of the epidermis and palisade layers of seed coat cells (Jofuku et al., 1994; Western et al., 2001). *TRANSPARENT TESTA GLABRA1* (*TTG1*), *ENHANCER OF GLABRA3* (*EGL3*), *TRANSPARENT TESTA8* (*TT8*), *MYB PROTEIN5* (*MYB5*) and *TRANSPARENT TESTA2* (*TT2)* form a WD40-bHLH-MYB complex that affect primarily mucilage synthesis (Koornneef, 1981; Western et al., 2001; Gonzalez et al., 2009; Li et al., 2009). This complex activates *TTG2* and *GLABRA2* (*GL2*; Koornneef, 1981; Walker et al., 1999; Western et al., 2001; Johnson et al., 2002). TTG2 and GL2 are both required for normal levels of mucilage biosynthesis. One of the roles of GL2 is to activate the transcription of the rhamnose synthase gene *MUCILAGE MODIFIED4* (*MUM4*; Usadel et al., 2004; Western et al., 2004). Another class of seed coat mucilage mutants was identified in genetic screens by normal amounts of mucilage but is fail to properly extrude when mature seeds are exposed to water. Four genes belonging to this class were identified: *MUM1* and *MUM2* (Western et al., 2001), *β-XYLOSIDASE1* (*BXL1*; Arsovski et al., 2009), and *SUBTILISIN-LIKE SERINE PROTEASE1.7* (*SBT1.7*; Rautengarten et al., 2008). Several evidences suggest that *MUM2*, *BXL1*, and *SBT1.7* are required for modifying the structure of pectin, one of the three

major polysaccharide groups of the cell wall, that maintain the mechanical properties of the wall (Carpita and Gibeaut 1993; Cosgrove, 1997). The third pathway that control mucilage release is defined by the transcription factor *MYB61*. This pathway appears to act in an independent pathway during mucilage release since it is not regulated either by MUM1 or TTG1 complex (Penfield et al., 2001; Arsovski et al., 2009; Arsovski et al., 2010).

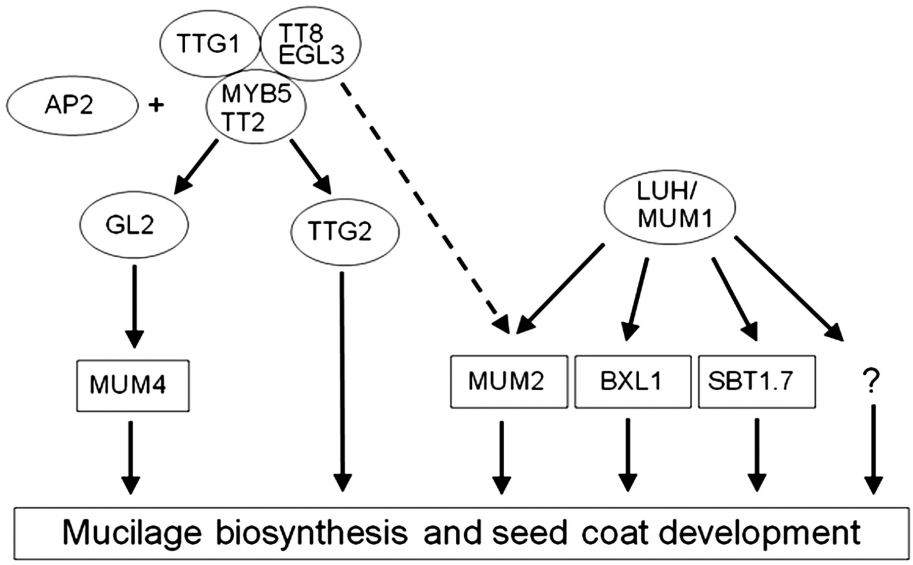


Figure 8 Proposed regulatory pathways for seed coat mucilage biosynthesis (from Huang et al., 2011). TTG1, EGL3/TT8, and MYB5/TT2 form a protein complex, which regulates *GL2* and *TTG2* expression. LUH/MUM1 is independent of the other transcription factors and can activate *MUM2*, *BXL1* and *SBT1.7*. If these protein, MUM2, BXL1 and SBT1.7, are also regulated by AP2 and/or the MYB5/TT2-EGL3/TT8-TTG1 complex is still unknown.

References

Abrahams, S., Lee, E., Walker, A.R., Tanner, G.J., Larkin, P.J., and Ashton, A.R. (2003). The *Arabidopsis TDS4* gene encodes leucoanthocyanidin dioxygenase (*LDOX*) and is essential for proanthocyanidin synthesis and vacuole development. Plant Journal **35**, 624-636

Abrahams, S., Tanner, G.J., Larkin, P.J., and Ashton, A.R. (2002). Identification and biochemical characterization of mutants in the proanthocyanidin pathway in Arabidopsis. *Plant Physiology* **130**, 561-576.

Alvarez, J., and Smyth, D. R. (1999). *CRABS CLAW* and *SPATULA*, two *Arabidopsis* genes that control carpel development in parallel with *AGAMOUS*. *Development* **126**, 2377-2386.

Arsovski, A.A., Haughn, G.W., Western, T.L. (2010). Seed coat mucilage cells ofArabidopsis thaliana as a model for plant cell wall research. *Plant Signal Behav.* **5** , 796–801.

Arsovski, A.A., Popma, T.M., Haughn, G.W., Carpita, N.C., McCann, M.C., and Western TL. (2009). AtBXL1 encodes a bifunctional β-d-xylosidase/α-l-arabinofuranosidase required for pectic arabinan modification in Arabidopsis mucilage secretory cells. *Plant Physiol* **150**, 1219–1234.

Baudry, A., Heim, M.A., Dubreucq, B., Caboche, M., Weisshaar, B. and Lepiniec, L. (2004) TT2, TT8, and TTG1 synergistically specify the expression of *BANYULS* and proanthocyanidin biosynthesis in *Arabidopsis thaliana*. *Plant Journal* **39**, 366–380.

Baxter, I.R., Young, J.C., Armstrong, G., Foster, N., Bogenschutz, N., Cordova, T., Peer, W.A., Hazen, S.P., Murphy, A.S., and Harper, J.F. (2005). A plasma membrane H^+-ATPase is required for the formation of proanthocyanidins in the seed coat endothelium of Arabidopsis thaliana. *Proceedings of the National Academy of Science USA* **102**, 2649– 2654.

Beeckman, T., De Rycke, R., Viane, R., and Inzé, D. (2000). Histological study of seed coat development in *Arabidopsis thaliana*. *J Plant Res* **113**, 139–148.

Berger, F. (1999). Endosperm development. *Curr. Opin. Plant Biol*. **2**, 28–32.

Berger, F. (2003). Endosperm, the crossroad of seed development. *Curr. Opin. Plant Biol*. **6**, 42–50.

Berger, F., Hamamura, Y., Ingouff, M., and Higashiyama, T. (2008). Double fertilization—caught in the act. *Trends Plant Sci* **13**, 437–443.

Carpita, N.C., and Gibeaut, D.M. (1993). Structural models of primary cell walls in flowering plants: consistency of molecular structure with the physical properties of the walls during growth. *Plant Journal* **3**, 1–30.

Christensen, C.A., Subramanian, S., and Drews, G.N. (1998). Identification of gametophytic mutations affecting female gametophyte development in *Arabidopsis*. *Dev. Biol.* **202**, 136–151.

Cosgrove, D.J. (1997). Assembly and enlargement of the primary cell wall in plants. *Annu Rev Cell Dev Biol* **13**, 171–201.

Debeaujon, I., Léon-Kloosterziel, K.M., and Koornneef, M. (2000). Influence of the testa on seed dormancy, germination and longevity in *Arabidopsis*. *Plant Physiol.* **122**, 403–413.

Debeaujon, I., Nesi, N., Perez, P., Devic, M., Grandjean, O., Caboche, M., and Lepiniec, L. (2003). Proanthocyanidin-Accumulating Cells in Arabidopsis Testa: Regulation of Differentiation and Role in Seed Development. *Plant Cell* **15**, 2514-2531.

Debeaujon, I., Peeters, A.J.M., Léon-Kloosterziel, K.M., and Koornneef, M. (2001). The *TRANSPARENT TESTA12* gene of Arabidopsis encodes a multidrug secondary transporter–like protein required for flavonoid sequestration in vacuoles of the seed coat endothelium. *Plant Cell* **13**, 853–872.

Devic, M., Guilleminot, J., Debeaujon, I., Bechtold, N., Bensaude, E., Koornneef, M., Pelletier, G., and Delseny, M. (1999). The *BANYULS* gene encodes a DFR-like protein and is a marker of early seed coat development. *Plant Journal* **19**, 387–398.

Dixon, R.A., Achnine, L., Kota, P., Liu, C.J., Reddy, M.S.S., and Wang, L.J. (2002). The phenylpropanoid pathway and plant defence - a genomics perspective. *Molecular Plant Pathology* **3**, 371-390.

Dresselhaus, T. (2006). Cell–cell communication during double fertilization. *Curr. Opin. Plant Biol*. **9**, 41–47.

Drews G.N., and Koltunow, A.M.G. (2011). The Female Gametophyte. *The Arabidopsis Book* 9: e0155. doi:10.1199/tab.0155.

Drews, G.N., Lee, D., and Christensen, C.A. (1998). Genetic analysis of female gametophyte development and function. *Plant Cell* **10**, 5-17.

Fan, C., Xing, Y., Mao, H., Lu, T., Han, B., Xu, C., et al. (2006). GS3, a major QTL for grain length and weight and minor QTL for grain width and thickness in rice, encodes a putative transmembrane protein. *Theor. Appl. Genet.* **112**, 1164–1171.

Gegas, V.C., Nazari, A., Griffiths, S., Simmonds, J., Fish, L., Orford, S., Sayers, L., Doonan, J.H., and Snape, J.W. (2010). A genetic framework for grain size and shape variation in wheat. *Plant Cell* **22**, 1046–1056.

Goldberg, R.B., Depaiva, G., and Yadegari, R. (1994). Plant embryogenesis—zygote to seed. *Science* **266**, 605–614.

Gonzalez, A., Mendenhall, J., Huo, Y., and Lloyd, A. (2009). TTG1 complex MYBs, MYB5 and TT2, control outer seed coat differentiation. *Dev Biol* **325**, 412–421.

Gross-Hardt, R., Lenhard, M., and Laux, T. (2002). WUSCHEL signaling functions in interregional communication during Arabidopsis ovule development. *Genes Dev.* **16**, 1129–1138.

Harper, J.L., Lovell, P.H., and Moore, K.G. (1970). The shapes and sizes of seeds. *Annu. Rev. Ecol. Syst.* **1**, 327-356.

Haughn, G.W., and Chaudhury, A. (2005). Genetic analysis of seed coat development in *Arabidopsis*. *Trends in Plant Science* **10**, 472-477.

Higashiyama, T., and Hamamura, Y. (2008). Gametophytic pollen tube guidance. *Sex. Plant Reprod.* **21**, 17-26.

Higashiyama, T., Kuroiwa, H., Kawano, S., and Kuroiwa, T. (1998). Guidance in vitro of the pollen tube to the naked embryo sac of torenia fournieri. *Plant Cell* **10**, 2019–2032.

Higashiyama, T., Yabe, S., Sasaki, N., Nishimura, Y., Miyagishima, S., Kuroiwa, H., and Kuroiwa, T. (2001). Pollen tube attraction by the synergid cell. *Science* **293**, 1480–1483.

Hirner, B., Fischer, W.N., Rentsch, D., Kwart, M., and Frommer, W.B. (1998). Developmental control of H^+/amino acid permease gene expression during seed development of Arabidopsis. *Plant Journal* **14**, 535–544.

House, C., Roth, C., Hunt, J., and Kover, P.X. (2010), Paternal effects in Arabidopsis indicate that offspring can influence their own size. *Proc Biol Sci* **277**, 2885–2893.
Huang, Z., Boubriak, I., Osborne, D.J., Dong, M., and Gutterman, Y. (2007). Possible role of pectin-containing mucilage and dew in reairing embryo DNA of seeds adapted to desert conditions. *Annals of Botany,* **101**, 277-283.
Huang, J., Debowles, D., Esfandiari, E., Dean, G., Carpita, N.C., and Haughn, G.W. (2011). The Arabidopsis transcription factor LUH/MUM1 is required for extrusion of seed coat mucilage. *Plant Physiol* **156**, 491–502.
Jacobson, D. J. (1998). Persistent, systemic, asymptomatic infections of Albugo. *Can. J. Bot. Revue Canadienne De Botanique* **76**, 739–750.
Jofuku, K.D., den Boer, B.G., Van Montagu, M., and Okamuro, J.K. (1994). Control of *Arabidopsis* flower and seed development by the homeotic gene APETALA2. *Plant Cell* **6**, 1211–1225.
Johnson, M. A. and Lord, E. M. (2006). Extracellular guidance cues and intracellular signaling pathways that direct pollen tube growth. In *The Pollen Tube: A Cellular and Molecular Perspective* **3** (ed. R. Malho), pp. 223-242. Heidelberg: Springer.
Johnson, C.S., Kolevski, B., Smyth, D.R. (2002). *TRANSPARENT TESTA GLABRA2*, a trichome and seed coat development gene of *Arabidopsis*, encodes a WRKY transcription factor. *Plant Cell* **14**, 1359–1375.
Kasahara, R.D., Portereiko, M.F., Sandaklie-Nikolova, L., Rabiger, D.S., and Drews, G.N. (2005). *MYB98* is required for pollen tube guidance and synergid cell differentiation in *Arabidopsis*. *Plant Cell* **17**, 2981–2992.
Kitamura, S., Shikazono, N., and Tanaka, A. (2004). *TRANSPARENT TESTA 19* is involved in the accumulation of both anthocyanins and proanthocyanidins in Arabidopsis. *Plant Journal* **37**, 104–114.
Kleindt, C.K., Stracke, R., Mehrtens, F., and Weisshaar, B. (2010). Expression analysis of flavonoid biosynthesis genes during Arabidopsis thaliana silique and seed development with a primary focus on the proanthocyanidin biosynthetic pathway. *BMC Research Notes* **3**: 255.
Koornneef M. (1981). The complex syndrome of *ttg* mutants. *Arabidopsis Information Service* **18**, 45–51.
Krannitz, P.G., Aarssen, L.W., and Dow, J.M. (1991). The effects of genetically based differences in seed size on seedling survival in *Arabidopsis thaliana* (Brassicacea). *Amer. J. Bot*., **78**, 446- 450.
Laux, T., Wurschum, T., and Breuninger, H. (2004) Genetic regulation of embryonic pattern formation. *Plant Cell*, **16** Suppl., S190–S202.
Lepiniec, L., Debeaujon, I., Routaboul, J.M., Baudry, A., Pourcel, L., Nesi, N., and Caboche, M. (2006). Genetics and biochemistry of seed flavonoids. *Annual Review of Plant Biology* **57**, 405–430.
Li, S.F., Milliken, O.N., Pham, H., Seyit, R., Napoli, R., Preston, J., Koltunow, A.M., and Parish, R.W. (2009). The *Arabidopsis* MYB5 transcription factor regulates mucilage synthesis, seed coat development, and trichome morphogenesis. *Plant Cell* **21**, 72–89.
Manning, P., Houston, K., and Evans, T. (2009) Shifts in seed size across experimental nitrogen enrichment and plant density gradients. *Basic Appl. Ecol.* **10**, 300–308.

Mansfield, S.G., Briarty, L.G., and Erni, S. (1991). Early embryogenesis in Arabidopsis thaliana. I. The mature embryo sac. *Canadian Journal of Botany* **69**, 447-460.
Manzaneda, A., Rey, P., and Alcantara, J. (2009). Conflicting selection on diaspore traits limits the evolutionary potential of seed dispersal by ants. *J. Evol. Biol.* **22**, 1407–1417.
McCormick, S. (1993). Male gametophyte development. *Plant Cell* **5**, 1265-1275.
McCormick, S. (2004). Control of male gametophyte development. *Plant Cell* **16**, Suppl: S142-S153.
Moles, A.T., Ackerly, D.D., Webb, C.O., Tweddle, J.C., Dickie, J.B., Pitman, A.J., and Westoby, M. (2005) Factors that shape seed mass evolution. *Proceedings of the National Academy of Science USA* **102**, 10540–10544.
Nesi, N., Debeaujon, I., Jond, C., Pelletier, G., Caboche, M., and Lepiniec, L. (2000). The *TT8* gene encodes a basic helix-loop-helix domain protein required for expression of *DFR* and *BAN* Genes in *Arabidopsis* siliques. *Plant Cell* **12**,1863-1878
Nowack, M.K., Ungru, A., Bjerkan, K.N., Grini, P.E., and Schnittger, A. (2010). Reproductive cross-talk: seed development in flowering plants. *Biochem Soc Trans* **38**, 604–612.
Orsi, C. H., and Tanksley, S. (2009). Natural variation in an ABC transporter gene associated with seed size evolution in tomato series. *PLoS Genet*. 5 e1000347. doi:10.1371/journal.pgen.1000347.
Penfield, S., Meissner, R.C., Shoue, D.A., Carpita, N.C., and Bevan, M.W. (2001). *MYB61* is required for mucilage deposition and extrusion in the Arabidopsis seed coat. *Plant Cell* **13**, 2777-2791.
Preuss, D. (1995). Being fruitful: Genetics of reproduction in Arabidopsis. *Trends Genet*. **11,** 146-153.
Rautengarten, C., Usadel, B., Neumetzler, L., Hartmann, J., Büssis, D., and Altmann, T. (2008). A subtilisin-like serine protease essential for mucilage release from *Arabidopsis* seed coats. *Plant Journal* **54**, 466–480.
Robinson-Beers, K., Pruitt, R.E., and Gasser, C.S. (1992). Ovule development in wild-type Arabidopsis and two female-sterile mutants. *Plant Cell* **4,** 1237-1249.
Routaboul, J.M., Kerhoas, L., Debeaujon, I., Pourcel, L., Caboche, M., Einhorn, J., and Lepiniec, L. (2006). Flavonoid diversity and biosynthesis in seed of *Arabidopsis thaliana*. *Planta* **224**, 96–107.
Russell, S.D. (1992). Double fertilization. *Int. Rev. Cytol.* **140**, 357–388.
Russell, S.D. (1996). Attraction and transport of male gametes for fertilization. *Sex. Plant Reprod.* **9**, 337–342.
Schneitz, K., Hülskamp, M., and Pruitt, R.E. (1995). Wild-type ovule development in *Arabidopsis thaliana*: a light microscope study of cleared whole-mount tissue. *Plant Journal* **7**, 731-749.
Silvertown, J. (1989). The paradox of seed size and adaptation. *Trends Ecol. Evol.* **4**, 24–26.
Smyth, D.R., Bowman, J.L., and Meyerowitz, E.M. (1990). Early flower development in Arabidopsis. *Plant Cell* **2**, 755-767.

Song, X., Huang, W., Shi, M., Zhu, M., and Lin, H. (2007). A QTL for rice grain width and weight encodes a previously unknown RING- type E3 ubiquitin ligase. *Nat. Genet.* **39**, 623–630.
Usadel, B., Kuschinsky, A.M., Rosso, M.G., Eckermann, N., and Pauly, M. (2004). RHM2 is involved in mucilage pectin synthesis and is required for the development of the seed coat in Arabidopsis. *Plant Physiol* **134**, 286–295.
van Went, J.L., and Willemse, M.T.M. (1984). Fertilization. In Embryology of Angiosperms, B. Johri, ed (Berlin: Springer-Verlag), pp. 273–318.
Walker, A. R., Davison, P. A., Bolognesi-Winfield, A. C., James, C. M., Srinivasan, N., Blundell, T. L., Esch, J. J., Marks, M. D. and Gray, J. C. (1999). The *TRANSPARENT TESTA GLABRA1* locus, which regulates trichome differentiation and anthocyanin biosynthesis in *Arabidopsis*, encodes a WD40 repeat protein. *Plant Cell* **11**, 1337-1349.
Western, T.L., Burn, J., Tan, W.L., Skinner, D.J., Martin-McCaffrey, L., Moffatt, B.A., and Haughn, G.W. (2001). Isolation and characterization of mutants defective in seed coat mucilage secretory cell development in *Arabidopsis*. *Plant Physiol* **127**, 998-1011.
Western, T.L., Skinner, D.J., and Haughn, G.W. (2000). Differentiation of mucilage secretory cells of the *Arabidopsis* seed coat. *Plant Physiol* **122**, 345-356.
Western, T.L., Young, D.S., Dean, G.H., Tan, W.L., Samuels, A.L., and Haughn, G.W. (2004). *MUCILAGE-MODIFIED4* encodes a putative pectin biosynthetic enzyme developmentally regulated by *APETALA2*, *TRANSPARENT TESTA GLABRA1*, and *GLABRA2* in the *Arabidopsis* seed coat. *Plant Physiol* **134**, 296-306.
Westoby, M., Falster, D.S., Moles, A.T., Vesk, P.A., and Wright, I.J. (2002). Plant ecological strategies: some leading dimensions of variation between species. *Annual Review of Ecology and Systematics* **33**, 125-159.
Westoby, M., Leishman, M., and Lord, J. (1996). Comparative ecology of seed size and dispersal. *Phil. Trans R. Soc. Lond. B* **351**, 1309–1318.
Windsor, J.B., Symonds, V.V., Mendenhall, J., and Lloyd, A.M. (2000). *Arabidopsis* seed coat development: morphological differentiation of the outer integument. *Plant Journal* **22**, 483–493.
Winkel-Shirley, B. (2002a). Biosynthesis of flavonoids and effects of stress. *Curr. Opin. Plant Biol.* **5**, 218–223.
Winkel-Shirley, B. (2002b). A mutational approach to dissection of flavonoid biosynthesis in Arabidopsis. In Phytochemistry in the Genomics and Post-Genomics Eras, J.T. Romeo and R.A. Dixon, eds (Oxford, UK: Pergamon-Elsevier Science), pp. 95–110.
Yadegari, R., and Drews, G.N. (2004). Female gametophyte development. *Plant Cell* **16**, Suppl, S133–141.

Chapter 1

The MADS box genes *SEEDSTICK* and *ARABIDOPSIS* B_{sister} play a maternal role in fertilization and seed development

Adapted from Mizzotti et al., 2011

This work was published on The Plant Journal
Article first published online: 16 JAN 2012
DOI: 10.1111/j.1365-313X.2011.04878.x

Summary

The haploid generation of flowering plants develops within the sporophytic tissues of the ovule. After fertilization, the maternal seed coat develops in a coordinated manner with formation of the embryo and endosperm. In the *arabidopsis bsister* (*abs*) mutant, the endothelium, which is the most inner cell layer of the integuments that surround the haploid embryo sac, does not accumulate proanthocyanidins and the cells have an abnormal morphology. However, fertility is not affected in *abs* single mutants. *SEEDSTICK* regulates ovule identity redundantly with *SHATTERPROOF 1* (*SHP1*) and *SHP2* while a role in the control of fertility was not reported previously. Here we describe the characterization of the *abs stk* double mutant. This double mutant develops very few seeds due to both a reduced number of fertilized ovules and seed abortions later during development. Morphological analysis revealed a total absence of endothelium in this double mutant. Additionally, massive starch accumulation was observed in the embryo sac. The phenotype of the *abs stk* double mutant highlights the importance of the maternal-derived tissues, particularly the endothelium, for the development of the next generation.

Introduction

Fertilization and seed formation are key events in the lifecycle of flowering plants. The seed can be considered as a functional unit required for the protection and propagation of the offspring represented by the embryo. The first step in seed development is the formation of ovules. In Arabidopsis, ovule primordia arise from the placenta at stage 8 of flower development, and differentiation is completed at stage 13 (Smyth et al., 1990), when the embryo sac is mature and can be fertilized (Schneitz et al., 1995). The MADS box gene *SEEDSTICK* (*STK*), which encodes a key regulator of ovule development, redundantly controls ovule identity, together with *SHATTERPROOF 1* (*SHP1*) and *SHP2* (Pinyopich et al., 2003). In the *stk shp1 shp2* triple mutant, integuments are converted into carpelloid structures and female gametophyte development is arrested just after megasporogenesis (Brambilla et al, 2007; Battaglia et al., 2008). Furthermore, the funiculus of *stk* single mutant ovules is larger than wild-type, and the mature seeds do not detach from the silique once they are mature (Pinyopich et al., 2003). Recently, we also showed that STK and SEPALLATA 3 (SEP3) together regulate the reproductive meristem (REM) transcription factor gene *VERDANDI* (*VDD*), which controls cell identity in the female gametophyte (Matias-Hernandez et al., 2010).

The functional role of integuments during ovule and seed development has been investigated for many years. Characterization of several Arabidopsis mutants highlighted the

role of integuments in many steps of ovule and seed development (for review see Bencivenga et al., 2011). These data support the possibility of an interaction between the ovule integuments and the developing gametophyte, as well as between the seed coat and the fertilization products (for review, see Nowack et al., 2010). However, it is still not clear how communication between the mother plant and the next generation is established, and what the messengers are. The existence of an interaction between ovule integuments and the developing embryo sac has been proposed on the basis of sporophytic ovule mutants, which show defects in embryo sac development (for review, see Bencivenga et al., 2011). For example, the Arabidopsis *inner no outer* (*ino*) mutant develops a normal inner integument but lacks the outer integument, and megagametogenesis is impaired in this sporophytic mutant (Christensen et al., 1997; Schneitz et al., 1997). Another sporophytic Arabidopsis mutant with gametophytic defects is *aintegumenta* (*ant*). In this mutant, the integuments are reduced or absent, and the embryo sac is not able to develop (Elliott et al., 1996; Klucher et al., 1996; Schneitz et al., 1997).

When double fertilization takes place, one sperm cell fertilizes the egg cell, giving rise to the embryo, and the other fertilizes the diploid central cell, producing the triploid endosperm. In response to fertilization, the ovule integuments differentiate into the seed coat. The seed coat provides a protected environment for embryo development and creates a barrier to prevent damage induced by external factors such as UV radiation or pathogens (Haughn and Chaudhury, 2005). The seed coat of Arabidopsis consists of five

cell layers: two originate from the outer integument, and the others derive from the inner integument. The innermost layer, the endothelium, develops from the inner integument by periclinal divisions at the four-nuclear embryo sac stage (Schneitz et al., 1995). Upon fertilization, proanthocyanidins are produced in the endothelium, and their oxidation is responsible for the brown colour of Arabidopsis seeds (Debeaujon et al., 2003). At the torpedo stage of embryo development, the endothelium cell layer begins to break down as the cellular endosperm expands (Andème Ondzighi et al., 2008).

Flavonoid biosynthesis in the innermost layer of the seed coat is an important aspect of seed coat differentiation. Screens for seed pigmentation phenotypes have lead to identification of several genes involved in flavonoid biosynthesis. Some of the mutants that were identified map to the *TRANSPARENT TESTA 16* (*TT16*) locus, which encodes the ARABIDOPSIS B_{sister} (ABS) MADS domain protein. ABS is necessary for proanthocyanidin accumulation in the endothelium of the seed coat, with the exception of the chalaza/micropyle area. Detailed morphological analysis of the endothelium in the *abs* mutant revealed that the cells of this layer had an altered morphology, with a parenchymal appearance and occasionally flattening, suggesting loss of cell identity. Despite these morphological observations, ovule function did not appear to be affected (Nesi et al., 2002).

Recently, an important role in the transport of nutrients has been proposed for the seed coat. Nutrients move centripetally from the

outer to the inner integuments via the apoplast to the endosperm and to the embryo. In this process, the endothelium plays an important role in protecting and nourishing the embryo (Stadler et al., 2005; Morley-Smith *et al.*, 2008).

Here we describe a new function for the Arabidopsis MADS domain transcription factor-encoding genes *STK* and *ABS*. We describe the role of STK and ABS in the maternal control of endothelium formation, as the *abs stk* double mutant completely lacks endothelium. Interestingly, the absence of endothelium is responsible for defects in the female gametophyte, reduced fertilization and defects during seed formation. Altogether, these defects lead to a severely reduced seed set. Our data show that the endothelium has a fundamental function in the interaction between the maternally derived integuments and the next generation which is protected by this sporophytic tissue.

Results

STK and ABS play a maternal role in ovule and seed development

Protein interaction studies showed that a MADS box protein complex comprising ABS, SEP3 and STK was formed in yeast (Kaufmann et al., 2005). Furthermore, *in situ* hybridization experiments revealed that *ABS* and *STK* mRNAs are both present in the innermost integument layer, the endothelium (Figure 1). Therefore, to identify unknown functions for STK and to investigate genetic and molecular interactions between ABS and STK, the *abs-6 stk-2* double mutant was generated. Both single mutants are fully fertile, but the *abs stk* double mutant showed a drastic reduction in fertility due to defects during ovule and seed formation (Figure 2).

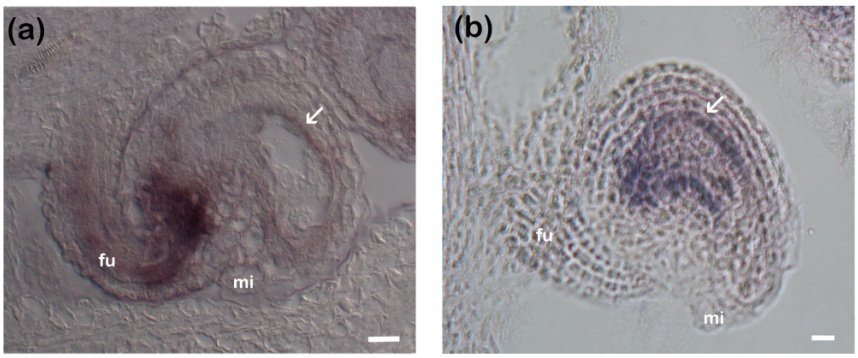


Figure 1. *In situ* hybridization. (a) Wild-type mature ovule: *STK* mRNA is present in the endothelium (white arrow). (b) Wild-type mature ovule: *ABS* is clearly expressed in the endothelium (white arrow). mi, micropyle; fu, funiculus. Scale bars = 20 µm.

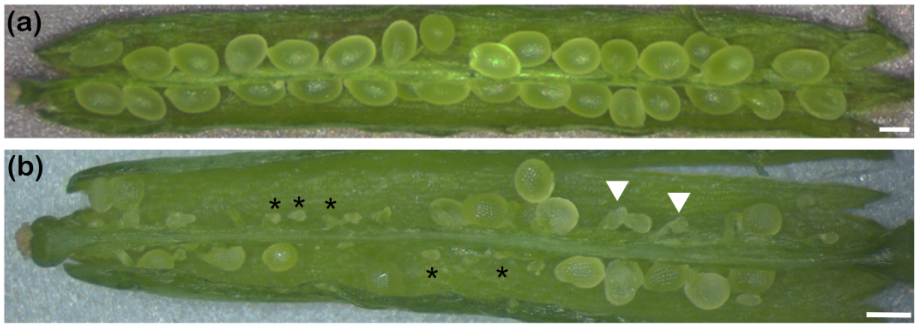


Figure 2. Wild-type and *abs stk* double mutant siliques. (a) Wild-type silique showing full seed set. (b) Silique of an *abs stk* double mutant containing aborted ovules (asterisk) and aborted seeds (arrowheads). Scale bars = 200 µm.

The ovules of the *stk* single mutant have bigger and longer funiculi, and upon fertilization the mature seeds are smaller than wild-type and do not detach from siliques (Pinyopich et al., 2003). The cells forming the endothelium in the *abs* mutant are flatter compared with wild-type, and proanthocyanidins are not synthesized in this integument layer upon fertilization (Nesi et al., 2002). However, neither ovule abortions nor seed arrest were observed in *abs* and *stk* single mutants (Nesi et al., 2002; Pinyopich et al., 2003). This suggests that the ovule and seed abortions observed in the *abs stk* double mutant are linked to the concomitant lack of STK and ABS activities.

As the seed phenotypes of *abs* and *stk* single mutants have a sporophytic origin (Nesi et al., 2002; Pinyopich et al., 2003), genetic experiments were performed to assess whether the *abs stk* double mutant phenotype also had a sporophytic nature. In the *abs*

stk double mutant, we observed that 643 ovules of the 1169 analysed (55%) aborted prior to fertilization. To quantify the seed abortion phenotype, we analysed siliques of wild-type and *abs stk* plants at various days after pollination (DAP) and counted the number of seeds that developed from the fertilized ovules (Table 1). The embryos were staged as previously described by Hsu et al. (2010). This analysis revealed that 98.7% of the developing embryos in wild-type siliques at 5 DAP were at early heart stage, but only 66.8% of the embryos had reached this stage of development in the *abs stk* mutant. At 13 DAP, only 58.1% of the *abs stk* developing embryos had reached the bent cotyledon stage, whereas 93.5% were at this stage of development in the wild-type. Finally, when the siliques were mature, 98.5% of the seeds of wild-type plants had completed their development, compared with only 24.4% in the *abs stk* double mutant. This analysis was also performed in the *abs* and *stk* single mutants, and, as expected, no differences were observed compared to wild-type (Table 1).

Table 1.
Ovule abortions and developing seeds in wild type and *abs*, *stk*, *abs stk* mutants

	Number of siliques analysed	Ovule abortions (Total ovules)	Total developing seeds (Total ovules)	Percentage	Total developing seeds (Fertilized ovules)	Percentage
0 DAP WT	24	60 (1149)		5.2%		
0 DAP *abs stk*	26	643 (1169)		55%		
0 DAP *abs*	24	43 (1081)		4%		
0 DAP *stk*	24	52 (1032)		5%		
5 DAP WT	12		512 (548)	93.4%	512 (519)	98.7%
5 DAP *abs stk*	24		326 (1085)	30%	326 (488)	66.8%
5 DAP *abs*	12		479 (503)	95.2%	479 (483)	99.2%
5 DAP *stk*	12		538 (577)	93.2%	538 (548)	98.2%
13 DAP WT	12		603 (645)	93.5%	603 (645)	93.5%
13 DAP *abs stk*	24		282 (1077)	26.2%	282 (485)	58.1%
13 DAP *abs*	12		566 (594)	95.3%	566 (570)	99.3%
13 DAP *stk*	12		585 (628)	93.2%	585 (597)	98%
Mature WT	12		592 (634)	93.4%	592 (601)	93.4%
Mature *abs stk*	24		120 (1092)	11%	120 (491)	24.4%
Mature *abs*	12		548 (593)	92.4%	548 (569)	96.3%
Mature *stk*	12		512 (560)	91.4%	512 (532)	96.2%

Furthermore, reciprocal crosses confirmed that these *abs stk* double mutant phenotypes are sporophytically controlled (Table S1). The role of STK and ABS in embryo and endosperm development was tested using a genetic approach: double heterozygous *abs/ABS stk/STK* plants were pollinated with *abs stk* homozygous double mutant pollen. Within the progeny of this cross, the *abs* and *stk* mutant alleles segregate in the embryo and endosperm, but the sporophytically derived seed coat was heterozygous for both genes. In segregating progeny, 25% of the seeds are expected to have embryo and endosperm homozygous for both *abs* and *stk*, which allowed us to analyse the role of STK and ABS in embryo and endosperm development regardless of their role in the integuments. As a control, we pollinated double heterozygous *abs/ABS stk/STK* plants with wild-type pollen. When

pollinating the *abs/ABS stk/STK* plants with *abs stk* homozygous double mutant pollen or wild-type pollen, we observed normal seed set, suggesting that the observed defects in the *abs stk* double mutant are sporophytically determined. Furthermore, these crosses demonstrate that the ABS and STK MADS domain proteins play a fundamental role, even before fertilization, in the molecular interaction between the integuments and the female gametophyte. After fertilization, they control communication between the seed coat and the fertilization products, i.e. the embryo and the endosperm.

To further investigate later seed developmental stages, we performed a germination assay. We tested seeds from *abs* and *stk* single mutant plants and those obtained from self fertilization of a plant heterozygous for both mutant alleles. As mentioned above, more than 90% of seeds develop normally in single mutant plants, but the percentage of mature seeds was only 11% in the *abs stk* double mutant (Table 1). The germination assay (Table 2) showed that seeds obtained from the single mutants, heterozygous double mutant and wild-type plants all had a germination rate of approximately 85%, whereas 76.7% of the *abs stk* double mutant seeds germinated. The small difference in germination rate between the double mutant seeds and the other genotypes is most likely due to the fact that some of the mature *abs stk* double mutant seeds were blocked at a very late stage of development, and even though morphologically indistinguishable, should not be considered as mature seeds. We assume that those *abs stk* double mutant

seeds that normally complete their development are able to germinate like wild-type seeds.

Table 2.
Total mature seeds developed and germination assay in wild type, *abs*, *stk*, *abs/ABS stk/STK*, and *abs stk*.

	Total Mature Seeds (Total Ovules)	Percentage	Germinated Seeds (Total Seeds)	Percentage
WT	592 (614)	96.4%	642 (733)	87.5%
abs	548 (593)	92.4%	504 (580)	86.9%
stk	512 (560)	91.4%	485 (592)	81.9%
abs/ABS stk/STK	552 (570)	96.8%	630 (726)	86.8%
abs stk	120 (1092)	11%	674 (879)	76.7%

Loss of the endothelium layer in the *abs stk* double mutant causes fertilization defects

To further investigate the defects that lead to the observed ovule and seed phenotypes in the *abs stk* double mutant, detailed histological, genetic and molecular analyses were performed. In the wild-type (Figure 3a) and *stk* and *abs* single mutants (Figure S1), ovule integuments and seed coat are composed of five layers. The mature ovule integuments and seed coats of *abs stk* double mutants are composed of four layers. Morphological analysis based on the shape of the cells showed that the innermost layer, the endothelium, was missing from the inner integument (Figure 3b). In addition, the remaining four integument layers showed an irregular shape compared to wild-type and the single mutants (Figure S1). To investigate how the absence of the endothelium in *abs stk* ovules could cause ovule sterility, the fertilization process and female gametophyte formation were

analysed in detail. In Arabidopsis, the mature embryo sac comprises seven cells: three antipodal cells, one diploid central cell, and one egg cell surrounded by two synergids (Mansfield et al., 1991). The fertilization process begins with hydration of the pollen grains and subsequent germination on the stigmatic tissue. Subsequently, the pollen tube grows and is attracted to the ovule micropyle. After entering a synergid, the pollen tube bursts to release the two sperm cells: one fuses with the egg cell and the other with the central cell of the mature female gametophyte (Drews et al., 1998).

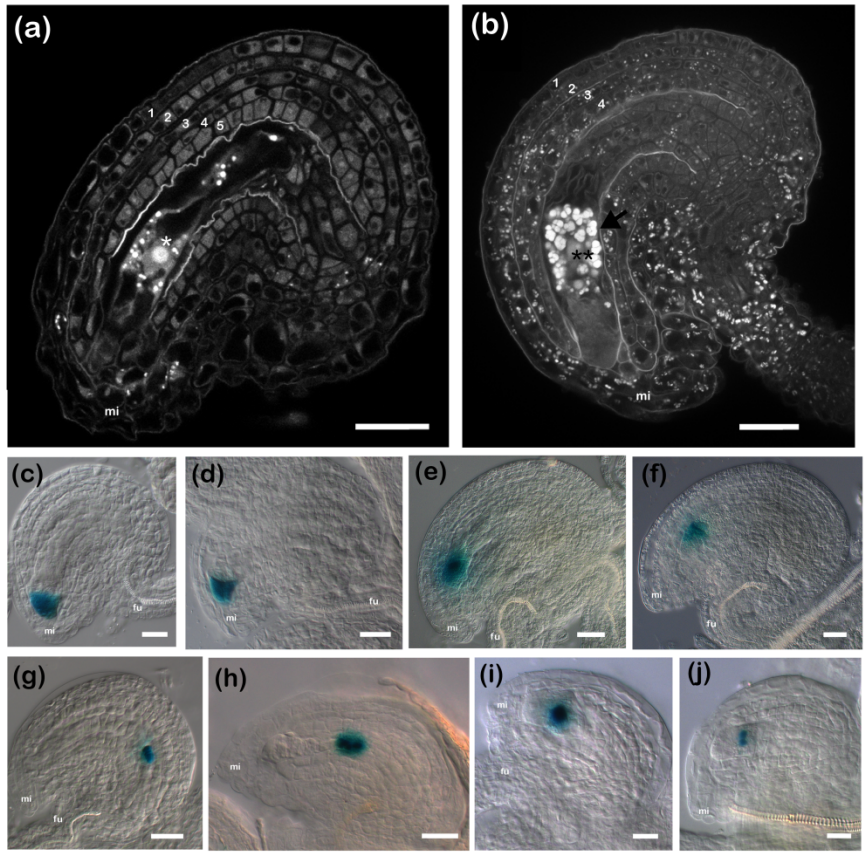


Figure 3. Morphological and molecular analysis of *abs stk* ovules. (a, b) Confocal analysis of wild-type (a) and *abs stk* (b) ovules. The integument of the wild-type ovule (a) has five layers (1, epidermis; 2, palisade; 3 and 4, two inner integument layers; 5, endothelium), but the double mutant seed coat (b) has only four layers: the innermost layer (endothelium) is missing. (c–j) Analysis of *abs stk* double mutant gametophyte cell identity. Crossing the *abs stk* double mutant with embryo sac specific reporter lines showed that female gametophyte cell identity was not altered in the double mutant. (c,d) Synergid cell marker expression in wild-type ovules (c) and *abs stk* mutant ovules (d). (e,f) Egg cell-specific marker expression in wild-type (e) and *abs stk* (f). (g,h) Antipodal cell marker expression in wild-type ovules (g) and in *abs stk* double mutant ovules (h). There is a slight difference in the position of the antipodal cells: in the *abs stk* double mutant, the antipodal cells are closer to the micropylar region of the ovule. (i,j) Central cell-specific marker expression in wild-type (i) and *abs stk* (j). Interestingly, the two polar nuclei do not always fuse. mi, micropyle; fu, funiculus. The white asterisk in (a) indicates the central cell. The two black asterisks in (b) indicates unfused polar nuclei. The white arrow in (b) indicates starch. Scale bars = 30 µm (a,b) and 20 µm (c–j).

In the *abs stk* double mutant, the ovules reach maturity (Figure 3b) as in wild-type (Figure 3a). To understand whether the observed ovule abortions are due to defects in determination of female gametophyte cell identity, embryo sac cell-specific reporter constructs were introduced into the *abs stk* double mutant. *abs stk* double mutants that are homozygous for an egg cell-specific marker (S. Sprunck, Department of Cell Biology and Plant Physiology, University of Regensburg, Germany, unpublished data), a synergid cell-specific marker (Gross-Hardt et al., 2007), a central cell-specific marker (Moll et al., 2008) or antipodal cell-specific marker (Matias-Hernandez et al., 2010) were used to determine the correct identity of the cells in the female gametophytes (n = 250). These analyses showed that cell identity was not affected in *abs stk* double mutant gametophytes (Figure 3c–j). However, the antipodal cells in the *abs stk* double

mutant (Figure 3h) appeared to be closer to the micropylar end than in wild-type ovules (Figure 3g). This phenotype is probably due to the reduced size of the embryo sac in the double mutant (Figure 3b, h). Another interesting observation is that, although the identity of the central cell was not affected, the two polar nuclei did not fuse in 15% of the observed *abs stk* ovules ($n = 250$) (Figure 3b, j), a phenotype that was never observed in wild-type embryo sacs at this stage (Figure 3i).

Morphological and cytological analysis of *abs stk* double mutant ovules indicated the presence of a large amount of starch in the embryo sac (Figures 3b and 4b). When we compared wild-type with *abs stk* double mutant ovules before fertilization, we observed that starch was mainly present at the micropylar region in wild-type embryo sacs (Figure 3a), as previously described by Mansfield et al. (1991), whereas a large amount of starch accumulated in the whole embryo sac in *abs stk* double mutant ovules (Figures 3b). After fertilization, starch was apparently used by the developing embryo and endosperm in wild-type ovules, and consequently the amount was drastically reduced (Figure 4e). In the *abs stk* double mutant, the number of ovules that showed a significant reduction in starch accumulation (Figure 4f) corresponded to the number of fertilized ovules (108/250), but the amount of starch was still high in the remaining ovules. For comparison, in the *abs* and *stk* single mutants, starch accumulation was similar to that in the wild-type (Figure S2).

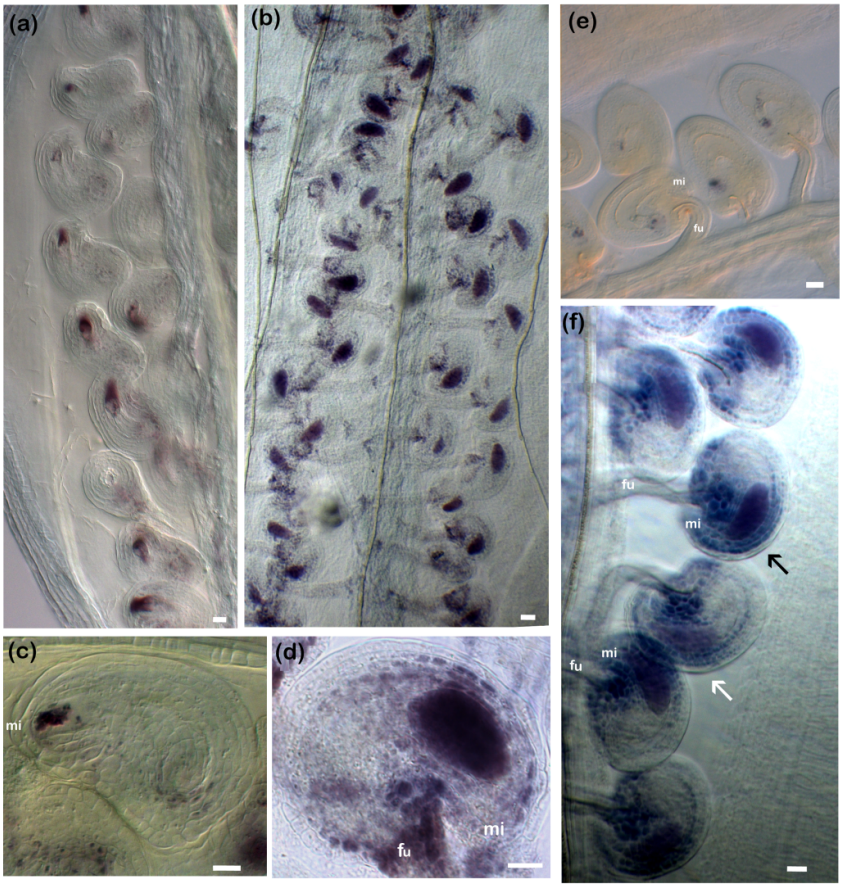


Figure 4. Lugol staining before and after fertilization. Wild-type carpel (a) and *abs stk* double mutant carpel (b) before fertilization: all ovules showed accumulation of starch. A more detailed analysis of the wild-type ovule (c) showed that starch accumulation was localized at the micropylar zone of the ovule. However, in the *abs stk* mutant (d), starch accumulated throughout the embryo sac. After fertilization, no starch accumulation was detected in wild-type ovules (e), but starch accumulation remained visible in the *abs stk* double mutant (f) (black arrow). In some ovules (white arrow), the amount of starch was reduced. mi, micropyle; fu, funiculus. Scale bars = 20 µm.

To investigate whether pollen tubes were attracted by the ovules, and whether they correctly entered the micropyle, aniline blue staining of wild-type and *abs stk* mutant pistils was performed. This

experiment showed that pollen tubes did indeed reach at all the *abs stk* double mutant ovules and entered the micropyle, indicating that this first part of the fertilization process was not affected (Figure 5a, b).

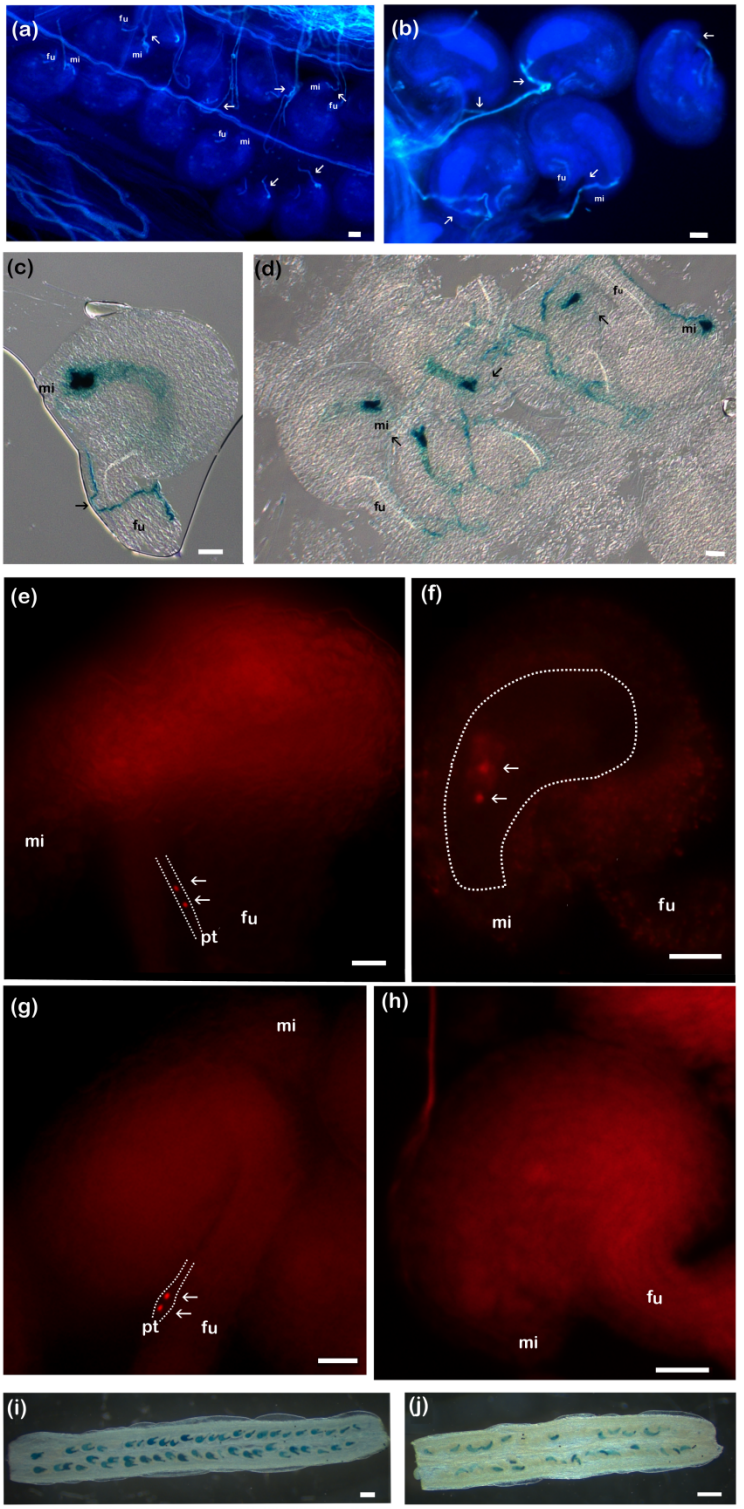

(a)
fu
mi
(b)
fu
mi
(c)
mi
fu
(d)
fu
mi
mi
fu
(e)
mi
fu
pt
(f)
mi
fu
(g)
mi
pt
fu
(h)
fu
mi
(i)
(j)

Figure 5. Pollen tube guidance, reception and burst, and sperm cell delivery/central cell fertilization. (a,b) Pollen tube guidance and reception: pollen tubes (white arrows) arrive and enter the micropyle of wild-type (a) and *abs stk* double mutant (b) ovules. (c,d) Fertilization of wild-type ovules (c) and *abs stk* double mutant ovules (d) with *LAT52:GUS* pollen showed that pollen tubes arrive at all the double mutant ovules (black arrows). In addition, the pollen tube burst is also evident close to the micropyle. (e–h) After bursting of the pollen tube, sperm cell migration was followed using the *pHTR10:HTR10-RFP* marker line in wild-type (e,f) and double mutant ovules (g,h). It is possible to follow the sperm cells (white arrows) in the pollen tube (dotted line) in both wild-type (e) and the *abs stk* mutant (g). After arriving in the micropyle, the two sperm cells (white arrows) were visible inside the wild-type embryo sac (dotted line) (f), but they were almost never visible inside the double mutant embryo sac in the double mutant (h). (i,j) Using the *pMINI3:GUS* marker line, 83% of the ovules in wild-type plants (*n* = 600) showed GUS expression (i), indicating that the central cell was fertilized and the triploid endosperm was formed. In the *abs stk* double mutant (j), only 43% of the ovules showed blue staining (*n* = 400). pt, pollen tube; mi, micropyle; fu, funiculus. Scale bars = 20 μm (a–h) and 150 μm (i,j).

To analyse whether sperm cells were released into *abs stk* mutant embryo sac, *abs stk* carpels were pollinated with pollen from plants containing a *pLAT52:GUS* transgene (Tsukamoto et al., 2010), which labels the pollen tube cytosol and allows investigation of pollen tube burst and release of the sperm cells (Figure 5c). This analysis confirmed that, as in the wild-type, pollen tube burst occurred in all *abs stk* ovules (Figure 5d). To further investigate the migration of the sperm cells in *abs stk* ovules, we used the *pHTR10:HTR10-RFP* reporter line (Aw et al., 2010). In this reporter line, sperm cell nuclei are labelled with RFP. Migration of sperm cell nuclei in wild-type ovules was clearly observed (Figure 5e, f). Surprisingly, sperm nuclei were visible at the micropylar region after pollen tube burst in only 10% of *abs stk* mutant ovules. In all other *abs stk* mutant ovules, we were unable to observe the sperm cells after the pollen tube entered the micropyle (Figure 5g, h). The

reason for this may be that the RFP signal was masked by the enormous amount of starch accumulated in *abs stk* ovules.

As pollen tubes do arrive at *abs stk* ovules, we analysed how many ovules were successfully fertilized using the *pMINI3*:*GUS* marker line. *MINI3* is expressed in the endosperm immediately after fertilization (Luo et al., 2005). This experiment showed that only 43% of the ovules (n = 400) were fertilized in *abs stk* carpels (Figure 5i), whereas 83% of the ovules were fertilized in wild-type control carpels (n = 600) (Figure 5j). This further confirms that, at least in a portion of the *abs stk* mutant embryo sacs, a sperm cell was able to migrate and to fertilize the central cell.

To confirm the formation of fertilized and hence triploid endosperm, we measured ploidy levels of developing seeds by flow cytometry. In wild-type seeds, in addition to 2C, 4C and 8C peaks, we observed a population of nuclei corresponding to triploid endosperm (3C and 6C) (Figure 6a, c). In the *abs stk* double mutant, the number of triploid endosperm nuclei was strongly reduced (Figure 6b, c) in comparison with wild-type and the single mutants (data not shown). Additionally, the 4C peak corresponding to diploid cells in G_2 phase was higher in the double mutant compared with wild-type. A higher 4C peak was also observed when comparing the *abs* and *stk* single mutants with wild-type plants (data not shown). These data suggest that fertilization of the central cell takes place in the *abs stk* double mutant, but the number of fertilized ovules is reduced. Moreover, the difference in the 4C peak suggests that ABS and STK are required for timely entry into mitosis.

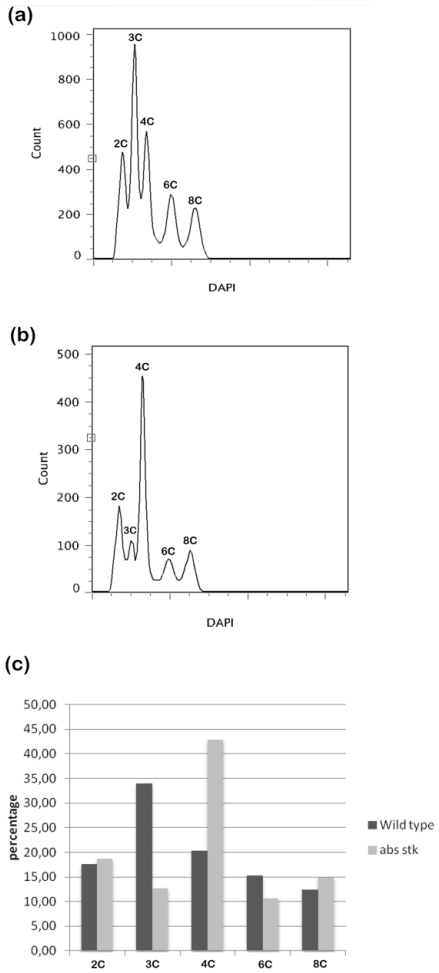


Figure 6. Flow cytometry ploidy analyses of the wild-type and *abs stk* double mutant. (a,b) DNA profile of the wild-type (a) and *abs stk* double mutant (b), showing a mixture of diploid (2C, 4C), endo-replicated (8C, most likely starting from a diploid DNA content) and triploid (3C, 6C) nuclei. The presence of triploid nuclei in developing *abs stk* seeds, although severely reduced in comparison to wild-type, suggests that at least a proportion of the seeds derive from a successful double fertilization. (c) Quantification of diploid (2C, 4C), endo-replicated (8C, most likely starting from a diploid DNA content) and triploid (3C, 6C) nuclei.

Discussion

One of the most intriguing aspects of the reproduction of flowering plants is the development of two different generations in the same organ, the ovule. In the ovule, the haploid embryo sac develops in strict coordination with the diploid ovule integuments (Nowack et al., 2010). After the double fertilization, zygotic tissues develop in a coordinated way with the integuments, which differentiate into the seed coat. Here we show, by a detailed functional analysis, that in the integuments the activity of the two MADS domain transcription factors (ABS and STK) is necessary to support double fertilization and seed development.

Genes such as *AINTEGUMENTA* (*ANT*), *BELL1* (*BEL1*) and *INNER NO OUTER* (*INO*) control the correct development of ovule integuments (for review, see Colombo et al., 2008). The *ant* mutant does not develop integuments (Elliott et al., 1996; Klucher et al., 1996; Baker et al., 1997; Schneitz et al., 1997), and only the inner integument develops in the *bel1* mutant, and at stage 12 of ovule development is converted into a carpelloid structure (Robinson-Beers et al., 1992; Modrusan et al., 1994; Reiser et al., 1995). In both *ant* and *bel1* mutants, gametophyte development is blocked at stage FG1 (Brambilla et al., 2007; Losa et al., 2010). In the *ino* mutant, which only develops the inner integument, megagametogenesis is blocked at FG5 (Christensen et al., 1997; Schneitz et al., 1997). These examples clearly indicate that correct development of the integuments is required for female gametophyte development, and highlight the importance of sporophytic tissues for development of the haploid generation (reviewed by Bencivenga et al., 2011). Interestingly, integument

development was also affected in the *abs stk* double mutant. In this double mutant, the innermost integument layer, the endothelium, is missing. Therefore, this double mutant provides a useful tool to study the function of the endothelium during seed development. Interestingly, ABS and STK appear to act redundantly in the formation of the endothelium even though they belong to different clades of the MADS box phylogenetic tree. Redundancy among distantly related MADS box genes has been described previously: for example, *AGAMOUS-LIKE 24* (*AGL24*) and *SHORT VEGETATIVE PHASE* (*SVP*) are redundant with *APETALA1* (*AP1*) during early stages of flower development (Gregis et al., 2006, 2008). Comparing the primary amino acid sequences of these proteins does not explain their redundancy, but redundancy might be due to the similarity in interactions they can make with other MADS domain factors (De Folter et al., 2005).

Previously, it was shown that co-suppression of two *STK* orthologues, *FBP7* and *FBP11*, in *Petunia hybrida* resulted in degeneration of the endothelium (Colombo et al., 1997), leading to the formation of seeds with a reduced amount of endosperm. Genetic analysis confirmed that this seed phenotype was completely sporophytically controlled, as shown here for the *abs stk* double mutant. The importance of the endothelium in ovule development and fertilization was also suggested by characterization of the Arabidopsis *pdi5* mutant (Andème Ondzighi et al., 2008). This mutant does not produce the disulfide isomerase PDI-5, which is involved in the timing of the programmed cell death in the endothelium. In the *pdi5* mutant, the endothelium cells

prematurely degenerate, resulting in partial loss of fertility (Andème Ondzighi et al., 2008).

Our studies using various gametophyte cell identity marker lines showed that cell identity was correctly determined in the embryo sac of the *abs stk* double mutant. Furthermore, we did not observe any arrest in gametophyte development as described for mutants with more severe integument defects. This suggests that the endothelium is not necessary for the progression of female gametophyte development. However, some effects were visible, such as the smaller size of the embryo sac and occasionally unfused central cell polar nuclei.

It has been suggested that an auxin gradient controls the identity of the gametophyte cells in the embryo sac (Pagnussat et al., 2009). In this respect, it is interesting to note that cell identity was not affected in the *abs stk* double mutant female gametophyte, despite the drastic reduction in embryo sac size and massive starch accumulation. These factors may interfere with creation of the postulated auxin gradient. Future experiments using auxin-responsive reporter lines in *abs stk* double mutants may clarify this. However, the absence of the endothelium has a clear effect on fertilization of the ovules. In the *abs stk* double mutant, only 45% of the ovules were fertilized. This reduction in fertilization is probably not due to defects in fusion of the polar nuclei, as polar nuclei fusion is also affected in the *ig binding protein* (*bip1*) and *bip2* double mutant, without any effect on ovule fertilization (Maruyama et al., 2010). In *Saccharomyces cerevisiae*, *BiP* genes have been shown to encode molecular chaperone Hsp70 proteins that are located in the endoplasmatic reticulum, which regulate nuclear

membrane fusion during mating. In the Arabidopsis *bip1 bip2* double mutant, the sperm nucleus fuses with only one of the two central nuclei. This causes the arrest of endosperm development and leads to seed abortion. Therefore, the seed abortions observed in the *abs stk* mutant may partly correspond to ovules in which polar fusion did not occur. However, as only 15% of the polar nuclei did not fuse, the polar nuclei phenotype could not completely explain the seed abortion phenotype (75% abortion among the fertilized ovules) observed in the *abs stk* double mutant. Furthermore, as reported in Table 1, we observed a block in seed development after the bent cotyledon stage (13 DAP). This *abs stk* double mutant phenotype could also not be explained by the formation of a diploid endosperm since in the *bip1 bip2* double mutant, seeds never reached the bent cotyledon stage (Maruyama et al., 2010).

The reduced fertilization efficiency in the *abs stk* mutant is not due to defects in pollen tube guidance as aniline blue staining of pollinated *abs stk* carpels showed that the pollen tubes arrived at the micropyle of all the ovules. Furthermore, pollen tube burst was observed in all ovules, indicating that sperm cells were correctly released. However, we could not further investigate the fertilization process because we observed sperm nuclei at the micropylar region in only 10% of the double mutant ovules. In all other ovules, no sperm nuclei were visible using the *pHTR10:HTR10-RFP* reporter line. Thus, at this point, we can only speculate about the possible reasons for these observations. It may be that sperm cells degenerated or did not properly fuse with the female gametes. However, as 43% of the ovules are fertilized, it is more likely that

sperm cells migrate to the egg and central cell, but the RFP signal is masked by the enormous starch accumulation observed in *abs stk* double mutant ovules. This hypothesis is supported by the fact that we observed a few times a very faint RFP signal from the nuclei in the ovule. Our flow cytometry data also suggest that fertilization of the central cell takes place in the *abs stk* double mutant. Interestingly, the flow cytometry analysis suggested that ABS and STK are also required for timely entry into mitosis. In relation to this, it is interesting to observe that the founding member of the MADS box gene family, MINI-CHROMOSOME MAINTENANCE 1 (MCM1) in yeast (and homologues in other organisms), is a key regulator of the cell cycle (Passmore et al., 1988). In fact, MCM1 has been shown to control the expression of the mitosis-promoting B-type cyclins CLB1 and CLB2. Consequently, cell cycle progression is compromised in *mcm1* mutant cells which accumulate in the G_2 phase (Althoefer et al., 1995), similar to what was observed for the *abs stk* double mutant. Moreover, another MADS box gene, *XAANTAL1* (XAL1)/*AGAMOUS-LIKE 12* (*AGL12*), is also involved in cell-cycle regulation, as the mutant has a significantly longer cell cycle duration (Tapia-Lopez et al., 2008). This suggests a potential role for plant MADS box genes, including *ABS* and *STK*, in control of cell-cycle progression. This may therefore represent a mechanism by which cell proliferation and differentiation are linked (Harashima and Schnittger, 2010).

In the *abs stk* mutant background, loss of endothelium correlates with starch accumulation. We propose that the endothelium plays a fundamental role in regulating glucose metabolism. The reason for

the reduced fertilization may be at least partially linked to this massive accumulation of starch, which could form a barrier to proper migration of the sperm cells to the egg and central cell. Carbohydrate metabolism in developing gametophytes is poorly understood, but it strongly influences plant fitness. Mutants with altered sucrose metabolism have recently been isolated that show defects during female gametophyte development and reduced fertility, for instance the *cytosolic phosphoglucomutase 2* (*cpm2*) *cpm3* double mutant (Egli et al., 2010) and the *sucrose transporter 2* (*suc2*) mutant (Gottwald et al., 2000). Moreover, the carbohydrate transporter gene *SUC1* was shown to be expressed in the female gametophyte (Feuerstein et al., 2010). Interestingly, the Arabidopsis *GLUCOSE-6-PHOSPHATE/PHOSPHATE TRANSLOCATOR 1* (*GPT1*) gene was shown to be important for male and female gametophyte development (Niewiadomski et al., 2005). In the ovaries of plants heterozygous for the *gpt1* mutation, 36% of the embryo sacs were defective in polar nuclear fusion, similar to what has been described for the *gametophytic factor 2* (*gfa2*) mutant (Christensen et al., 2002; Niewiadomski et al., 2005). In the *gpt1* mutant, de-regulation of metabolic pathways is probably the cause of gametophyte defects. These examples indicate that tight regulation of metabolic pathways is required in the female gametophyte, and disturbance of these causes gametophyte defects.

In conclusion, we have identified a new function for the MADS domain protein-encoding genes *ABS* and *STK*. Despite the fact that these genes belong to different clades of the MADS box phylogenetic tree, they redundantly regulate endothelium

formation, as the complete absence of endothelium is detectable only in the *abs stk* double mutant and not in *abs* and *stk* single mutants. Our results show that fertilization is under sporophytic control, and that the endothelium is an important component contributing to ovule fertility. Furthermore, we also show that the endothelium is important during seed development, as it is probably essential for regulating the flux of nutrients, as evidenced by the massive accumulation of starch in the embryo sac of the *abs stk* double mutant. All these data indicate an essential role of maternal tissues for correct and balanced nutrition of the next generation that develops within the seeds.

Experimental Procedures

Plant material and growth conditions

Arabidopsis thaliana wild-type (ecotype Columbia) and transgenic plants were grown at 22°C under short-day conditions (8 h light/16 h dark) and long-day conditions (16 h light/8 h dark). The *stk-2* allele contains a 74 nt insertion near the splice site of the 3rd intron (Pinyopich et al., 2003). The *abs-6* allele contains a T-DNA insertion in the 3′ region of the 1st intron, 51 nt upstream of the start of the 2nd exon (De Folter et al., 2006).

PCR-based genotyping

Identification of the *STK* wild-type and mutant alleles was performed by PCR analysis using oligonucleotides AtP204 (5′-GCTTGTTCTGATAGCACCAACACTAGCA-3′) and AtP561 (5′-GGAACTCAAAGAGTCTCCCATCAG-3′). The mutant allele gives a 399 bp DNA fragment, and the wild-type allele gives a 325 bp DNAfragment.

For identification of the *ABS* wild-type allele, oligonucleotides AtP3077 (5′-ATGGGTAGAGGGAAGATAGAGATAAAGAA-3′) and AtP3078 (5′-TTAATCATTCTGGGCCGTTGGATCGTTTT-3′) were used. The wild-type allele gives a 1899 bp DNA fragment. Identification of the *abs* mutant allele was performed using oligonucleotides AtP3079 (5′-TTTCTCCATATTGACCATCATACTCATTG-3′) and AtP3078 (5′-TTAATCATTCTGGGCCGTTGGATCGTTTT-3′). The mutant allele gives a 1200 bp DNA fragment.

Expression analysis by *in situ* hybridization

DIG-labelled RNA probes for detection and hybridization of *ABS* and *STK* were prepared as described by Ambrose et al. (2000). Sections of plant tissue were hybridized with digoxigenin-labelled *ABS* antisense probe, amplified using primers TT16For (5′-ATGACGACCAGGAGCAATTG-3′) and TT16Rev (5′-AGAACTCAAGTGCATTGTGC-3′), and with digoxigenin-labelled *STK* antisense probe, amplified using primers AtP2563 (5′-ATCTAAGAACTAAGGTAGCAGAAGT-3′) and AtP2564 (5′-TCTTAATCATTACACAACACAAATTGC-3′).

Confocal laser scanning analysis

For integument morphological analysis, plants were emasculated, and 24 h after emasculation, pistils were fixed as described by Braselton et al. (1996). The samples were excited using a 532 nm laser, and emission was detected between 570 and 740 nm. The samples were observed using a Leica SP5 confocal laser scanning microscope (http://www.leica.com/).

Pollen tube guidance, reception and burst analysis

For *in vivo* pollen tube guidance experiments, pistils were emasculated and pollinated after 24 h with wild-type pollen. After 16–18 h, pistils were carefully isolated from the plants and fixed in a solution of acetic acid and absolute ethanol (1:3), cleared with 8 N sodium hydroxide and labelled with aniline blue (Sigma, http://www.sigmaaldrich.com/).

For *in vivo* pollen tube reception and burst of the tubes, wild-type and double mutant pistils were emasculated and crossed after 24 h

with *pLAT52:GUS* pollen. After 16–18 h, the pistils were carefully collected and stained for GUS activity (Liljegren et al., 2000). Samples were incubated in clearing solution (Brambilla et al., 2007), dissected under a Leica MZ6 stereo microscope, and observed using a Zeiss Axiophot D1 microscope equipped with differential interference contrast (DIC) optics (http://www.zeiss.com/). Images were captured using an Axiocam MRc5 camera (Zeiss) with axiovision software (version 4.1).

Sperm cell migration analysis

For sperm cell migration experiments, pistils were emasculated and crossed after 24 h with the *pHTR10:HTR10-RFP* marker line. Pistils were collected after 16–18 h, samples were dissected under a Leica MZ6 stereo microscope, and images were obtained using a Zeiss Axiophot D1 microscope equipped with DIC optics and a rhodamine filter set.

Cytological analysis

For cytological analysis of ovules, Lugol staining was performed. Pistils were isolated from closed and open flowers, fixed and cleared with the same solutions used for aniline blue staining, and labelled with Lugol's solution. Stained pistils were observed using a Zeiss Axi-overt 200 DIC microscope.

The gametophytic cell identity reporter lines used in here encode a nuclear localization signal that is in-frame with the GUS reporter gene. The egg cell-specific marker was kindly provided by Stefanie Sprunck (unpublished data). The synergid cell-specific marker was kindly provided by Ueli Grossniklaus (Institute of Plant Biology,

University of Zurich, Switzerland) (Gross-Hardt et al., 2007). The central cell-specific marker was kindly provided by Rita Gross-Hardt (Department of Developmental Genetics, University of Tübingen, Germany) (Moll et al., 2008). The antipodal cell-specific marker, kindly provided by Rita Gross-Hardt, was generated as described by Yu et al. (2005): the promoter of At1g36340 was amplified using primers 5′-AGTGAGGCGCGCCTGATCATTAAGTTTAGGGGT-3′ and 5′-AGTGATTAATTAATTACGAGAAATCACCAAAC-3′, and cloned upstream from the NLS_GUS reporter into pGIIBar binary vector (Gross-Hardt et al., 2007) (cloning details are available upon request).

For female gametophyte cell identity determination, marker lines were used as female and pollinated with *abs stk* pollen. In the F_1 generation, heterozygous plants were self-fertilized, and the presence/absence of the mutant alleles for *abs* and *stk* was analysed in the F_2 generation by PCR.

The presence of the reporter genes was analysed by GUS staining, confirming the correct expression in wild-type background. For GUS staining, flowers were emasculated and harvested 12 h after pollination as described by Liljegren et al. (2000). Samples were incubated in chloral hydrate:glycerol:water solution 8:1:2, dissected and observed using a Zeiss Axiophot D1 microscope equipped with DIC optics.

Central cell fertilization and ploidy analyses

To confirm the fertilization of the central cell, *abs stk* double mutant pistils were pollinated with *pMINI3:GUS* pollen (Luo et al., 2005).

After 48 h, pistils were collected and GUS staining was performed as described by Liljegren et al. (2000). Samples were incubated in clearing solution, dissected and observed using a Zeiss Axiophot D1 microscope equipped with DIC optics.

For flow cytometry analysis, seeds at 6 DAP were taken from the siliques, and crushed in 2 ml test tubes with nuclear extraction buffer (CyStain UV-precise kit, Partec, http://www.partec.com/). All samples were subsequently stained with nuclear staining solution (CyStain UV-precise kit) containing 4′,6-diamidino-2-phenylindole (DAPI) as previously described (Nowack et al., 2007). The ploidy level, represented by the mean peak position in a DAPI fluorescence intensity histogram, was calibrated against the 2C nuclear DNA content peak derived from a preparation of young rosette leaves (Nowack et al., 2007). Data were presented using cyflow ploidy analyser software (Partec).

Acknowledgements

We would like to thank Martin Yanofsky (Section of Cell and Developmental Biology, University of California at San Diego, CA, USA) for providing the *stk-2* mutant, Richard Immink (Plant Research International, Wageningen University & Research Centre, The Netherlands) for the *abs-6* mutant, Rita Gross-Hardt (Department of Developmental Genetics, University of Tübingen, Germany) for the central cell marker line and the antipodal marker line, Stefanie Sprunck (Department Cell Biology and Plant Physiology, University of Regensburg, Germany) for the egg cell marker line, Ueli Grossniklaus (Institute of Plant Biology, University of Zurich, Switzerland) for the synergid cell marker line, Ming Luo (Commonwealth Scientific and Industrial Research Organization, Plant Industry Division, Australia) for p*MINI3*:GUS, Ravishankar Palanivelu (School of Plant Science, University of Arizona, AZ, USA) for p*LAT52*:GUS, and Frédéric Berger (Department of Biological Sciences, University of Singapore, Singapore) for the p*HTR10*:*HTR10*-RFP marker. We also thank Xin'Ai Zhao (Institut de Biologie Moléculaire des Plantes du Centre National de la Recherche Scientifique, Strasbourg, France) for her help with flow cytometry. For the *STK in situ* hybridization analysis, we would like to thank Valeria Gagliardini (Institute of Plant Biology, University of Zurich, Switzerland). We also thank Barbara Ambrose (Assistant Curator of Plant Genomics, New York Botanical Garden, NY) for her help with the *ABS in situ* hybridization experiments. Finally, thanks also to Sonia Sacchi, Antonella Stillitano and Lara Grasseni for help with GUS experiments. This work was supported by an EU-ITN fellowship (ITN-SYSFLO project) to M.A.M. and a fellowship from the Università degli Studi di Milano to C.M. This work was also supported by grant 'Action Thématique et Incitative sur Programme' from the Centre National de la Recherche Scientifique and a

European Research Council Starting Independent Researcher grant to A.S.

References

Althoefer, H., Schleiffer, A., Wassmann, K., Nordheim, A., and Ammerer, G. (1995). Mcm1 Is Required To Coordinate G2-Specific Transcription in *Saccharomyces cerevisiae*. *Molecular And Cellular Biology* **15**, 5917-5928.

Andème Ondzighi, C., Christopher, D.A., Cho, E.J., Chang, S.C., and Staehelin L.A. (2008). *Arabidopsis* Protein Disulfide Isomerase-5 Inhibits Cysteine Proteases during Trafficking to Vacuoles before Programmed Cell Death of the Endothelium in Developing Seeds. *Plant Cell* **20**, 2205-2220.

Ambrose, B.A., Lerner, D.R., Ciceri, P., Padilla, C.M., Yanofsky, M.F., and Schmidt, R.J. (2000). Molecular and Genetic Analyses of the *Silky1* Gene Reveal Conservation in Floral Organ Specification between Eudicots and Monocots. *Molecular Cell* **5**, 569-579.

Aw, S.J., Hamamura Y., Chen Z., Schnittger A., and Berger F. (2010). Sperm entry is sufficient to trigger division of the central cell but the paternal genome is required for endosperm development in *Arabidopsis*. *Development* **137**, 2683-2690.

Baker, S.C., Robinson-Beers, K., Villanueva, J.M., Gaiser J.C., and Gasser, C.S. (1997). Interactions Among Genes Regulating Ovule Development in *Arabidopsis thaliana*. *Genetics* **145**, 1109-1124.

Battaglia, R., Brambilla, V., and Colombo, L. (2008). Morphological analysis of female gametophyte development in the *bel1 stk shp1 shp2* mutant. *Plant Biosystems* **142**, 643-649.

Bencivenga, S., Colombo, L., and Masiero, S. (2011). Cross talk between the sporophyte and the megagametophyte during ovule development. *Sexual Plant Reproduction* **24**, 113-121.

Brambilla, V., Battaglia, R., Colombo, M., Masiero, S., Bencivenga, S., Kater, M.M., and Colombo, L. (2007). Genetic and molecular interactions between BELL1 and MADS box factors support ovule development in *Arabidopsis*. *Plant Cell* **19**, 2544-2556.

Braselton, J.P., Wilkinson, M.J., and Clulow, S.A. (1996). Feulgen staining of intact plant tissues for confocal microscopy. *Biotechnic & Histochemistry*. **71**, 84-87.

Christensen, C.A., Gorsich, S.W., Brown, R.H., Jones, L.G., Brown, J., Shaw, J.M., and Drews, G.N. (2002). Mitochondrial GFA2 is required for synergid cell death in Arabidopsis. *Plant Cell* **14**, 2215-2232.

Christensen, C.A., King, E.J., Jordan, J.R., and Drews, G.N. (1997). Megagametogenesis in *Arabidopsis* wild type and the *Gf* mutant. *Sexual Plant Reproduction* **10**, 49-64.

Colombo, L., Battaglia, R., and Kater, M.M. (2008). *Arabidopsis* ovule development and its evolutionary conservation. *Trends in Plant Science* **13**, 444-450.

Colombo, L., Franken, J., Van der Krol, A.R., Wittichy, P.E., Donsy, H.J.M., and Angenent, G.C. (1997). Downregulation of Ovule-Specific MADS Box Genes from Petunia Results in Maternally Controlled Defects in Seed Development. *Plant Cell* **9**, 703-715.

De Folter, S., Immink, R.G., Kieffer, M., Parenicová, L., Henz, S.R., Weigel, D., Busscher, M., Kooiker, M., Colombo, L., Kater, M.M., Davies, B., and Angenent, G.C. (2005). Comprehensive interaction map of the Arabidopsis MADS Box transcription factors. *Plant Cell.* **17**, 1424-33.

De Folter, S., Shchennikova, A.V., Franken, J., Busscher, M., Baskar, R., Grossniklaus, U., Angenent, G.C., and Immink, R.G. (2006). A Bsister MADS-box gene involved in ovule and seed development in petunia and Arabidopsis. *Plant Journal* **47**, 934-946.

Debeaujon, I., Nesi, N., Perez, P., Devic, M., Grandjean, O., Caboche, M., and Lepiniec, L. (2003). Proanthocyanidin-Accumulating Cells in Arabidopsis Testa: Regulation of Differentiation and Role in Seed Development. *Plant Cell* **15**, 2514-2531.

Drews, G.N., Lee, D., and Christensen, C.A. (1998). Genetic analysis of female gametophyte development and function. *Plant Cell* **10**, 5-17.

Egli, B., Kölling, K., Köhler, C., Zeeman, S.C., and Streb, S. (2010). Loss of cytosolic phosphoglucomutase compromises gametophyte development in Arabidopsis. *Plant Physiology* **154**, 1659-1671.

Elliott, R.C., Betzner, A.S., Huttner, E., Oakes, M.P., Tucker, W.Q., Gerentes, D., Perez, P., and Smyth, D.R. (1996). AINTEGUMENTA, an APETALA2-like gene of *Arabidopsis* with pleiotropic roles in ovule development and floral organ growth. *Plant Cell* **8**, 155-168.

Feuerstein, A., Niedermeier, M., Bauer, K., Engelmann, S., Hoth, S., Stadler, R., and Sauer, N. (2010). Expression of the AtSUC1 gene in the female gametophyte, and ecotype-specific expression differences in male reproductive organs. *Plant Biology* **12,** 105-114.

Gregis, V., Sessa, A., Colombo, L., and Kater, M.M. (2006). *AGL24*, *SHORT VEGETATIVE PHASE*, and *APETALA1* Redundantly Control *AGAMOUS* during Early Stages of Flower Development in *Arabidopsis*. *Plant Cell* **18**, 1373-1382.

Gregis, V., Sessa, A., Colombo, L., and Kater, M.M. (2008). *AGAMOUS-LIKE24* and *SHORT VEGETATIVE PHASE* determine floral meristem identity in Arabidopsis. *Plant Journal* **66**, 891-902.

Gross-Hardt, R., Kägi, C., Baumann, N., Moore, J.M., Baskar, R., Gagliano, W.B., Jürgens, G., and Grossniklaus, U. (2007). LACHESIS restricts gametic cell fate in the female gametophyte of Arabidopsis. *PLoS Biology* **5,** 47-53.

Gottwald, J.R., Krysan, P.J., Young, J.C., Evert, R.F., and Sussman, M.R. (2000). Genetic evidence for the *in planta* role of phloem-specific plasma membrane sucrose transporters. *Proceedings of the National Academy of Sciences* **97,** 13979-13984.

Harashima, H., and Schnittger, A. (2010). The integration of cell division, growth and differentiation. *Current Opinion in Plant Biology* **13**, 66–74.

Haughn, G.W., and Chaudhury, A. (2005). Genetic analysis of seed coat development in *Arabidopsis*. *Trends in Plant Science* **10**, 472-477.

Hsu, S.C., Belmonte, M.F., Harada, J.J., and Inoue, K. (2010). Indispensable Roles of Plastids in *Arabidopsis thaliana* Embryogenesis. *Current Genomics* **11**, 338-349.

Kaufmann, K., Anfang, N., Saedler, H., and Theissen, G. (2005). Mutant analysis, protein–protein interactions and subcellular localization of the Arabidopsis Bsister (ABS) protein. *Molecular Genetics Genomics* **274**, 103-118.

Klucher, K.M., Chow, H., Reiser, L., and Fischer, R.L. (1996). The AINTEGUMENTA gene of *Arabidopsis* required for ovule and female gametophyte development is related to the floral homeotic gene APETALA2. *Plant Cell* **8**, 137-153.

Liljegren, S., Ditta, G., Eshed, Y., Savidge, B., Bowman, J., and Yanofsky, M. (2000). *SHATTERPROOF* MADS-box genes control seed dispersal in *Arabidopsis*. *Nature* **404**, 766-769.

Losa, A., Colombo, M., Brambilla, V., and Colombo, L. (2010). Genetic interaction between AINTEGUMENTA (ANT) and the ovule identity genes SEEDSTICK (STK), SHATTERPROOF1 (SHP1) and SHATTERPROOF2 (SHP2). *Sexual Plant Reproduction* **23**, 115-122.

Luo, M., Dennis, E.S., Berger, F., Peacock, W.J., and Chaudhury, A. (2005). *MINISEED3* (*MINI3*), a *WRKY* family gene, and *HAIKU2* (*IKU2*), a leucine-rich repeat (*LRR*) *KINASE* gene, are regulators of seed size in *Arabidopsis*. *Proceedings of the National Academy of Sciences* **102**, 17531-17536.

Maruyama, D., Endo, T., and Nishikawa, S. (2010). BiP-mediated polar nuclei fusion is essential for the regulation of endosperm nuclei proliferation in *Arabidopsis thaliana*. *Proceedings of the National Academy of Sciences* **107**, 1684-1689.

Mansfield, S.G., Briarty, L.G., and Erni, S. (1991). Early embryogenesis in Arabidopsis thaliana. I. The mature embryo sac. *Canadian Journal of Botany* **69**, 447-460.

Matias-Hernandez, L.M., Battaglia, R., Galbiati, F., Rubes, M., Eichenberger, C., Grossniklaus, U., Kater, M.M., and Colombo, L. (2010). *VERDANDI* is a direct target of the MADS domain ovule identity complex and affects embryo sac differentiation in *Arabidopsis*. *Plant Cell* **22**, 1702-1715.

Modrusan, Z., Reiser, L., Feldmann, K.A., Fischer, R.L., and Haughn, G.W. (1994). Homeotic transformation of ovules into carpel-like structures in *Arabidopsis. Plant Cell* **6,** 333-349.

Moll, C., von Lyncker, L., Zimmermann, S., Kägi, C., Baumann, N., Twell, D., Grossniklaus, U., and Gross-Hardt, R. (2008). CLO/GFA1 and ATO are novel regulators of gametic cell fate in plants. *Plant Journal* **56**, 913-922.

Morley-Smith, E.R., Pike, M.J., Findlay, K., Köckenberger, W., Hill, L.M., Smith, A.M., and Rawsthorne, S. (2008). The transport of sugars to developing embryos is not via the bulk endosperm in oilseed rape seeds. *Plant Physiology* **147**, 2121-2130.

Nowack, M.K., Shirzadi, R., Dissmeyer, N., Dolf, A., Endl, E., Grini, P.E., and Schnittger, A. (2007). Bypassing genomic imprinting allows seed development. *Nature* **447**, 312–315.

Nowack, M.K., Ungru, A., Bjerkan, K.N., Grini, P.E., and Schnittger, A. (2010). Reproductive cross-talk: seed development in flowering plants. *Biochem Soc Trans* **38**, 604–612.

Niewiadomski, P., Silke Knappe, S., Geimer, S., Fischer, K., Schulz, B., Unte, U.S., Rosso, M.G., Ache, P., Flugge, U-I., and Schneider, A. (2005). The Arabidopsis Plastidic Glucose 6-Phosphate/Phosphate Translocator GPT1 Is Essential for Pollen Maturation and Embryo Sac Development. *Plant Cell* **17**, 760-775.

Nesi, N., Debeaujon, I., Jond, C., Stewart, A.J. Jenkins, G.I., Caboche, M., and Lepiniec, L. (2002). The *TRANSPARENT TESTA16* locus encodes the ARABIDOPSIS BSISTER MADS domain protein and is required for proper development and pigmentation of the seed coat. *Plant Cell* **14**, 2463-2479.

Pagnussat, G.C., Alandete-Saez, M., Bowman J.L., and Sundaresan, V. (2009). Auxin-dependent patterning and gamete specification in the Arabidopsis female gametophyte. *Science* **26**, 1684-1689.

Passmore, S., Maine, G.T., Elble, R., Christ, C., and Tye, B.K. (1988). Saccharomyces cerevisiae protein involved in plasmid maintenance is necessary for mating of MAT alpha cells. *Journal of Molecular Biology* **204**, 593-606.

Pinyopich, A., Ditta, G.S., Savidge, B., Liljegren, S.J., Baumann, E., Wisman, E., and Yanofsky, M.F. (2003). Assessing the redundancy of MADS-box genes during carpel and ovule development. *Nature* **424**, 85-88.

Reiser, L., Modrusan, Z., Margossian, L., Samach, A., Ohad, N., Haughn, G.W., and Fischer, R.L. (1995). The *BELL1* gene encodes a homeodomain protein involved in pattern formation in the *Arabidopsis* ovule primordium. *Cell* **83**, 735-742.

Robinson-Beers, K., Pruitt, R.E., and Gasser, C.S. (1992). Ovule development in wild-type Arabidopsis and two female-sterile mutants. *Plant Cell* **4,** 1237-1249.

Schneitz, K., Hülskamp, M., Kopczak, S.D., and Pruitt, R.E. (1997). Dissection of sexual organ ontogenesis: A genetic analysis of ovule development in *Arabidopsis thaliana*. *Development* **124**, 1367-1376.

Schneitz, K., Hülskamp, M., and Pruitt, R.E. (1995). Wild-type ovule development in *Arabidopsis thaliana*: a light microscope study of cleared whole-mount tissue. *Plant Journal* **7**, 731-749.

Smyth, D.R., Bowman, J.L., and Meyerowitz, E.M. (1990). Early flower development in Arabidopsis. *Plant Cell* **2**, 755-767.

Stadler, R., Lauterbach, C., and Sauer, N. (2005). Cell-to-cell movement of green fluorescent protein reveals post-phloem transport in the outer integument and identifies symplastic domains in Arabidopsis seeds and embryos. *Plant Physiology* **139**, 701-712.

Tapia-Lopez, R., Garcia-Ponce, B., Dubrovsky, J.G., Garay-Arroyo, A., Perez-Ruiz, R.V., Kim, S.H., Acevedo, F., Pelaz, S., and Alvarez-Buylla, E.R. (2008). An *AGAMOUS*-Related MADS-Box Gene, XAL1 (AGL12), Regulates Root Meristem Cell Proliferation and Flowering Transition in Arabidopsis. *Plant Physiology* **146**, 1182-1192.

Tsukamoto, T., Qin, Y., Huang, Y., Dunatunga, D., and Palanivelu, R. (2010). A role for LORELEI, a putative glycosylphosphatidylinositol-anchored protein, in *Arabidopsis thaliana* double fertilization and early seed development. *Plant Journal* **62**, 571-588.

Yu, H.J., Hogan, P., and Sundaresan, V. (2005). Analysis of the female gametophyte transcriptome of Arabidopsis by comparative expression profiling. *Plant Physiology* **139**,1853-1869.

Supporting Information

Figure S1

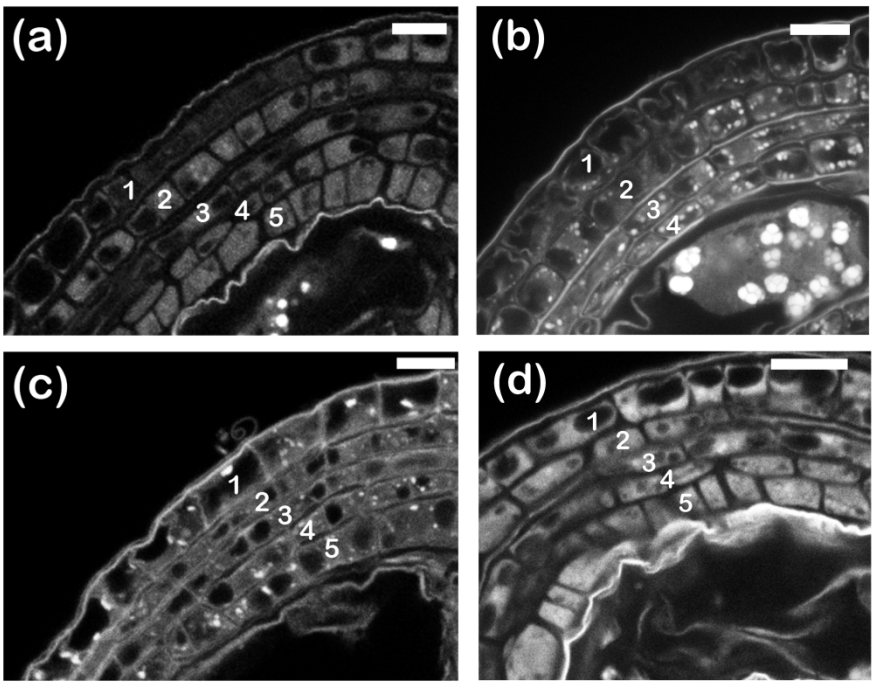


Figure S1. Morphological analysis of integuments. Wild- type (a), *abs* (c) and *stk* ovules integuments (d) are composed of five layers. The *abs stk* integuments (b) are composed of four layers: the missing layer is the endothelium. In the double mutant also the remaining four integument layers showed an irregular shape when compared to wild-type and to the single mutants. Scale bars: 10 µm.

Figure S2

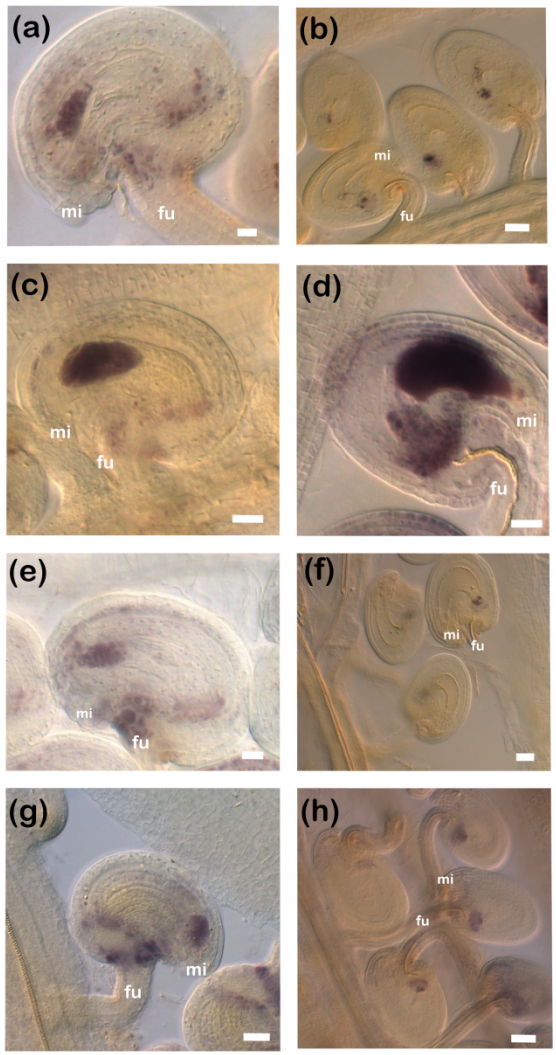


Figure S2. Lugol staining before and after fertilization in wild-type, *abs stk*, *abs* and *stk* mutants. Wild-type (a), *abs stk* (c), *abs* (e) and *stk* (g) ovules before fertilization. All the ovules showed starch accumulation. After fertilization there is no starch accumulation detectable in wild-type (b), *abs* (f) or *stk* (h) ovules, whereas in the *abs stk* double mutant (d) the starch accumulation is still visible as before. (mi, micropyle; fu, funiculus). Scale bars: 20 µm.

Table S1

Table S1.
Reciprocal crosses between wild type and *abs stk* mutant. Ovule abortions, seed abortions and developing seeds analysed at 5 DAP.

	Total ovules	Ovule abortions (Percentage)	Seed abortions (Percentage)	Developing seeds (Percentage)
WT X *abs stk*	166	10 (6%)	8 (5%)	148 (89%)
abs stk X WT	326	171 (52%)	45 (14%)	110 (34%)

Table S1. Reciprocal crosses between wild-type and *abs stk* mutant. Ovule abortions, seed abortions and developing seeds analysed at 5 DAP.

Chapter 2

The MADS-box factor SEEDSTICK (STK) plays a central role in the control of metabolic pathways during seed development in *Arabidopsis thaliana*.

Summary

The sporophytic tissues of the ovule protect the female gametophyte developing inside. After fertilization, the maternal seed coat grows, in coordination with the embryo and endosperm, and undergoes several changes including accumulation of proanthocyanidins and mucilage. The MADS-box gene *SEEDSTICK* regulates ovule identity redundantly with *SHATTERPROOF 1* (*SHP1*) and *SHP2* and is involved in female gametophyte differentiation, endothelium formation and fertilization. Here we report new functions of this transcription factor during seed development. *stk* mutant seeds present defect in seed coat morphology and abnormal proanthocyanidins accumulation. In addition, *stk* mutant seeds present problems in mucilage release. Our data reveal new functions of the MADS-box gene *SEEDSTICK* after fertilization highlighting the importance of this transcription factor indicated as a key regulator of seed development.

Introduction

Seed development is an extremely complex process that requires the coordination in growth and development of three distinct structures: the integuments, the embryo and the endosperm. All these elements together contribute to the final seed size and to ensure the survival of the progeny (Ingram, 2010). The mature seed coat of Arabidopsis consists of five cell layers: two of them originating from the ovule outer integument while the others derive from the inner ovule integument. Following fertilization, the innermost layer, namely the endothelium, synthesizes proanthocyanidins (PAs) colourless compounds that, after oxidation, are responsible for the brown pigmentation of the seeds (Nesi et al., 2002; Haughn and Chaudhury, 2005). The cells of the other two inner integument layers do not seem to differentiate further and they crush together as the seed develops. The genetic control of seed proanthocyanidins biosynthesis has been largely investigated through the isolation and molecular characterization of *transparent testa* (*glabra*), *tt*(*g*) mutants, which are affected in seed coat pigmentation (Winkel-Shirley, 2001; Debeaujon et al., 2003; Sharma and Dixon, 2005; Kitamura et al., 2010). Transcription factors encoding genes belonging to the TT group as well as proanthocyanidins biosynthetic genes have been identified to form a molecular network controlling PAs biosynthesis. An endothelium-specific transcription complex, composed of the TTG1, TT8 and TT2 proteins, acts upstream the *TTG2* gene and the flavonoid biosynthetic genes *BANYLUS* (*BAN*; Walker et al., 1999; Johnson et al., 2002; Baudry et al., 2004). The activity of these proteins is

required for proper endothelium cells differentiation. One of the major regulatory step in the specific activation of the expression of flavonoid structural genes is controlled by TT8, a bHLH factor required for expression of two flavonoid late biosynthetic genes: *DIHYDROFLAVONOL 4-REDUCTASE* (*DFR*) and *BANYULS* (*BAN*). Another gene involved in the flavonoid accumulation and a master regulator of endothelial cells differentiation is the MADS-box transcription factor *TRANSPARENT TESTA16* / *ARABIDOPSIS* B_{sister} *TT16*/*ABS* (Nesi et al., 2002; Debeaujon et al., 2003; de Folter et al., 2006; Mizzotti et al., 2011). *abs* mutant seeds are affected in the three layers belonging to the inner integument. Proanthocyanidins are completely absent in the mutant and the cells of the endothelium do not properly develop. *ABS* and the *TRANSPARENT TESTA1* genes are responsible for BAN expression regulation in the core region of the endothelium but not in the micropyle and the chalazal area (Lepiniec et al., 2006). Another MADS-box gene specifically expressed in the endothelium is *AGL6* (Schauer et al., 2009; Koo et al., 2010), however its function is still unclear since the *agl6* single mutant has no phenotype, which might be due to redundancy with some other MADS-box genes.

The seed coat provides a fascinating system for developmental studies since it has an active metabolism and represents an excellent model system for cellular processes including PA production, cell wall synthesis and modification and mucilage production and release (Lepiniec et al., 2006; Arsovski et al., 2010). The epidermal layer of seed coat indeed during seed coat development, produces and secretes large amount of

pectinaceous carbohydrate mucilage. The mucilage is a seed component that strongly contributes to seed physiology and improve germination is the mucilage. Seed mucilage is mainly composed of pectin, a polysaccharide that is secreted by the epidermal layer to the apical tangential regions of the cell and forms a doughnut shaped pocket between the plasma membrane and primary cell wall (Beeckman et al., 2000; Western et al., 2000; Windsor et al., 2000; Arsovski et al., 2009). Two important genes involved in promoting mucilage biosynthesis are *ENHANCER OF GLABRA3* (*EGL3*) and *TT8* that are partially redundant and they are also required for epidermal cell development in the seed coat (Zhang et al., 2003; Li et al., 2009). A transcription factor complex composed of EGL3 and TT8 is able to interact with the MYB5 and TTG1 proteins. This complex regulates the expression of the *TTG2* and *GLABRA2* (*GL2*) transcription factor encoding genes that are important for the control of epidermal cell differentiation (Zhang et al., 2003; Gonzalez et al., 2009; Li et al., 2009; Arsovski et al., 2010). The MYB61 transcription factor defines a separate pathway involved in seed coat formation since it is not regulated by the EGL3/TT8 complex and till now the targets of MYB61 await discovery (Penfield et al., 2001; Arsovski et al., 2009; Arsovski et al., 2010). Loss of function mutants of each of these regulators resulted in a reduced amount of mucilage and flattened columellae. A second class of mucilage genes identified by genetic screens produces a normal amount of mucilage that do not properly extrude upon seed hydration. Several genes were identified by the characterization of mutant defective in mucilage release upon hydration: *MUCILAGE-MODIFIED1* and *2* (*MUM1* and *MUM2*), *β*-

XYLOSIDASE1 (*BXL1*), and *SUBTILISIN-LIKE SERINE PROTEASE1.7* (*AtSBT1.7*;). Those genes are all defective in mucilage release upon hydration and *MUM2*, *BXL1*, and *AtSBT1.7* are positively regulates by LEUNIG-HOMOLOG (LUH/MUM1; Western et al., 2001; Rautengarten et al., 2008; Arsovski et al., 2009; Huang et al., 2011).

Here we report the functional characterization of *SEEDSTICK* (*STK*) during seed development. The function of the MADS domain transcription factor STK has been extensively studied during ovule identity determination (Favaro et al., 2003**;** Pinyopich et al., 2003; Brambilla et al., 2007) and female gametophyte differentiation (Matias-Hernandez et al., 2010). In these processes *STK* acts redundantly with the *SHATTERPROOF1* (*SHP1*) and *SHP2* MADS-box genes as a master regulator of cell differentiation. The *stk* single mutant has shorter siliques with irregularly spaced seeds. The funiculus is longer in this mutant and mature seeds are not released due to a defect in the formation of the seeds abscission zone (Pinyopich et al., 2003). Furthermore, we have recently reported that STK plays a redundant role with the MADS-box factor ABS to regulate early stages of endothelium formation (Mizzotti et al., 2011). Hereby we focus our attention on the specific role of STK during seed coat formation. We found that *stk* mutant seeds have defects both at very early and later stages during seed coat differentiation. Our results demonstrate that *STK* is required for seed size determination, endothelial cell differentiation and mucilage extrusion. Furthermore, we identified direct target genes of the STK transcription factor showing that this

MADS domain factor acts as a master regulator of seed metabolic pathways.

Result

STK is involved in seed coat development and proanthocyanidins accumulation

In order to understand the contribution of STK during seed development, we have performed reciprocal crosses to reveal the sporophytic role of *STK*: only when *stk* mutant carpels were pollinated with wild-type pollen the obtained seeds presented a small size (Figure 1d). On the contrary wild-type carpels pollinated with *stk* mutant pollen produced a progeny with a normal seeds size (Figure 1c). Moreover the progeny of heterozygous seeds *STK*/*stk* showed a wild type seed size indicating that seed size phenotype is conferred by the maternal genotype of STK locus and it is therefore a maternal effect.

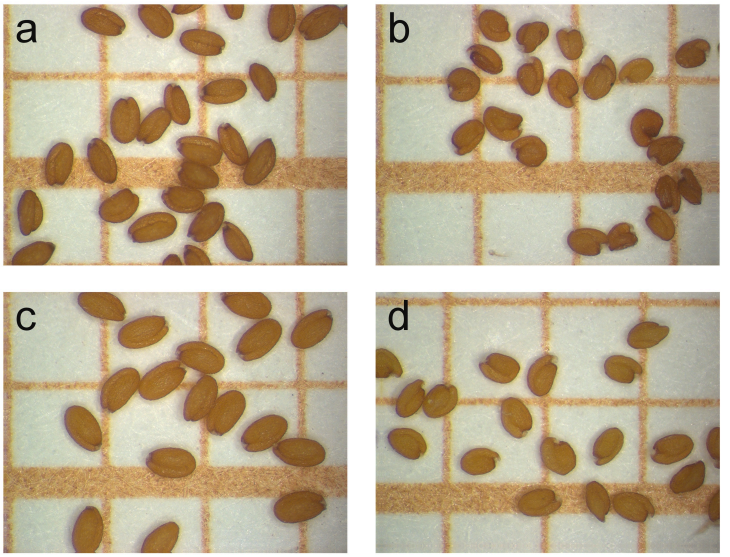


Figure 1. Influence of *stk* mutation on seed size. *stk* single mutant seeds are rounder and smaller (b) than wild-type ones (a). Reciprocal crosses with wild-type plants reveal that wild-type carpels pollinated with *stk* mutant pollen have seeds with wild-type size (c); whereas, *stk* mutant carpels pollinated with wild-type pollen have seeds with *stk*

phenotype (d). These data confirm that seed size is conferred by the maternal genotype of STK locus.

To further analyse the sporophytic role of *STK* we performed a detailed morphological analysis of the integuments. The mature seed coat derives from the two ovule integuments: the two outer layers of the seed coat (oi) derive from the outer ovule integument, while from the inner ovule integument originate the three internal layers (ii). The two outer layers of seed coat are composed of large, vacuolated cells at the micropylar and the chalazal pole, but in the curving zone the cells are smaller (Beeckman et al., 2000; Figure 2a). The other inner integument layers (ii2 and ii1') do not differentiate further and they crush together as the seed develops (Haughn and Chaudhury, 2005). The cells of the innermost layer, the endothelium (ii1), are tiny, isodiametric, regularly spaced and contain small vacuoles. After fertilization the endothelium produced proanthocyanidins (PAs) responsible for the brown coloration of seed coat subsequent to their oxidation (Nesi et al., 2002; Haughn and Chaudhury, 2005; Kleindt et al., 2010; Figure 2a). The proanthocyanidins are epicatechin and catechin polymers but in the Arabidopsis testa only the cis flavan-3-ol (epicatechin) are present as colorless polymers localized in the vacuole. Our analysis revealed that *stk* mutant seed coat presents morphological and structural defects. The cells of the endothelium layer are not isodiametric like the wild-type ones and the cells of all the layers seem to be more crushed and not completely stretched (Figure 2b). Morphological analysis suggest that the MADS-box factor STK might plays a role during PAs production: toluidine blue

staining on *stk* mutant revealed the presence of PAs not only in the endothelium, as in the wild-type, but also in the second layer of inner integument (ii2; Figure 2a, b). We performed vanillin assay to specifically detect flavan-3-ols and their proanthocyanidin polymers (Debeaujon et al., 2003) and confirmed that the compounds accumulate in the second layer of the *stk* mutant inner integument are PAs (Figure 2d, asterisk).

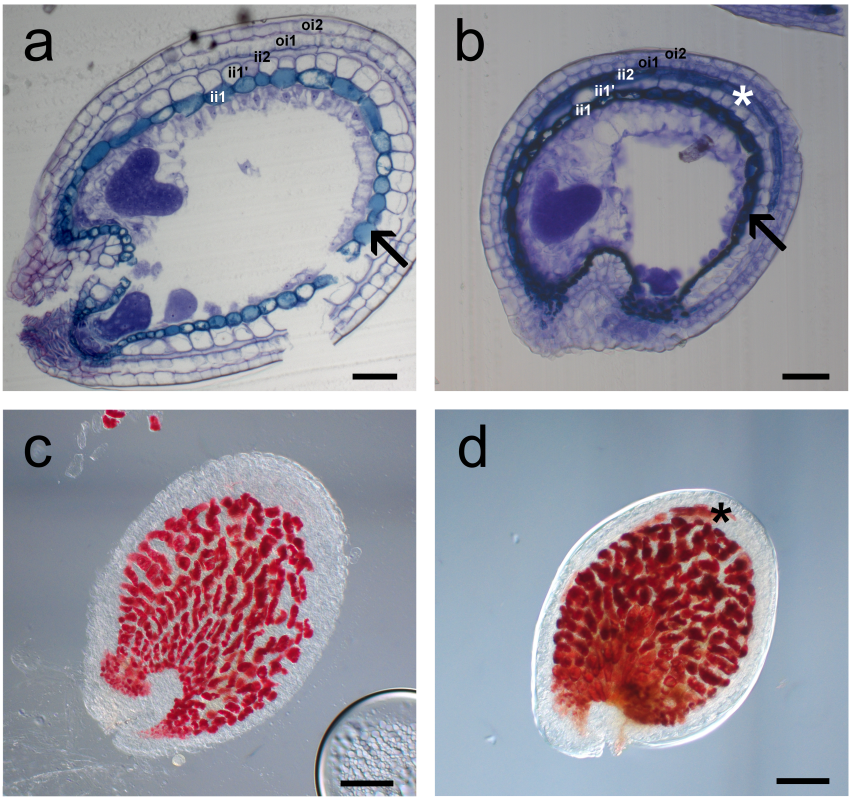


Figure 2. *stk* mutant seeds accumulate PAs ectopically. Toluidine blu staining revealed the presence of PAs (arrow) in the endothelium layer (ii1) in wild-type (a) and *stk* mutant seeds (b). Seeds stained with the vanillin: wild-type (c) and *stk* mutant the second layer of the inner integument (ii2; b, d, asterisk). Scale bars = 30 μm.

It is already known from literature that at the immature stage of seed development, most PAs are solvent-soluble, and then, with the progression of maturation, they are gradually insolubilized (Routaboul et al., 2006; Kitamura et al., 2010). Therefore in order to verify the PAs composition, we performed our analysis both at the immature (6 Day After Pollination – DAP) and at the mature stage of seed development and in both the stages we analyzed soluble and insoluble PAs. The first analysis was performed by acid hydrolysis as previously described by Tohge et al. (2005), measuring the absorbance at 520 nm. Figure 3 shows the mean of the triplicates and the standard deviation bar. Statistical significance was determined by Student's *t* test and *P* values <0.05 were considered to be statistically significant. The analysis of soluble PAs (Figure 3a) revealed that at 6 DAP the amount of PAs is similar in the wild-type and in the mutant. The same compounds, soluble PAs, detected at the mature stage are higher in the *stk* mutant compared to the wild-type (Figure 3a). Insoluble PAs (Figure 3b) at 6 DAP are higher in the wild-type respect to the mutant. The same compounds, insoluble

PAs, detected at the mature stage revealed no differences between the wild-type and the *stk* mutant (Figure 3b).

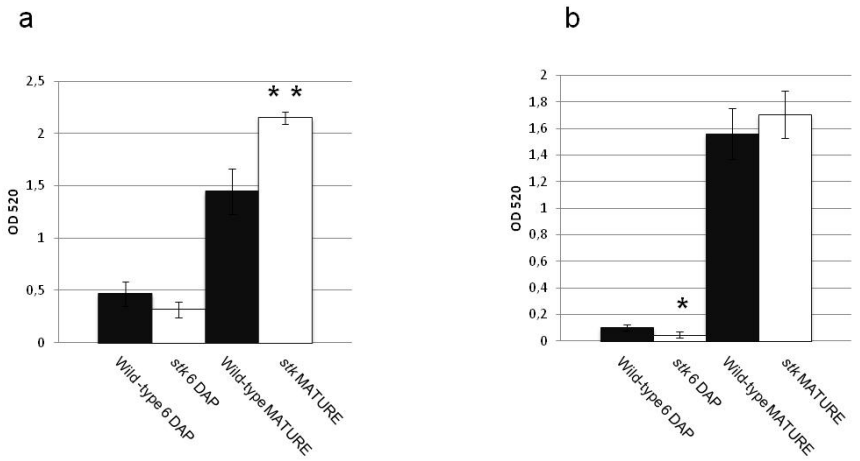


Figure 3. Proanthocyanidin analysis by acidic hydrolysis. Soluble proanthocyanidins (a) and insoluble proanthocyanidins (b) were determined according to 'Experimental procedures'. Error bars represent SD of three independent measurements. Statistical Student's *t* test was performed: * $P < 0.05$, ** $P < 0.01$.

To better describe PAs composition in *stk* mutant seeds, PAs extracts were analyzed by LC-MS and complete metabolic profiles were obtained. Peaks that could be designated as known compounds were selected and analyzed and are reported in Table S1. We performed the analysis both at the immature (6 DAP) and at the mature stage of seed development and in both the stages we analyzed soluble and insoluble PAs. For each samples three biological replicates were performed and the analysis showed obvious similarities among the triplicate samples of each genotype. The insoluble PAs at 6 DAP couldn't be detected, while the same compounds, insoluble PAs, in mature seeds do not revealed differences between the wild-type and the mutant (data not shown). Nevertheless, the levels of soluble PA oligomers (from dimers to nonamer) at 6 DAP was the same in the wild-type and in the *stk* mutant, but the level of epicatechin monomers was higher

in the mutant compared to the wild-type (Figure 4a). In the metabolic profiles of soluble PAs only six metabolites were detected in mature seeds. Wild-type and *stk* mutant seeds contained the same levels of PAs dimers and trimer; however the level of epicatechin monomer, pentamer and hexamer was different (Figure 4b). In particular, the level of pentamer and hexamer in the wild-type was higher compared to the level of the same compounds in the mutant. On the contrary the level of epicatechin monomers was higher in the *stk* mutant, as already showed in the metabolic profiles of immature seeds. Therefore these data indicate an higher level of soluble PAs in the immature and mature mutant seeds and in particular the epicatechin level is affected.

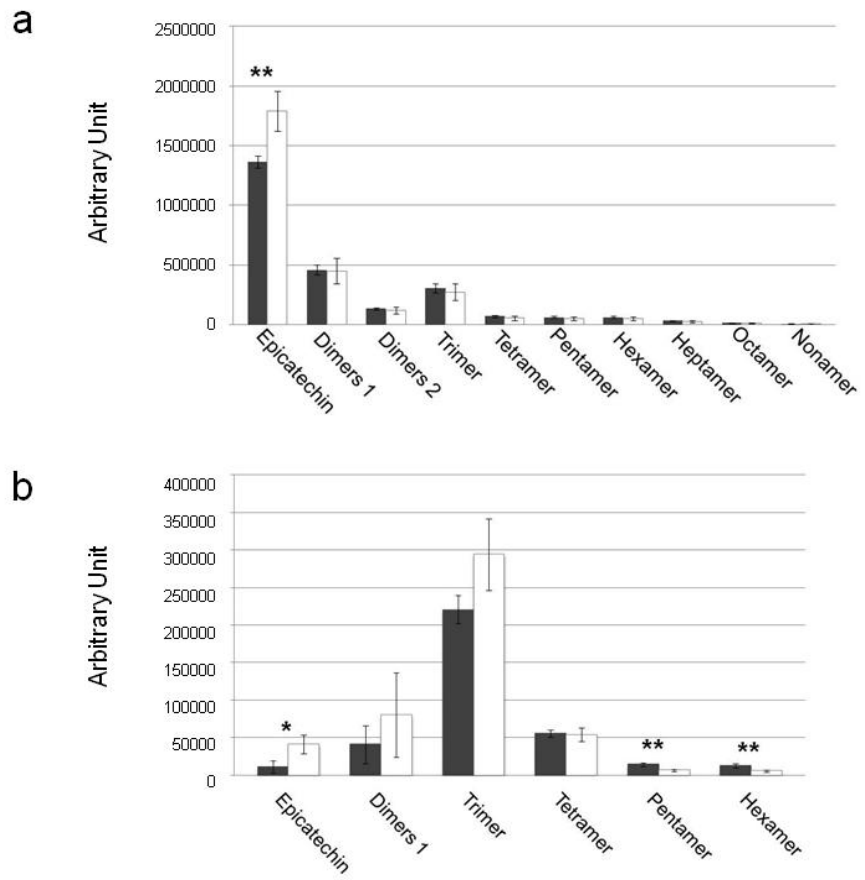


Figure 4 Proanthocyanidins analysis by LC-MS. Soluble PAs were detected in wild-type (black bars) and *stk* mutant (white bars) at the immature stage (a) and mature stage (b) of seed development. Error bars represent SD of three independent measurements. Statistical Student's *t* test was performed: * $P < 0.05$, ** $P < 0.01$.

STK is involved in mucilage release

Another molecule strongly contributing to the seed physiology and improving germination is represented by the mucilage. In order to investigate a possible role of STK during mucilage release we analyzed mucilage production in *stk* mutant seeds. In wild-type plants, seeds hydration leads to the inflate of the mucilage, that cause the bursting of the primary cell wall and the release of mucilage (Western et al., 2000; Windsor et al., 2000; Arsovski et

al., 2009). Upon hydration, mucilage release is visible using the Ruthenium Red, a pectin-staining dye (Hanke and Northcote, 1975), which revealed the presence of a pink staining surrounding wild-type seeds (Figure 5a). On the contrary, Ruthenium Red staining indicated that the *stk* mutant seeds released only a thin layer of mucilage upon hydration (Figure 5b). Morphological analysis of seed coat epidermal layer did not show obvious differences when comparing *stk* mutant cells with wild-type cells. In both the genotypes, we observed a phase of growth by vacuolar expansion, followed by the biosynthesis and deposition of amyloplasts (Figure 5e, h). Starting from 7 DAP the starch granules become bigger and the mucilage, both in wild-type and in *stk* mutant seeds, is secreted in the extracellular space between the plasma membrane and the cell wall. The amyloplasts and the vacuole are delimited to a column in the center of the cell (Figure 5f, i). Finally around 10 DAP, secondary cell wall material is deposited around the narrow cytoplasmic column and the vacuole and forms the columella (Figure 5g, j; Beeckman et al., 2000; Western et al., 2000; Windsor et al., 2000). To confirm the morphological data, we compared the surfaces of dry wild-type and *stk* mutant seeds (Figure 5k, n). The epidermal cells of *stk* mutant seeds showed the typical hexagonal shape with the columella at the center of the cell. Upon imbibitions in water the cell wall of wild-type seeds broke, the mucilage is released and leaves behind a depression around the columella (Figure 5l). On the contrary, imbibed *stk* mutant seeds revealed no differences compared to *stk* dry seeds and confirmed that the primary cell wall fails to break

and the mucilage is not extruded from the *stk* mutant epidermal cells (Figure 5o).

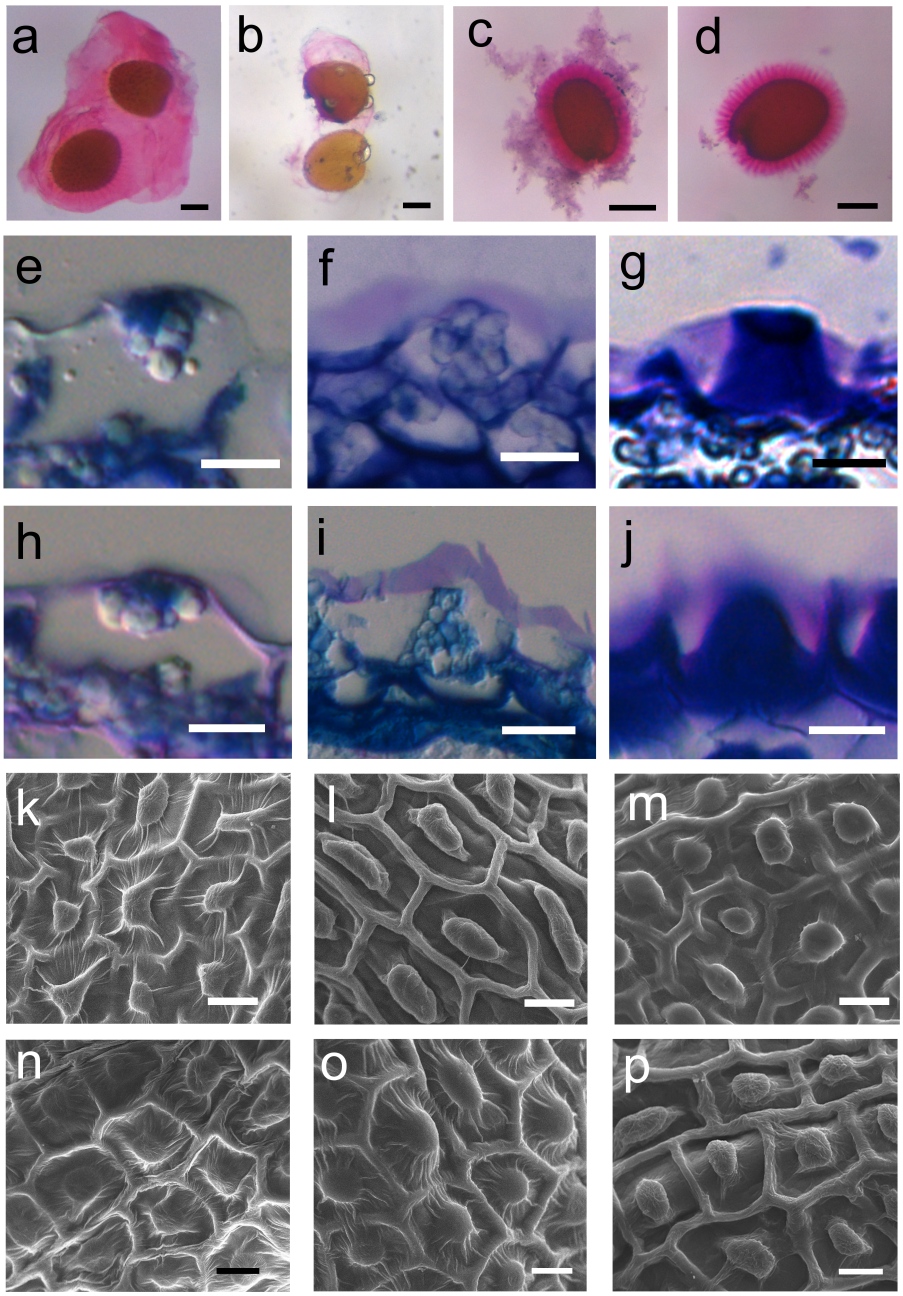


Figure 5. Mucilage release is defective in *stk* mutant. Ruthenium Red staining reveals the presence of a thick, pink-staining capsule of mucilage around the wild-type seed imbibed in water (a), while *stk* mutant seed show a significantly reduced or completely absence of mucilage release (b). EDTA imbibitions caused mucilage extrusion both in wild-type (c) and *stk* mutant seeds (d). In the wild-type (e) and *stk* mutant (h) seed coat epidermal cell amyloplasts are visible. No differences can be detected in amyloplasts accumulation and mucilage deposition in wild-type (f) and stk mutant (i). Also the columella formation does not present differences between wild-type (g) and mutant (j). SEM analysis revealed that the epidermal layer of wild-type seeds show a reticulate appearance (k). In *stk* mutant epidermal cells (n), cell size is reduced compared to WT (Compare (k) with (n)), but there are no other morphological differences. After imbibition, deep hollows are visible around the columellae of wild-type epidermal cells (l). In *stk* mutant seed imbibition does not change seed coat morphology indicating that mucilage has not been extruded (o). On the contrary, EDTA imbibition caused mucilage extrusion both in wild-type (m) and *stk* mutant seeds (p). Scale bars = 30 μm (a-d) and 20 μm (e-p).

The lack of mucilage release from *stk* mutant epidermal cell could be linked to a mechanical resistance of the outer primary cell wall or to abnormal mucilage composition (Western et al., 2001; Rautengarten et al., 2008; Walker et al., 2011). The stability of pectin fraction of cell walls can be influenced by the degree of esterification and the formation of calcium bridges. In order to analyze if these events could influence the mechanical resistance of the outer wall, we used different chemical reagents: *stk* and wild-type seeds were imbibed in the presence of weak alkali (Na_2CO_3), strong alkali (KOH) and strong cation chelators (EDTA). Seeds were imbibed for 2 hours in the different chemical reagents, before staining in the Ruthenium Red. Na_2CO_3 (1 M) and the weak alkali extract pectins by cleavage of cross-linking ester linkages (Selvendran and Ryden, 1990; McCartney and Knox, 2002; Dean et al., 2007); this treatment caused the break of the primary cell wall and subsequent mucilage release both in wild-type and *stk*

mutant seeds (Figure S1c, S1d). KOH (1 M) and the strong alkali are able to extracts cross-linking glycans from cellulosic microfibrils (Fry, 2000; Dean et al., 2007). Both the wild-type and the *stk* mutant seeds treated with KOH released the mucilage from the epidermal layer (Figure S1e, S1f). EDTA (0,5 M) and heavy cation chelators, through the draw away of Ca^{2+} ions from the cell wall pectins, allow the increase of mucilage hydration and the weakening of the primary cell wall (Dean et al., 2007, Arsovski et al., 2009). EDTA imbibitions caused mucilage extrusion in the wild-type and in the *stk* mutant seeds (Figure 5c, d). SEM analysis on wild-type and *stk* mutant seeds treated with EDTA confirm that the treatment with this chelators cause the rapture of the cell wall of wild-type and mutant seeds and the release of the mucilage that leaves behind a depression around the columella (Figure 5m, p). The chemical treatments described above showed the ability to extrude mucilage from *stk* mutant epidermal cells. These data suggest that the hydration properties of *stk* mucilage are not altered. On the base of the data obtained it will be interesting to analyze the mucilage composition of the *stk* mutant seeds to understand if the defect in mucilage release is linked to abnormal mucilage composition or to the cell wall.

To test if the problem in mucilage release in *stk* mutant can compromise seed germination abilities, seeds were germinated by placing on filter paper wetted with water or aqueous solutions of polyethylene glycol (PEG) 6000, at varying concentrations, to reduce water potential. The percentages of germinated seeds were scored for 7 days (Figure 6). Wild-type seeds didn't show problems in germination by PEG concentration up to 18% with a germination

percentage of 92% (Figure 6a). Beyond this concentration the germination efficiency strongly decreased. In contrast, *stk* mutant seeds showed a decrease of germination efficiency already at 18% with a germination percentage of 62% (Figure 6b). This analysis highlight that *stk* seeds have a germination efficiency lower than wild-type seeds with PEG concentration from 15% up to 21% and the difference in germination percentage is enhanced with the increase of PEG.

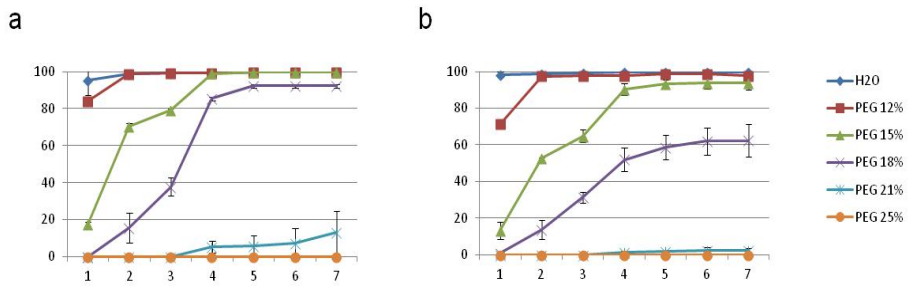


Figure 6. Seed germination on wetted paper containing polyethylene glycol. Germination of the wild-type (a) and the *stk* mutant seeds (b) on increasing concentrations of PEG were scored for 7 days. Data points represent the mean and standard deviation of three independent experiments.

STK is a key regulator controlling metabolic network during seed coat development

Morphological and metabolomic data suggested that the lack of STK activity is linked to defects in secondary metabolites pathway during seed coat formation. To identify specific TFs altered in *stk* mutant background, expression profile of genes involved in PAs accumulation and in mucilage release was analyzed. More precisely, we analyzed the bHLH-encoding genes *TRANSPARENT*

TESTA8 (*TT8*) that is involved in PAs biosynthesis, and *ENHANCER OF GLABRA3* (*EGL3*) that acts redundantly with *TT8* in the control of anthocyanin biosynthesis and in the production of seed coat mucilage (Nesi et al., 2000; Zhang et al., 2003; Baudry et al., 2004). We analyzed the MADS-box genes *TRANSPARENT TESTA 16* / *ARABIDOPSIS* B_{SISTER} (*TT16*/*ABS*), which was shown to be necessary for PAs biosynthesis and normal endothelium cell morphology (Nesi et al., 2002; de Folter et al., 2006), and *AGAMOUS-LIKE6* (*AGL6*) that is specifically expressed in the endothelium layer (Schauer et al., 2009). Concerning those genes specifically involved in mucilage release, we studied the expression profile of the *R2R3-MYB* gene *MYB61* (Penfield et al., 2001), the *SUBTILISIN-LIKE SERINE PROTEASE1.7* (*AtSBT1.7*; Rautengarten et al., 2008) and the *MUCILAGE MODIFIED2* (*MUM2*; Dean et al., 2007) that are defective in mucilage release upon hydration. The expression of these genes was analyzed through quantitative real-time PCR in the wild-type and in *stk* mutant background using RNA extracted from siliques of 3-4 DAP (Day After Pollination) for the genes involved in PAs production, and siliques at 8-10 DAP for the genes involved in mucilage release. Moreover the expression profile of *ABS* was also tested in not pollinated inflorescence in order to define the relation between STK and *ABS* on the base of their role in endothelium formation (Mizzotti et al., 2011). The expression analysis of those genes revealed that they are all repressed by STK: in the *stk* mutant their expression is enhanced compared to the wild-type (Figure 7a, b). This analysis confirmed the role of STK in secondary metabolites production and mucilage released and suggests a key role for STK

in the complex regulatory network that control seed coat formation. In order to determine which of these up-regulated genes are direct target of STK during seed development we performed a ChIP (Chromatin ImmunoPrecipitation) assay with a specific antibody against the STK protein. We performed the ChIP assay on wild-type inflorescence and siliques until 6 DAP. Chromatin extracted from wild-type leaves was used as negative control since *STK* is not expressed in this tissue. As positive control in the ChIP assay we used the binding of STK to the *VERDANDI* (*VDD*) promoter (Matias-Hernandez et al., 2010). Since MADS domain proteins recognize and bind CArG boxes, the genomic sequence corresponding to 3 Kb upstream of the ATG start codon, all exons and introns and 1 kb downstream of the STOP codon of the selected genes were analysed for the presence of putative CArG motifs [CC(A/T)6GG] (Riechmann and Meyerowitz, 1997). Bioinformatics analysis revealed the presence of putative CArG boxes in all the sequences that were analyzed. Testing the direct binding of STK to all the putative CArG sequences allowed us to demonstrate that STK directly interacts with the regulatory regions of *EGL3* and *ABS* (Figura 7c). On the contrary, we did not detect any interaction between STK and the genomic regions of *TT8, AGL6, MYB61, MUM2* and *AtSBT1.7.*

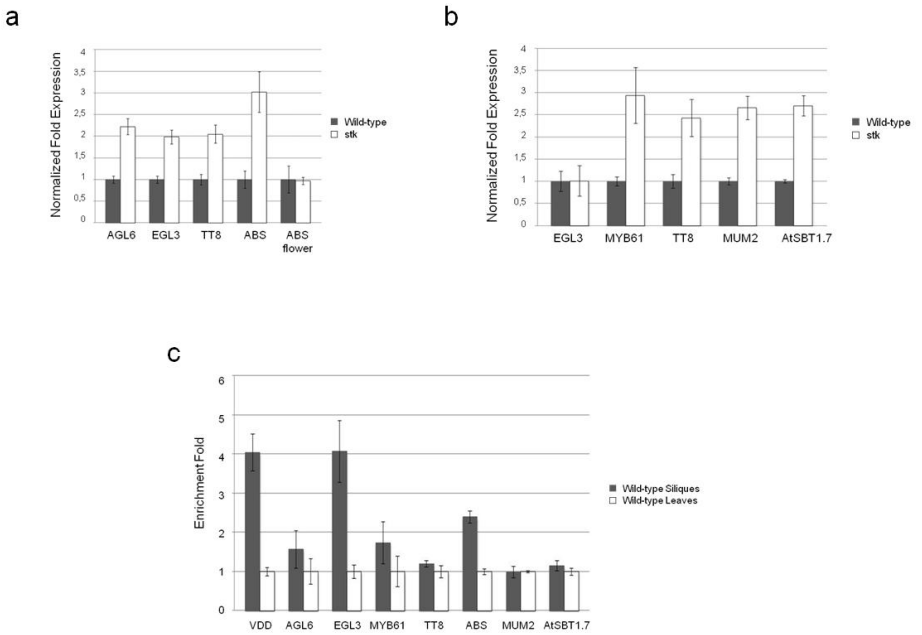


Figure 7. Expression profile of genes involved in PAs production and mucilage release in wild-type and *stk* mutant by Real Time PCR. (a) Quantitative real-time RT-PCR performed on cDNA obtained from flower and siliques from 3 to 4 DAP and from unpollinated flowers for *ABS*. The relative mRNA levels indicate that the expression of all these genes is up-regulated in absence of STK protein in the young silique. The relative mRNA levels of unpollinated flowers indicate that in absence of STK protein the expression of *ABS* is similar to the wild-type one. Error bars represent the propagated error value using three replicates. (b) Quantitative real-time RT-PCR performed on cDNA obtained from siliques from 8 to 10 DAP. The relative mRNA levels indicate that in the mature seeds the expression of all these genes is up-regulated in absence of STK protein. Error bars represent the propagated error value using three replicates. (c) ChIP enrichment tests by quantitative real-time PCR show that STK specific binding to the CArG boxes of *EGL3* and *ABS*. The material from wild-type leaves was used as a negative control since *STK* is not expressed in this tissue. Fold enrichment was calculated over the negative controls. Error bars represent the propagated error value using three replicates.

In order to confirm the expression data and identify a wider range of genes involved in PAs accumulation and mucilage release that are regulated by STK, RNA-seq analysis was performed. RNA was collected from inflorescences and siliques untill 6 DAP both from

wild-type and *stk* mutant background and the resulting cDNA was sequenced using the Solexa/Illumina techonologies. This procedure was repeated in duplicate. The sequences obtained were aligned to cDNAs of Arabidopsis using CLC Bio software. Statistical significance was determined by Student's *t* test and *P* values <0.05 were considered to be statistically significant. The data concerning the PAs production genes confirmed that *TT8* is repressed by STK: the fold change indicates that TT8 is expressed 1.5 time more in the mutant background and this difference is statistically significant (*P* values <0.05). The RNA-seq data of all the other genes involved in PAs accumulation and previously analyzed by real time PCR (*EGL3*, *AGL6* and *ABS*), confirmed that these genes are all repressed by STK but this repression seems not to be statistically significant. The same result was obtained for the mucilage release genes *MUM2*, *MYB61* and *AtSBT1.7*: they are repressed by STK but this repression seems not to be statistically significant. Besides this the RNA-seq data analysis revealed that STK repress also other genes involved in the PAs biosynthetic pathway. In particular the expression of the transparent testa genes *TT1* and *TT2* is up-regulated in *stk* with an expression level that is, respectively, 2.4 and 2 times higher in the mutant. Moreover two of the flavonoid late biosynthetic genes *DFR* and *BAN* are up-regulated in *stk* mutant as well as *MYB5*, that is part of the regulatory complexes controlling the epidermal cell differentiation.

Discussion

The MADS-box gene *STK* plays a crucial role during seed development in *Arabidopsis*

The molecular function of the MADS-box gene *STK* has been already described during ovule identity determination (Favaro et al., 2003; Pinyopich et al., 2003; Brambilla et al., 2007), female gametophyte differentiation (Matias-Hernandez et al., 2010), endothelium formation and fertilization process (Mizzotti et al., 2011). In the spite of what has been previously reported, we found that STK also plays a pivotal role after the double fertilization events and it is involved in different aspects of seed coat formation including metabolic control of key pathway in seed development. Here we have conducted a detailed characterization of mutant plants lacking *STK* function, and presented evidences for its role in seed coat development; its requirement for PAs accumulation in the endothelium and for mucilage release from epidermal cells upon imbibition. In *stk* mutant seeds both outer and inner seed coat layers are affected. Our data indicate that the MADS-box gene *STK* is necessary for proper integument development since in the *stk* mutant seed coat the cells of the endothelium layer are not isodiametric and the cells of all the layers seem to be more crushed and not completely stretched. The reciprocal crosses indicate that *stk*, through the control of integument development, is involved in the maternal control of seed size determination.

STK regulates the expression of genes involved in seed coat differentiation and PAs production

Morphological analysis revealed the in *stk* mutant seeds PAs are accumulated also outside from the endothelium. By acid hydrolysis, some differences were detected in the mutant respect to the wild-type; however this type of approach could not be considered really precise since it is based on the measurement of the absorbance and there could be other compounds, different from PAs, which adsorb at the same wavelength. Through LC-MS approach we demonstrated that the level of epicatechin monomers was higher in the mutant compared to the wild-type. However the level of pentamer and the hexamer seems to indicate the opposite, since the level of these compounds is higher in the wild-type; although if we consider the total level of PAs compounds, it results higher in the mutant than in the wild-type, confirming the morphological analysis. The regulation of flavonoids and proanthocyanidins production has been extensively studied (for review see Lepiniec et al., 2006). A regulatory complex composed by TTG1, TT8/EGL3, MYB5 and TT2 proteins positively regulates the expression of *BAN* (Zhang et al., 2003; Baudry et al., 2004; Gonzalez et al., 2009; Li et al., 2009). *BAN* encodes for the core enzyme of proanthocyanidin biosynthesis: a anthocyanidin reductase that convert anthocyanidins to their corresponding flavan-3-ols. In this complexes regulatory network that control PAs accumulation in the endothelium layer, *STK* seems to play a key role: on the base of our data, STK repress the expression of genes involved in the regulation of *BAN*. *EGL3* is directly repressed by STK, while *TT8* is repressed in an indirect way since there are no

evidence of a direct binding of STK protein to the *TT8* promoter. Also *MYB5* and *TT2* are repressed by STK protein, as highlighted by the RNA-seq data, and future ChIP analysis on the promoter of these genes will define if they are direct or indirect target of STK. A possible explanation for STK role in the repression of all these genes is that STK controls endothelium cell differentiation through the spatial regulation of these gene: the expression of these genes involved in PAs accumulation is confined inside the endothelium layer by the STK protein. In absence of STK activity these genes are ectopically expressed and PAs are accumulated also outside form the endothelium as demonstrated by the phenotype of *stk* mutant. RNA-seq data indicates that STK represses *BAN* expression; this regulation could be a direct regulation of *BAN* expression or could be mediated by ABS, by TT1 or by the TTG1 complex. This further regulation highlights the importance of STK in the PAs production pathway: it repress, in a direct or indirect way, the expression of the anthocyanidin reductase gene (*BAN*) that convert anthocyanidins to their corresponding flavan-3-ols.

STK activity influence also *ABS* expression: *ABS* is a direct target of the MADS-box factor STK and *ABS* transcripts are more abundant in *stk* mutant background exclusively after the fertilization event. The *ABS* gene is already reported in literature as an important regulator of endothelial differentiation, acting upstream other transcription factors (Nesi et al., 2002; Debeaujon et al., 2003; Haughn and Chaudhury, 2005). Moreover, yeast three hybrid assay demonstrated that a MADS-box protein complex composed of ABS, STK and SEP3 is formed in yeast (Kaufmann et al., 2005). Our previous data indicated that the presence of both

these genes is strictly necessary for endothelium formation and for plant fertility (Mizzotti et al., 2011). Integration of previous data with our results indicates that both the ABS and STK factors are master regulators of inner seed coat differentiation. Different models might explain, at the molecular level, which is the relationship between these MADS-box factors. They might have a function in endothelium formation before fertilization, when STK do not regulate *ABS* expression, while later STK protein might act as a repressor of *ABS* transcription. Another possibility is that STK controls endothelium cell differentiation through the spatial regulation of the *ABS* gene. In absence of STK activity the *ABS* gene is ectopically expressed as demonstrated by the seed phenotype in *stk* mutant background. Here, we detected an accumulation of proanthocyanidins in different layers of the inner integument making therefore possible that different cells acquire endothelial identity as a consequence of the ectopic expression of the *ABS* MADS-box transcription factor. A similar mechanism might explain the increased accumulation of *AGL6* transcripts in *stk* mutant background. In wild-type plant, the *AGL6* encoding gene is specifically expressed in the endothelium (Schauer et al., 2009; Koo et al., 2010). The STK transcription factor might act as a repressor or spatial regulator of the *AGL6* gene.

STK has a key role in outer seed coat differentiation and mucilage release

Another important features of seed development is the mucilage: it strongly contribute to the seed physiology and improve germination. Our data revealed that *stk* mutant seeds do not released mucilage upon hydration in water. Seed mucilage, that is dispensable for germination under laboratory condition, is essential for its hygroscopic properties and, as expected, the germination efficiency of *stk* mutant seeds is reduced respect to the wild-type. Since no differences were detected in the mucilage accumulation and columella formation in the *stk* mutant, the defect in mucilage release may be the result of a problem in the mechanical resistance of the outer primary cell wall, or an insufficient mucilage expansion caused by a change in mucilage composition. However the fact that the mucilage was released from *stk* mutant seeds when imbibited in EDTA indicate that there are no change in the composition or structure of the polysaccharide components that reduce the hydrophilic potential of the mucilage and point to a problem in mechanical resistance of the outer primary cell wall. Future analysis of the mucilage composition will help us to better elucidated if STK could also have a role in this pathway. The expression analysis and the RNA-seq data revealed that the MADS-box encoding gene *STK* plays a key role also during outer seed integument differentiation. Expression analysis on genes involved in outer seed coat development revealed that transcripts accumulation of the genes *MYB61*, *MUM2*, *SBT1.7*, *EGL3* and *TT8* is higher in *stk* mutant background. Based on the literature, the *TT8* gene acts redundantly with the *EGL3* gene during mucilage

production and release (Zhang et al., 2003). The protein complex composed of the transcription factors TT8, MYB5, TTG1 and EGL3 acts upstream *GL2* and *TTG2* in the control of mucilage production and release (Western et al., 2001; Gonzalez et al., 2009; Li et al., 2009). On the basis of our data, STK directly repress *EGL3*, indirectly repress *TT8*, while the MYB5 repression, highlighted by the RNA seq data, is still to be analyzed to clarify if it is a direct or an indirect repression. Another class of mucilage gene are those defective in mucilage release upon hydration: *MUM1, MUM2, ATBXL1* and *AtSBT1.7* (Western et al., 2001; Dean et al., 2007; Rautengarten et al., 2008; Arsovski et al., 2009). The phenotypes of *mum1, mum2, atbxl1* an *atsbt1.7* mutants demonstrate that mucilage synthesis and secretion to the apoplast is not sufficient to guarantee extrusion of mucilage when seeds are exposed to water and the same phenotype was observed also in *stk*. Our data indicate that STK regulates the expression of *MUM2* and *AtSBT1.7* and the regulation of these genes should be done through other partners. The mucilage release is also controlled by the *MYB61* transcription factor appears defining a third pathway that control mucilage release but that is not regulated by either by MUM1 or TTG1 complex (Penfield et al., 2001; Arsovski et al., 2009; Arsovski et al., 2010). Also this third pathway of mucilage release is controlled by STK although in an indirect way since on the base of the ChIP data *MYB61* is not a direct target of STK. On the base of our expression and RNA-seq data it's possible to conclude that STK is a key regulator of the outer cell layer of the seed coat. In particular STK regulates the expression of the TT8/TTG1/TT2/MYB5/EGL3 protein complex. Transcript of *MUM2*,

AtSBT1.7 and *MYB61* are enhanced in *stk* mutant background indicating that STK acts as a repressor of these genes. However ChIP assay data point to an indirect regulation of these genes. STK seems to be a new regulator of *MUM2* and *AtSBT1.7*, different from MUM1. In conclusion, STK seems to be a key player of the mucilage release and it act as a repressor in all the three different pathway known till now to regulate mucilage production and release: the pathway of the TTG1 complex, the pathway of MYB61 and the pathway specifically involved in mucilage release with *MUM2, ATBXL1* and *AtSBT1.7* genes. In all these three pathway STK act as a repressor. It is now of fundamental importance to analyze the *stk* mutant mucilage composition in order to define if STK role in mucilage release is due to a problem in mucilage composition or to a problem in cell wall properties.

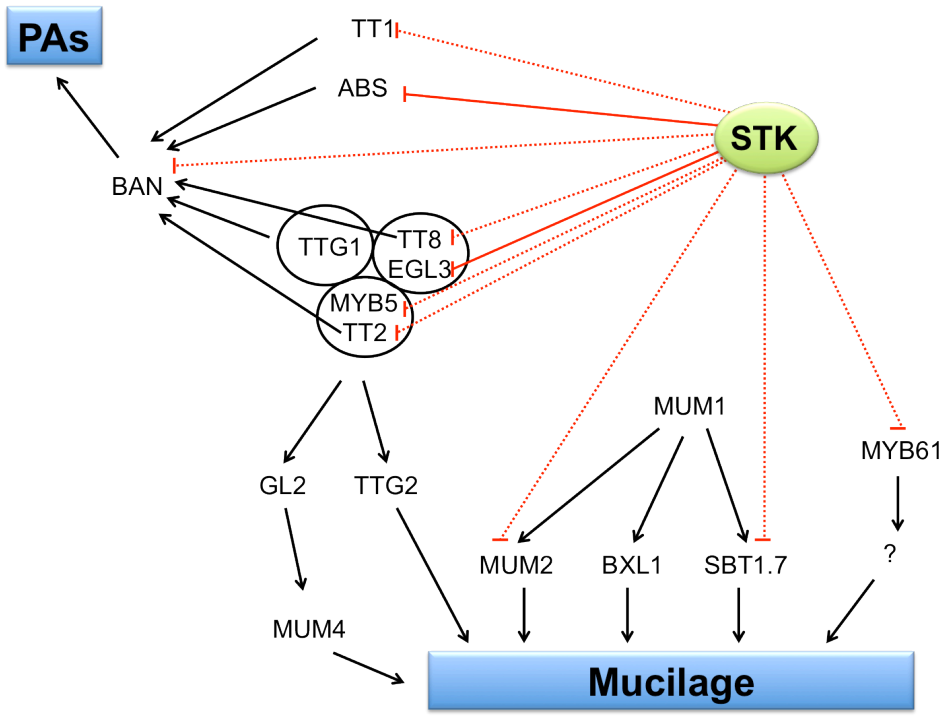


Figure 8. STK is a key regulator of the metabolic pathway. Proposed genetic pathway for the regulation of proanthocyanidins production and mucilage production and release on the base of the expression analysis, ChIP assay and RNA-seq data. Continuos lines are the direct interaction demonstrated by ChIP assay, dotted lines are the interaction for which ChIP assay was negative or not performed yet.

In conclusion, our data revealed that the MADS-box gene STK is a key regulator of metabolic pathways. It is directly implicated in transcriptional regulation of transcription factors involved in PAs accumulation and mucilage release in the integument layer where these genes are not required and it might redundantly play a role with another transcription factor in the positive control of those metabolic pathways in the correct layers.

Experimental Procedures

Plant Material and Growth Conditions.

Arabidopsis thaliana wild-type (ecotype Columbia) and mutant plants were grown at 22°C under short-day (8 h light/16 h dark) or long-day (16 h light/8 h dark) conditions. The Arabidopsis *stk* mutant was kindly given by M. Yanofsky (Pinyopich et al., 2003). The *stk-2* allele contains a 74 nucleotides insertion near the splice site of third intron.

PCR-Based Genotyping

Identification of the STK wild type and mutant alleles were performed by PCR analysis using oligonucleotide AtP204 (5'-GCTTGTTCTGATAGCACCAACACTAGCA -3') and oligonucleotide AtP561 (5'- GGAACTCAAAGAGTCTCCCATCAG -3'). The mutant allele gives a 399 bp DNA fragment, the wild type allele gives a 325 bp DNA fragment.

Morphological Analysis

To analyze seed size, dried seeds were photographed on graph paper using a stereomicroscopy. For integument morphological analysis Arabidopsis thaliana wild-type (ecotype Columbia) and *stk* mutant plants were fixed followed the manufacter's instruction for Technovit 7100 embedding (Heraeus Kulzer). Section of 0.8 µm of plant tissue were stained in 0.5% (w/v) toluidine blue O. Samples were observed using a Zeiss Axiophot D1 microscope (http://zeiss.com/) equipped with differential interface contrast (DIC) optics. Images were recorded with an Axiocam MRc5 camera (Zeiss) using the Axiovision program (version 4.1). The

whole-mount vanillin assay for PA detection was performed as described previously (Debeaujon et al., 2000). Vanillin (vanilaldehyde) can condense specifically to PAs and flavan-3-ol precursors to give a bright-red product in acidic conditions. Clearing of seeds was obtained after overnight incubation in ethanol : acetic acid (9:1). Microscopic observations were performed using a Zeiss Axiophot D1 microscope (http://zeiss.com/) equipped with differential interface contrast (DIC) optics. Images were recorded with an Axiocam MRc5 camera (Zeiss) using the Axiovision program (version 4.1). For mucilage release whole seeds were stained by shaking in a 0.01% (w/v) ruthenium red (Sigma) for 90 min. Seeds treated with Na_2CO_3 (1 M), KOH (1 M) and EDTA (0,5 M) were imbibed for 2 hours in the different chemical reagents, before staining in the Ruthenium Red. After ruthenium red staining the samples were rinsed in dH_2O prior to visualization. Seeds were observed and photographed using a stereomicroscopy. For mucilage extrusion SEM was performed on wild-type and mutant plant before and after imbibition. The dried seeds were put over night at 37°C before proceed with the analysis. Imbibed seeds were air dried overnight on filter paper and then treated as dry seeds. Dried and imbibed seeds were gold coated using a sputter coater (SEMPREP2; Nanotech) and observed with a LEO 1430 scanning electron microscope (LEO Electron Microscopy).

Determination of PA composition

PA extraction and acid hydrolysis were performed according to the method of Tohge et al. (2005). PAs were extracted from immature seeds (6 DAP) by grinding them in 70% acetone containing 5.26 mM $Na_2S_2O_5$, followed by sonication for 20 min. Following centrifugation at 13 000 g for 5 min, the supernatant was evaporated and resuspended in 2:10:3 of HCl:butanol:70% acetone. The absorbance at 520 nm of this resuspended solution was then determined to quantify the level of anthocyanins present. After hydrolysis at 95°C for 60 min, the absorbance at 520 nm was determined and correspond to the contents of anthocyanins plus extractable PAs. Subtraction of the first absorbance value from the second was defined as the soluble PA fraction. The pellet obtained following extraction with 70% acetone was also evaporated, resuspended in the HCl/butanol solution, and hydrolyzed to define the insoluble PAs present.

Preparation of Extracts

Immature and mature seeds (30 mg) were frozen in liquid nitrogen and ground to a fine powder using an analytical mill (IKA; A11 basic). Then, the soluble portion of PAs was extracted from frozen tissue with 75% methanol:water (v/v) containing 0.1% formic acid. The mixture was vortexed for 30 s, sonicated for 30 min at room temperature, vortexed again for 30 s, centrifuged (13 000 rpm, 10 min). The supernatant containing the soluble PAs, was analyzed by LC-MS. The remaining pellet was washed with methanol 50%, centrifuge (13 000 rpm, 10 min), washed again with methanol 100% and centrifuged (13 000 rpm, 10 min). The samples were dry in a speed vacuum for 1 hour at 30°C and then hydrolyzed with

NaOh (2N) for 15 min at 60°C. The mixture was vortexed for 30 s and HCl 4N was added. The lipids were extracted and discarded with hexane: the hexane was added to the mixture, centrifuge (13 000 rpm, 10 min) and the upper phase was throw away. The insoluble PAs was extracted three time with Ethyl Acetate, the extraction were combined and dry in speed vacuum for 1 hour at 30° C. The pellet was dissolved in acetone:water:acetic acid (70:29.5:0.5 v/v/v), vortexed, sonicated for 15 min and centrifuged (13 000 rpm, 10 min). The supernatant containing the insoluble PAs, was analyzed by LC-MS.

Targeted Profiling of proanthocyanidins

The profiling of PAs in extracts of seeds was performed by MS analyses, performed by the UPLC-qTOF instrument (Waters High Definition MS System; Synapt), with the UPLC column connected online to a photo diode array detector (Waters, Acquity), and then to the MS detector, equipped with an electrospray probe. Separation of metabolites and detection of the eluted compound masses was performed as described by Mintz-Oron et al. (2008) and Adato et al. (2009). Masses were detected in the m/z range of 50 to 1500 D with the following settings: capillary voltage at 3.0 kV, cone voltage at 28 eV, collision energy at 4 eV, and argon was used as a collision gas. For MS/MS, 10 to 60 eV were used (for both ionization modes). The metabolites were putatively identified as follows: the elemental composition, selected according to the accurate masses and the isotopic pattern using the MassLynx software , and MS/MS fragments were compared with those found in the literature (Hanhineva et al., 2008; Kitamura et al., 2010).

Relative quantification of the compounds was performed with the QuanLynx program version 4.1 (Waters) using the data acquired in the negative mode. Peak areas were used for the hierarchical clustering of the SAs with MeV version 4.5.1 software (http://www.tm4.org /mev). Peak areas after ln transformation and quantile normalization inside each group of replicates were used for the analysis.

Germination test

Fresh harvested seeds were placed on filter paper discs sealed in an Petri dish and moistened with 2 mL of water or polyethylene glycol (PEG) 6000 solution from 12 to 25% concentration (Panreac). Seeds were stratified for 3 days at 4°C. Seedling establishment was scored as the appearance of the radical. Each treatment was performed in triplicate with ~50 seeds per genotype per treatment.

RNA-seq analysis

The RNAs were extract from wild-type and *stk* mutant inflorescence and siliques till 6 DAP with the Qiagen Kit according to the manufacturer's instructions. DNA contaminations were removed using the PROMEGA RQ1 RNase-Free DNase according to the manufacturer's instructions. RNA quality was measured with the Nanodrop and the integrity was analyzed by electrophoresis gel. In order to confirm that in *stk* mutant samples STK was not expressed, STK expression was checked by real time PCR with primer RT 780 (5'- TGCGATGCAGAAGTTGCGCTC -3') and RT 781 (5'- AGTACGCGGCATTGATTTCTTG -3'). The library was

prepared with the Illumina TruSeq mRNA-seq kit and sequenced with the Illumina Lane single-read 50bp. The obtained data, 30M of reads for each sample, were analyzed with the CLC Bio software.

Expression Analysis

Quantitative real-time RT-PCR experiments were performed on cDNA obtained from siliques from 3 to 4 day after pollination and from 8 to 10 day after pollination. Total RNA was extracted using the LiCl method (Verwoerd et al., 1989). DNA contamination was removed using the Ambion TURBO DNA-free DNase kit according to the manufacturer's instructions (http://ambion.com/). The treated RNA was subjected to reverse transcription using the ImProm-IITM reverse transcription system (Promega). Genes of interest transcripts were detected using a Sybr Green Assay (iQ SYBR Green Supermix; Bio-Rad) with different reference genes. The real-time PCR assay was conducted in triplicate and was performed in a Bio-Rad iCycler iQ Optical System (software version 3.0a). Relative enrichment of genes of interest transcripts was calculated normalizing the amount of mRNA against a different normalizator genes (ubiquitin, actin, PPa2 and SAND (Hong et al. 2010)) fragment. Diluted aliquots of the reverse-transcribed cDNAs were used as templates in quantitative PCR reactions containing the iQ SYBR Green Supermix (Bio-Rad). The difference between the cycle threshold (Ct) of gene and that of reference gene (ΔCt = CtGENE – CtREFERENCE) was used to obtain the normalized expression of that gene, which corresponds to $2^{-\Delta Ct}$. The expression of the genes was analysed using the set of primer pairs reported in the table S2.

ChIP and Quantitative Real-Time PCR Analysis

The genomic regions located 3 kb upstream of the ATG, 1 kb downstream of the stop codon and in the exons and introns of the selected genes involved in seed development were analyzed to identify the perfect CArG boxes sequence or CArG sequences with one or two mismatch. ChIP experiments were performed as a modified version of a previously reported protocol (Gregis et al, 2008); STK polyclonal antibody was obtained against the synthetic peptide: NH2-RTKVAEVERYQHH-COOH. Antibodies were produce by Primm. Enrichment of the target region was determined using a Sybr Green Assay (iQ_ SYBR Green Supermix; Bio-Rad). The quantitative real-time PCR assay was conducted in triplicate and was performed in a Bio-Rad iCycler iQ optical system (software version 3.0a). Relative enrichment was calculated normalizing the amount of immunoprecipitated DNA against an *ACTIN2/7* (*ACT2/7*) fragment and against total INPUT DNA. In particular, for the binding of STK to the selected genomic regions, the affinity of the purified sample obtained from the WT Col siliques and inflorescence was compared with the affinity-purified sample obtained from the WT Col leaves, which was used as negative control. To determine the efficiency of the Chromatine Immuno Precipitations we used *VDD* third CArG as positive control (Matias-Hernandez et al., 2010). Fold enrichment was calculated using the formulas of a previously reported protocol (Matias-Hernandez et al., 2010). The expression of the genes was analysed using these set of primer pairs reported in table S3.

Accession Number

Sequence data from this article can be found in the GenBank/EMBL data libraries under the following accession numbers: SEEDSTICK, At4g09960.

References

Adato, A., Mandel, T., Mintz-Oron, S., Venger, I., Levy, D., Yativ, M., Domínguez, E., Wang, Z., De Vos, R.C.H, Jetter, R., Schreiber, L., Heredia, A., Rogachev, I., Aharoni A. (2009). Fruit-Surface Flavonoid Accumulation in Tomato Is Controlled by a *SlMYB12*-Regulated Transcriptional Network. *PLoS Genet* **5**, e1000777.

Arsovski, A.A., Haughn, G.W., and Western, T.L. (2010). Seed coat mucilage cells of Arabidopsis thaliana as a model for plant cell wall research. *Plant Signal Behav* **5**, 796–801.

Arsovski, A.A., Popma, T.M., Haughn, G.W., Carpita, N.C., McCann, M.C., and Western TL. (2009). AtBXL1 encodes a bifunctional β-d-xylosidase/α-l-arabinofuranosidase required for pectic arabinan modification in Arabidopsis mucilage secretory cells. *Plant Physiol* **150**, 1219–1234.

Baudry, A., Heim, M.A., Dubreucq, B., Caboche, M., Weisshaar, B. and Lepiniec, L. (2004) TT2, TT8, and TTG1 synergistically specify the expression of *BANYULS* and proanthocyanidin biosynthesis in *Arabidopsis thaliana*. *Plant Journal* **39**, 366–380.

Beeckman, T., De Rycke, R., Viane, R., and Inzé, D. (2000). Histological study of seed coat development in *Arabidopsis thaliana*. *J Plant Res* **113**, 139–148.

Brambilla, V., Battaglia, R., Colombo, M., Masiero, S., Bencivenga, S., Kater, M.M., and Colombo, L. (2007). Genetic and molecular interactions between BELL1 and MADS box factors support ovule development in *Arabidopsis*. *Plant Cell* **19**, 2544-2556.

De Folter, S., Shchennikova, A.V., Franken, J., Busscher, M., Baskar, R., Grossniklaus, U., Angenent, G.C., and Immink, R.G. (2006). A Bsister MADS-box gene involved in ovule and seed development in petunia and Arabidopsis. *Plant Journal* **47**, 934-946.

Dean, G.H., Zheng, H., Tewari, J., Huang, J., Young, D.S., Hwang, Y.T., Western, T.L., Carpita, N.C., McCann, M.C., Mansfield, S.D., and Haughn, G.W. (2007). The *Arabidopsis MUM2* gene encodes a β-galactosidase required for the production of seed coat mucilage with correct hydration properties. *Plant Cell* **19**, 4007–4021.

Debeaujon, I., Léon-Kloosterziel, K.M., and Koornneef, M. (2000). Influence of the testa on seed dormancy, germination and longevity in *Arabidopsis*. *Plant Physiol.* **122**, 403–413.

Debeaujon, I., Nesi, N., Perez, P., Devic, M., Grandjean, O., Caboche, M., and Lepiniec, L. (2003). Proanthocyanidin-Accumulating Cells in Arabidopsis Testa: Regulation of Differentiation and Role in Seed Development. *Plant Cell* **15**, 2514-2531.

Favaro, R., Pinyopich, A., Battaglia, R., Kooiker, M., Borghi, L., Ditta, G., Yanofsky, M.F., Kater, M.M., and Colombo, L. (2003). MADS-box protein complexes control carpel and ovule development in Arabidopsis. *Plant Cell* **15**, 2603–2611.

Fry, S.C. (2000). The Growing Plant Cell Wall: Chemical and Metabolic Analysis. (Caldwell, NJ: The Blackburn Press).

Gonzalez, A., Mendenhall, J., Huo, Y., and Lloyd, A. (2009). TTG1 complex MYBs, MYB5 and TT2, control outer seed coat differentiation. *Dev Biol* **325**, 412–421.

Gregis, V., Sessa, A., Colombo, L., and Kater, M.M. (2008). *AGAMOUS-LIKE24* and *SHORT VEGETATIVE PHASE* determine floral meristem identity in Arabidopsis. *Plant Journal* **66**, 891- 902.
Hanhineva, K., Rogachev, I., Kokko, H., Mintz-Oron, S., Venger, I., Kärenlampi, S., and Aharoni, A. (2008). Non-targeted analysis of spatial metabolite composition in strawberry (Fragaria×ananassa) flowers. *Phytochemistry* **69**, 2463-2481.
Hanke, D.E., and Northcote, D.H. (1975). Molecular visualization of pectin and DNA by ruthenium red. *Biopolymers* **14**, 1–17.
Haughn, G.W., and Chaudhury, A. (2005). Genetic analysis of seed coat development in *Arabidopsis*. *Trends in Plant Science* **10**, 472-477.
Hong, S.M., Bahn, S.C., Lyu, A., Jung, H.S., and Ahn, J.H. (2010). Identification and testing of superior reference genes for a starting pool of transcript normalization in *Arabidopsis*. *Plant Cell Physiol* **51**, 1694–1706.
Huang, J., Debowles, D., Esfandiari, E., Dean, G., Carpita, N.C., and Haughn, G.W. (2011). The Arabidopsis transcription factor LUH/MUM1 is required for extrusion of seed coat mucilage. *Plant Physiol* **156**, 491–502.
Ingram, G.C. (2010). Family life at close quarters: communication and constraint in angiosperm seed development. *Protoplasma* **247**, 195-214.
Johnson, C.S., Kolevski, B., Smyth, D.R. (2002). *TRANSPARENT TESTA GLABRA2*, a trichome and seed coat development gene of *Arabidopsis*, encodes a WRKY transcription factor. *Plant Cell* **14**, 1359–1375.
Kaufmann, K., Anfang, N., Saedler, H., and Theissen, G. (2005). Mutant analysis, protein– protein interactions and subcellular localization of the Arabidopsis Bsister (ABS) protein. *Molecular Genetics Genomics* **274**, 103-118.

Kitamura, S., Matsuda, F., Tohge, T., Yonekura-Sakakibara, K., Yamazaki, M., Saito, K., and Narumi, I. (2010). Metabolic profiling and cytological analysis of proanthocyanidins in immature seeds of *Arabidopsis thaliana* flavonoid accumulation mutants. *Plant Journal* **62**, 549–559.
Kleindt, C.K., Stracke, R., Mehrtens, F., and Weisshaar, B. (2010). Expression analysis of flavonoid biosynthesis genes during Arabidopsis thaliana silique and seed development with a primary focus on the proanthocyanidin biosynthetic pathway. *BMC Research Notes* **3**, 255.
Koo, S.C., Bracko, O., Park, M.S., Schwab, R., Chun, H. J., Park, K. M., Seo, J.S., Grbic, V., Balasubramanian, S., Schmid, M., Godard, M., Yun, D., Lee, S.Y., Sang Y., Cho, M.Y., Weigel, D., and Kim, M.C. (2010). Control of Lateral Organ Development and flowering time by the *Arabidopsis thaliana* MADS-box gene AGAMOUS-LIKE6. *Plant J.* **62**, 807–816.
Lepiniec, L., Debeaujon, I., Routaboul, J.M., Baudry, A., Pourcel, L., Nesi, N., and Caboche, M. (2006). Genetics and biochemistry of seed flavonoids. *Annual Review of Plant Biology* **57**, 405–430.
Li, S.F., Milliken, O.N., Pham, H., Seyit, R., Napoli, R., Preston, J., Koltunow, A.M., and Parish, R.W. (2009). The *Arabidopsis* MYB5 transcription factor regulates mucilage synthesis, seed coat development, and trichome morphogenesis. *Plant Cell* **21**, 72–89.
Matias-Hernandez, L.M., Battaglia, R., Galbiati, F., Rubes, M., Eichenberger, C., Grossniklaus, U., Kater, M.M., and Colombo, L. (2010). *VERDANDI* is a

direct target of the MADS domain ovule identity complex and affects embryo sac differentiation in *Arabidopsis*. *Plant Cell* **22**, 1702-1715.
McCartney, L., and Knox, J.P. (2002). Regulation of pectic polysaccharide domains in relation to cell development and cell properties in the pea testa. *J Exp Bot* **53**, 707-713.
Mintz-Oron, S., Mandel, T., Rogachev, I., Feldberg, L., Lotan, O., Yativ, M., Wang, Z., Jetter, R., Venger, I., Adato, A., and Aharoni, A. (2008). Gene expression and metabolism in tomato fruit surface tissues. *Plant Physiology* **147**, 823–851.
Mizzotti, C., Mendes, M.A., Caporali, E., Schnittger, A., Kater, M.M., Battaglia, R., and Colombo, L. (2011). The MADS box genes *SEEDSTICK* and *ARABIDOPSIS* B_{sister} play a maternal role in fertilization and seed development. *Plant Journal* Dec **16**. doi: 10.1111/j.1365-313X.2011.04878.x.
Nesi, N., Debeaujon, I., Jond, C., Pelletier, G., Caboche, M., and Lepiniec, L. (2000). The *TT8* gene encodes a basic helix-loop-helix domain protein required for expression of *DFR* and *BAN* Genes in *Arabidopsis* siliques. *Plant Cell* **12**,1863-1878
Nesi, N., Debeaujon, I., Jond, C., Stewart, A., Jenkins, G.I., Caboche, M., Lepiniec, L. (2002). The TRANSPARENT TESTA16 locus encodes the *ARABIDOPSIS BSISTER MADS* domain protein and is required for proper development and pigmentation of the seed coat. *Plant Cell **14**, 2463-2479.*
Penfield, S., Meissner, R.C., Shoue, D.A., Carpita, N.C., and Bevan, M.W. (2001). *MYB61* is required for mucilage deposition and extrusion in the Arabidopsis seed coat. *Plant Cell* **13**, 2777-2791.
Pinyopich, A., Ditta, G.S., Savidge, B., Liljegren, S.J., Baumann, E., Wisman, E., and Yanofsky, M.F. (2003). Assessing the redundancy of MADS-box genes during carpel and ovule development. *Nature* **424**, 85-88.
Rautengarten, C., Usadel, B., Neumetzler, L., Hartmann, J., Büssis, D., and Altmann, T. (2008). A subtilisin-like serine protease essential for mucilage release from *Arabidopsis* seed coats. *Plant Journal* **54**, 466–480.
Riechmann, J.L. and Meyerowitz, E.M. (1997). Determination of floral organ identity by Arabidopsis MADS domain homeotic proteins AP1, AP3, PI, and AG is independent of their DNA-binding specificity. *Molec. Biol. Cell* **8**, 1243-1259.
Routaboul, J.M., Kerhoas, L., Debeaujon, I., Pourcel, L., Caboche, M., Einhorn, J., Lepiniec, L. (2006). Flavonoid diversity and biosynthesis in seed of Arabidopsis thaliana. *Planta* 224, 96 –107.
Schauer, S.E., Schluter, P.M., Baskar, R., Gheyselinck, J., Bolanos, A., Curtis, M.D., and Grossniklaus, U. (2009). Intronic regulatory elements determine the divergent expression patterns of AGAMOUS-LIKE6 subfamily members in Arabidopsis. *Plant Journal* **59**, 987–1000.
Selvendran, R.R., and Ryden, P. (1990). Isolation and analysis of plant cell walls. In *Methods In Plant Biochemistry*, Vol. **2**, Carbohydrates (P.M. Dey and J.B. Harbourne, eds.) pp. 549-579. Academic Press, London.
Sharma, S.B., and Dixon, R.A. (2005). Metabolic engineering of proanthocyanidins by ectopic expression of transcription factors in Arabidopsis thaliana. *Plant Journal* **44**, 62–75.
Tohge, T., Matsui, K., Ohme-Takagi, M., Yamazaki, M., Saito, K. (2005). Enhanced radical scavenging activity of genetically modified *Arabidopsis* seeds. *Biotechnol Lett* **27**, 297–303.

Verwoerd, T.C., Dekker, B.M., Hoekema, A. (1989). A small-scale procedure for the rapid isolation of plant RNAs. *Nucleic Acids Res **17***, 2362.

Walker, A. R., Davison, P. A., Bolognesi-Winfield, A. C., James, C. M., Srinivasan, N., Blundell, T. L., Esch, J. J., Marks, M. D. and Gray, J. C. (1999). The *TRANSPARENT TESTA GLABRA1* locus, which regulates trichome differentiation and anthocyanin biosynthesis in *Arabidopsis*, encodes a WD40 repeat protein. *Plant Cell* **11**, 1337-1349.

Walker, M., Tehseen, M., Doblin, M.S., Pettolino, F.A., Wilson, S.M., Bacic, A. and Golz, J.F. (2011). The transcriptional regulator LEUNIG_HOMOLOG regulates mucilage release from the *Arabidopsis* testa. *Plant Physiol* **156**, 46–60.

Western, T.L., Burn, J., Tan, W.L., Skinner, D.J., Martin-McCaffrey, L., Moffatt, B.A., and Haughn, G.W. (2001). Isolation and characterization of mutants defective in seed coat mucilage secretory cell development in *Arabidopsis*. *Plant Physiol* **127**, 998-1011.

Western, T.L., Skinner, D.J., and Haughn, G.W. (2000). Differentiation of mucilage secretory cells of the *Arabidopsis* seed coat. *Plant Physiol* **122**, 345-356.

Windsor, J.B., Symonds, V.V., Mendenhall, J., and Lloyd, A.M. (2000). *Arabidopsis* seed coat development: morphological differentiation of the outer integument. *Plant Journal* **22**, 483–493.

Winkel-Shirley, B. (2001). Flavonoid biosynthesis: a colorful model for genetics, biochemistry, cell biology and biotechnology. *Plant Physiol* **126**, 485–493.

Zhang, F., Gonzalez, A., Zhao, M., Payne, C.T., and Lloyd, A. (2003). A network of redundant bHLH proteins functions in all TTG1-dependent pathways of *Arabidopsis*. *Development* **130**, 4859–4869.

Supporting Information

Figure S1

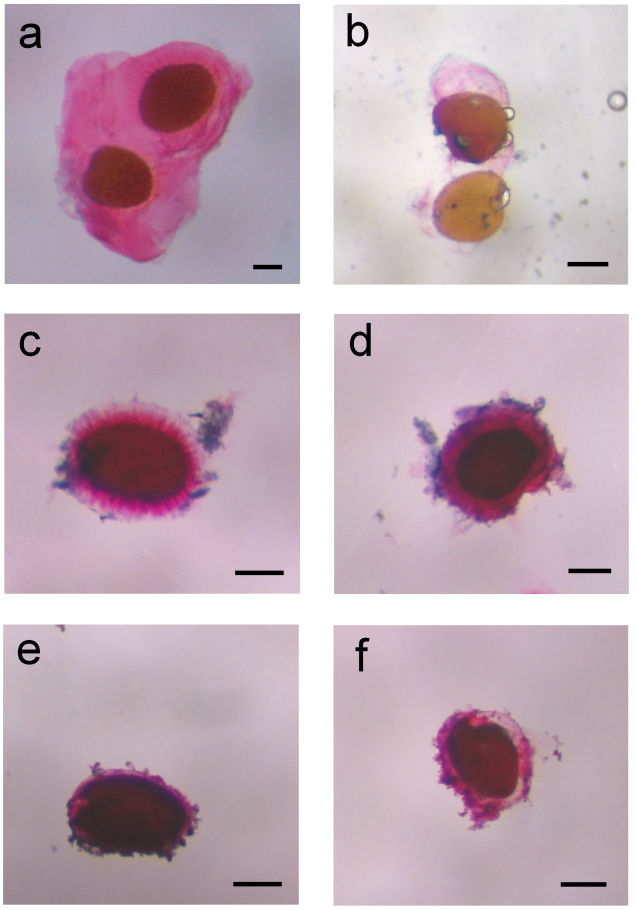


Figure S1. Mucilage release is defective in *stk* mutant. Ruthenium Red staining reveals the presence of a thick, pink-staining capsule of mucilage around the wild-type seed imbibed in water (a), while *stk* mutant seed show a significantly reduced or completely absence of mucilage release (b). Treatment with weak alkali such as Na_2CO_3 caused mucilage extrusion both in wild-type (c) and *stk* mutant seeds (d). Also the treatment with strong alkali like KOH caused mucilage extrusion both in wild-type (e) and *stk* mutant seeds (f). Scale bars = 200 µm.

Table S1

Retention time (min)	Mass (m/z)	Polarity	Annotation
6,83	289,07	Negative	(Epi)Catechin
6,1	577,13	Negative	Dimer1
10,65	577,13	Negative	Dimer2
7,74	865,2	Negative	Trimer
8,24	1153,26	Negative	Tetramer
8,52	720,15	Negative	Pentamer
8,96	864,19	Negative	Hexamer
9,36	1008,71	Negative	Heptamer
9,71	1152,75	Negative	Octamer
10,1	1296,79	Negative	Nonamer

Table S1. List of the annotated metabolites shown in Figure 4.

Table S2

TT8 for	ATGAAGAAGCCGAAGACGAA
TT8 rev	CTTGTGGGGTGTGACATGAG
EGL3 for	AACCAGGAGTGTTGGAGTGG
EGL3 rev	CGGAAGCTCGTCTAGTGACC
MYB61 for	ACTCGCTGGTTTGCAGAGAT
MYB61 rev	GTGTTTGGGTCAATGCCTCT
AGL6 for	GCAACACCGAACCCTTTTTA
AGL6 rev	TGGCATCGTGGTCTAATCAA
TT16 for	GCAGCAACAGTTGGAGAATC
TT16 rev	TCCCAGCTTGTTGAAACTCC
MUM2 for	TCAAGTGGGCAGGTCAAATG
MUM2 rev	AAAAGAGCGGCATGGAAAGC
AtSBT1.7 for	GAAGATCATTGGAGCTAGCG
AtSBT1.7 rev	ACATCCTAGAGCCCAACAAG
UBQ for	CTGTTCACGGAACCCAATTC
UBQ rev	GGAAAAAGGTCTGACCGACA
ACT8 for	CTCAGGTATTGCAGACCGTATGAG
ACT8 rev	CTGGACCTGCTTCATCATACTCTG
PPa2 for	CAGCAACGAATTGTGTTTGG
PPa2 rev	AAATACGCCCAACGAACAAA
SAND for	CAGACAAGGCGATGGCGATA
SAND rev	GCTTTCTCTCAAGGGTTTCTGGGT

Table S2. Set of primer pairs used in the expression analysis assay.

Table S3

ACTIN2/7 for	CCAATCGTGAGAAAATGACTCAG
ACTIN2/7 rev	CCAAACGCAGAATAGCATGTGG
VDD CArG3 *for*	GGAAATATGACGCTTGTCTTTTTAG
VDD CArG3 *rev*	CAGAAACAGCAATATGCTCGTG
MYB61 for	TTGAAGCGTGTTTTATACGTCA
MYB61 rev	ATTGCGTTCATCATTGTTCTTC
AGL6 for	CGAGTTTGGTAGTGTTGGGT
AGL6 rev	CAAAACATGATCCGACTCTTGA
TT16 for	GAAGTTTAGACCCGTTCAAG
TT16 rev	ATGCTGAAACTCGAACACTG
TT8 for	AAAGATAAGAGGCTACCGCG
TT8 rev	ATTCTCAAGCTCATGGACCC
EGL3 for	TCCGTGCAATTAATGCGAGC
EGL3 rev	CTAACGCCGCAGATGATGATG
MUM2 for	GCAAAACCTCAACACCTAGG
MUM2rev	AATGGTCCAATCTTGTTTTG
AtSBT1.7 for	TAGAACAGTTTTGGAGAGCC
AtSBT1.7rev	TGACTCACGAATGCATTACG

Table S3. Set of primer pairs used in the ChIP assay.

Discussion

The development of seeds is one of the major innovations in the evolution of vascular plants that lead to their successful colonization of the Earth (Ingram 2010; Linkies et al. 2010). Beside this, seeds and the plants which produce them, have acquired an essential role in our life: seeds constitute a major proportion of the diet in many human cultures. Seeds are not important only for nutrition but also as raw materials for the manufacture of industrial chemicals, and other products. Also the seed coat has economic significance, as the source of cotton fibres, and during processing of some seed-based products such as coffee and cocoa, the seed coat must be removed.

In addition to their importance in human cultures, the seeds present a feature that make them an attractive system to study the control and the coordination of growth: seed development in angiosperm is indeed an extremely complex process that require the strictly coordination in growth and development of the embryo, endosperm and seed coat (Ingram 2010). This feature makes the seeds an excellent system to study the coordination between different structures during growth.

The role of the integuments during ovule development

The first step in seed development is the formation of the embryo sac enclosed in the ovule integuments (Nowack et al., 2010). Functional role of integuments during ovule development has been investigated for many years and the analysis of several mutants suggest a possible interaction between the integuments and the developing gametophyte though it is still not clear the real nature of the messengers. (for review see Nowack et al., 2010; Bencivenga et al., 2011). Several studies have already demonstrated that the correct integument development is necessary for the proper female gametophyte development. In *aintegumenta* (*ant*) and *bell1* (*bel*) mutants, for instance, the integuments are not developed or only partially developed and in these mutants the female gamethopyte is blocked (Robinson-Beers et al., 1992; Modrusan et al., 1994; Reiser et al., 1995; Elliott et al. 1996; Klucher et al. 1996; Baker et al. 1997; Schneitz et al. 1997; Brambilla et al., 2007; Losa et al., 2010). In our work we studied the double mutant *seedstick* / *arabidopsis bsister* (*stk abs*) that is affected in integument

development since the innermost layer of the integuments, namely the endothelium, is completely missing. In this double mutant the female gametophytes are able to complete their development indicating that the phenotype is less severe than the other mutants with integuments defect (Chapter 1 of this thesis). Moreover all the cells of the female gametophyte have their proper identity though some effects were visible, such as the smaller size of the embryo sac and the occasionally unfused central cell polar nuclei. These results indicate that the most inner layer of the integuments is not necessary for the progression of the female gametophyte.

The role of the integuments during the fertilization process

A defining feature of angiosperms is the reproduction by double fertilization. Each pollen grain contains two sperm cells that are transferred from the anthers to the stigma where it forms a pollen tube that grows inside the carpels to reach the female gametophyte. The guidance of the pollen tube through the sporophytic tissue to reach the female gametophyte is based on several mechanisms such as chemo-attraction, mechanical guidance and growth stimulation though the major chemo-attractant is still unidentified (Dresselhaus, 2006; Higashiyama and Hamamura, 2008). The pollen tube ceases to grow after entering the embryo sac and releases its contents into one of the synergid cells (Berger et al., 2008). The sperm cells are released inside the degenerating synergid and one sperm cell fertilizes the egg cell, forming the zygote, while the other sperm cell fertilizes the diploid

central cell to produce the triploid endosperm (van Went and Willemse, 1984; Russell, 1992, 1996; Berger et al., 2008). The analysis of the double mutant *stk abs* highlighted the role of the endothelium during the fertilization process (Chapter 1 of this thesis). Indeed in the *stk abs* double mutant only 45% of the embryo were fertilized and, among the fertilized ovules, 75% of seed are aborted. This phenotype could be explained by the unfusion of the polar nuclei but only in a partial way since the polar nuclei that are not fused correspond to 15% of the ovules. Furthermore this reduction fertility is not related neither to defects in pollen tube guidance nor to pollen tube burst. Morphological analysis of the *stk abs* developing embryo revealed a massive starch accumulation that could represent a barrier to proper migration of the sperm cells. Different mutants with altered sucrose metabolism have been isolated and they present stunted growth, retarded development, and sterility. The *cytosolic phosphoglucomutase2* (*cpm2*) *cpm3* double mutant and the *sucrose transporter2* (*suc2*) mutant, for instance, present defects during female gametophyte development and reduced fertility (Gottwald et al., 2000; Egli et al., 2010). These mutants point to indicate that in the female gametophyte there must be a tight regulation of metabolic pathways and disturbance of these cause gametophyte defects. Moreover our results on the *stk abs* double mutant indicate that fertilization is also under sporophytic control and that the endothelium is an important component contributing to ovule fertility. Furthermore, on the base of our data we assume that the endothelium is critical during seed development and its role is probably based on the regulation of the nutrients fluxes. According

to our results the integuments during fertilization are essential for a correct and balanced nutrition of the next generation besides being essential for fertilization.

The role of the integuments during seed development

In response to fertilization the ovule integuments grow and develop is strictly coordination with the development of the embryo and the endosperm. The seed coat provides protection to the embryo from adverse environmental effects such as UV damage, mechanical stress and desiccation and it assist in germination and dispersal too (Windsor et al., 2000; Haughn and Chaudhury, 2005; Nowack et al., 2010). The seed coat participates in many important processes during seed development such as transport of nutrients from the funiculus to the developing embryo, protection of the embryo, and control of the length of the dormancy period (Debeaujon et al., 2000). The Arabidopsis seed coat consists of five cell layers with different fate: the cells of the endothelium during the first week after fertilization synthesize proanthocyanidin (PAs), which accumulate in the central vacuole. The proanthocyanidin are later oxidized, imparting a brown color to the seed coat (Debeaujon et al., 2003). The cells of the other two inner integument layers are crushed together as the seed develops while the cells of both outer integument layers accumulate amyloplasts during the growth phase. Moreover the cells of the epidermal layer synthesize and secrete a large quantity of mucilage into the apoplast that contribute to seed physiology and improve germination. The isolation and molecular characterization of

transparent testa (*glabra*), *tt*(*g*) mutants, which are affected in seed coat pigmentation, has allowed to define the genetic control of seed PAs biosynthesis (Winkel-Shirley, 2001; Debeaujon et al., 2003; Sharma and Dixon, 2005; Kitamura et al., 2010). The protein complex composed by TT8, EGL3 (ENHANCER OF GLABRA3), MYB5, TT2 and TTG1 is a master regulator of PAs biosynthesis since it directly promotes the expression of *BAN* (*BANLYUS*). *BAN* encode for the core enzyme of the PAs production: an anthocyanidin reductase that convert anthocyanidins to their corresponding flavan-3-ols (Zhang et al., 2003; Baudry et al., 2004; Gonzalez et al., 2009; Li et al., 2009). Aside from this protein complex, the regulation of *BAN* expression is actuated by ABS and TT1 protein that control BAN expression in the core region of the endothelium, but not in the micropyle and chalazal areas (Lepiniec et al., 2006). In our work we studied the single mutant *seedstick* (*stk*) that is affected in integuments development and is also involved in PAs accumulation (Chapter 2 of this thesis). On the base of ChIP assay and RNA-seq analysis we concluded that *STK* has a pivotal role in PAs production acting as a repressor of all the genes involved in the PAs accumulation in the endothelium. STK is in particular repress the expression of four out of five genes of the TTG1 complex and it repress also the other pathway that control *BAN* expression: the TT1 and the ABS pathways.

Another important features of seed development are the production and release of mucilage that contribute to seed physiology and improve germination. The regulation of mucilage production and release is under the control of the protein complex composed by TT8, EGL3, MYB5, TT2 and TTG1. This complex regulates the

expression of *TTG2* and *GLABRA2* (*GL2*) that are involved in the generation of mucilage in the outer layer of the seed coat (Western et al., 2000; Windsor et al., 2000). Other genes involved in mucilage release are the genes regulated by the MUCILAGE-MODIFIED1 (MUM1) protein: *MUM2*, *β-XYLOSIDASE1* (*BXL1*) and *SUBTILISIN-LIKE SERINE PROTEASE1.7* (*AtSBT1.7*). Mutants for these genes produced normal amount of mucilage but it does not properly extrude upon seed hydration (Western et al., 2001; Rautengarten et al., 2008; Arsovski et al., 2009; Huang et al., 2011). The same mutant phenotype was also reported for the transcription factor MYB61 but it defines a separate pathway (Penfield et al., 2001; Arsovski et al., 2009; Arsovski et al., 2010). In our work (Chapter 2 of this thesis) we demonstrated the *STK* is also a key regulator of mucilage release. STK repress all the different pathway of mucilage production and release. In particular it repress the MYB61 pathway while in the pathway activate by MUM1 it act as a repressor of *MUM2* and *AtSBT1.7* genes. The regulation of the third pathway, the pathway regulated by GL2 and TTG2, is carried out through the regulation of the protein complex TTG1, TT8, EGL3, MYB5 and TT2. Morphological data revealed that STK is involved in mucilage released upon imbibition and treatment with different chemical reagents suggested that the hydration properties of the mucilage are not affected, however it is now important to analyse the mucilage composition in order to define if the problem is due to altered mucilage composition or to defects in cell wall.

Our data demonstrated that *STK* is essential for integument development and for the secondary metabolites production and

release and according to these data we can conclude that *STK* is a central player in seed development.

References

Arsovski, A.A., Haughn, G.W., and Western, T.L. (2010). Seed coat mucilage cells of Arabidopsis thaliana as a model for plant cell wall research. *Plant Signal Behav* **5**, 796–801.

Arsovski, A.A., Popma, T.M., Haughn, G.W., Carpita, N.C., McCann, M.C., and Western TL. (2009). AtBXL1 encodes a bifunctional β-d-xylosidase/α-l-arabinofuranosidase required for pectic arabinan modification in Arabidopsis mucilage secretory cells. *Plant Physiol* **150**, 1219–1234.

Baker, S.C., Robinson-Beers, K., Villanueva, J.M., Gaiser J.C., and Gasser, C.S. (1997). Interactions Among Genes Regulating Ovule Development in *Arabidopsis thaliana*. *Genetics* **145**, 1109-1124.

Baudry, A., Heim, M.A., Dubreucq, B., Caboche, M., Weisshaar, B. and Lepiniec, L. (2004) TT2, TT8, and TTG1 synergistically specify the expression of *BANYULS* and proanthocyanidin biosynthesis in *Arabidopsis thaliana*. *Plant Journal* **39**, 366–380.

Bencivenga, S., Colombo, L., and Masiero, S. (2011). Cross talk between the sporophyte and the megagametophyte during ovule development. *Sexual Plant Reproduction* **24**, 113-121.

Berger, F., Hamamura, Y., Ingouff, M., and Higashiyama, T. (2008). Double fertilization—caught in the act. *Trends Plant Sci* **13**, 437–443.

Brambilla, V., Battaglia, R., Colombo, M., Masiero, S., Bencivenga, S., Kater, M.M., and Colombo, L. (2007). Genetic and molecular interactions between BELL1 and MADS box factors support ovule development in *Arabidopsis*. *Plant Cell* **19**, 2544-2556.

Debeaujon, I., Léon-Kloosterziel, K.M., and Koornneef, M. (2000). Influence of the testa on seed dormancy, germination and longevity in *Arabidopsis*. *Plant Physiol.* **122**, 403–413.

Debeaujon, I., Nesi, N., Perez, P., Devic, M., Grandjean, O., Caboche, M., and Lepiniec, L. (2003). Proanthocyanidin-Accumulating Cells in Arabidopsis Testa: Regulation of Differentiation and Role in Seed Development. *Plant Cell* **15**, 2514-2531.

Dresselhaus, T. (2006). Cell–cell communication during double fertilization. *Curr. Opin. Plant Biol*. **9**, 41–47.

Egli, B., Kölling, K., Köhler, C., Zeeman, S.C., and Streb, S. (2010). Loss of cytosolic phosphoglucomutase compromises gametophyte development in Arabidopsis. *Plant Physiology* **154**, 1659-1671.

Elliott, R.C., Betzner, A.S., Huttner, E., Oakes, M.P., Tucker, W.Q., Gerentes, D., Perez, P., and Smyth, D.R. (1996). AINTEGUMENTA, an APETALA2-like gene of *Arabidopsis* with pleiotropic roles in ovule development and floral organ growth. *Plant Cell* **8**, 155-168.

Gonzalez, A., Mendenhall, J., Huo, Y., and Lloyd, A. (2009). TTG1 complex MYBs, MYB5 and TT2, control outer seed coat differentiation. *Dev Biol* **325**, 412–421.

Gottwald, J.R., Krysan, P.J., Young, J.C., Evert, R.F., and Sussman, M.R. (2000). Genetic evidence for the *in planta* role of phloem-specific plasma membrane sucrose transporters. *Proceedings of the National Academy of Sciences* **97,** 13979-13984.

Haughn, G.W., and Chaudhury, A. (2005). Genetic analysis of seed coat development in *Arabidopsis*. *Trends in Plant Science* **10**, 472-477.
Higashiyama, T., and Hamamura, Y. (2008). Gametophytic pollen tube guidance. *Sex. Plant Reprod.* **21**, 17-26.
Huang, J., Debowles, D., Esfandiari, E., Dean, G., Carpita, N.C., and Haughn, G.W. (2011). The Arabidopsis transcription factor LUH/MUM1 is required for extrusion of seed coat mucilage. *Plant Physiol* **156**, 491–502.
Ingram, G.C. (2010). Family life at close quarters: communication and constraint in angiosperm seed development. *Protoplasma* **247**, 195-214.
Kitamura, S., Matsuda, F., Tohge, T., Yonekura-Sakakibara, K., Yamazaki, M., Saito, K., and Narumi, I. (2010). Metabolic profiling and cytological analysis of proanthocyanidins in immature seeds of *Arabidopsis thaliana* flavonoid accumulation mutants. *Plant Journal* **62**, 549–559.
Klucher, K.M., Chow, H., Reiser, L., and Fischer, R.L. (1996). The AINTEGUMENTA gene of *Arabidopsis* required for ovule and female gametophyte development is related to the floral homeotic gene APETALA2. *Plant Cell* **8**, 137-153.
Lepiniec, L., Debeaujon, I., Routaboul, J.M., Baudry, A., Pourcel, L., Nesi, N., and Caboche, M. (2006). Genetics and biochemistry of seed flavonoids. *Annual Review of Plant Biology* **57**, 405–430.
Li, S.F., Milliken, O.N., Pham, H., Seyit, R., Napoli, R., Preston, J., Koltunow, A.M., and Parish, R.W. (2009). The *Arabidopsis* MYB5 transcription factor regulates mucilage synthesis, seed coat development, and trichome morphogenesis. *Plant Cell* **21**, 72–89.
Linkies, A., Graeber, K., Knight, C., and Leubner-Metzger, G. (2010). The evolution of seeds. *New Phytol* **186**, 817–831.
Losa, A., Colombo, M., Brambilla, V., and Colombo, L. (2010). Genetic interaction between AINTEGUMENTA (ANT) and the ovule identity genes SEEDSTICK (STK), SHATTERPROOF1 (SHP1) and SHATTERPROOF2 (SHP2). *Sexual Plant Reproduction* **23**, 115-122.
Modrusan, Z., Reiser, L., Feldmann, K.A., Fischer, R.L., and Haughn, G.W. (1994). Homeotic transformation of ovules into carpel-like structures in *Arabidopsis. Plant Cell* **6,** 333-349.
Nowack, M.K., Ungru, A., Bjerkan, K.N., Grini, P.E., and Schnittger, A. (2010). Reproductive cross-talk: seed development in flowering plants. *Biochem Soc Trans* **38**, 604–612.
Penfield, S., Meissner, R.C., Shoue, D.A., Carpita, N.C., and Bevan, M.W. (2001). *MYB61* is required for mucilage deposition and extrusion in the Arabidopsis seed coat. *Plant Cell* **13**, 2777-2791.
Rautengarten, C., Usadel, B., Neumetzler, L., Hartmann, J., Büssis, D., and Altmann, T. (2008). A subtilisin-like serine protease essential for mucilage release from *Arabidopsis* seed coats. *Plant Journal* **54**, 466–480.
Reiser, L., Modrusan, Z., Margossian, L., Samach, A., Ohad, N., Haughn, G.W., and Fischer, R.L. (1995). The *BELL1* gene encodes a homeodomain protein involved in pattern formation in the *Arabidopsis* ovule primordium. *Cell* **83**, 735-742.
Robinson-Beers, K., Pruitt, R.E., and Gasser, C.S. (1992). Ovule development in wild-type Arabidopsis and two female-sterile mutants. *Plant Cell* **4,** 1237-1249.
Russell, S.D. (1992). Double fertilization. *Int. Rev. Cytol.* **140**, 357–388.

Russell, S.D. (1996). Attraction and transport of male gametes for fertilization. *Sex. Plant Reprod.* **9**, 337–342.

Schneitz, K., Hulskamp, M., Kopczak, S.D., and Pruitt, R.E. (1997). Dissection of sexual organ ontogenesis: A genetic analysis of ovule development in *Arabidopsis thaliana*. *Development* **124**, 1367-1376.

Sharma, S.B., and Dixon, R.A. (2005). Metabolic engineering of proanthocyanidins by ectopic expression of transcription factors in Arabidopsis thaliana. *Plant Journal* **44**, 62–75.

van Went, J.L., and Willemse, M.T.M. (1984). Fertilization. In Embryology of Angiosperms, B. Johri, ed (Berlin: Springer-Verlag), pp. 273–318.

Western, T.L., Burn, J., Tan, W.L., Skinner, D.J., Martin-McCaffrey, L., Moffatt, B.A., and Haughn, G.W. (2001). Isolation and characterization of mutants defective in seed coat mucilage secretory cell development in *Arabidopsis*. *Plant Physiol* **127**, 998-1011.

Western, T.L., Skinner, D.J., and Haughn, G.W. (2000). Differentiation of mucilage secretory cells of the *Arabidopsis* seed coat. *Plant Physiol* **122**, 345-356.

Windsor, J.B., Symonds, V.V., Mendenhall, J., and Lloyd, A.M. (2000). *Arabidopsis* seed coat development: morphological differentiation of the outer integument. *Plant Journal* **22**, 483–493.

Winkel-Shirley, B. (2001). Flavonoid biosynthesis: a colorful model for genetics, biochemistry, cell biology and biotechnology. *Plant Physiol* **126**, 485–493.

Zhang, F., Gonzalez, A., Zhao, M., Payne, C.T., and Lloyd, A. (2003). A network of redundant bHLH proteins functions in all TTG1-dependent pathways of *Arabidopsis*. *Development* **130**, 4859–4869.